CP4O

CryoSat Plus for Oceans

ESA/ESRIN Contract No. 4000106169/12/I-NB

D2.1 Preliminary Analysis Report (PAR)

VERSION 1.0, 1st June 2013

ESA/ESRIN Technical Officer: Jérôme Benveniste

Author Organisation Details

AUTHOR/MANAGER/COLLABORATOR LIST

Main Author(s)	Affiliation	Signature
M. Naeije	TUDelft	
D Cotton	SatOC	
Project Manager	**Affiliation**	
D. Cotton	SatOC	
Collaborators	**Affiliation**	

DISTRIBUTION LIST

Who	Affiliation

CP4O	Preliminary Analysis Report	D2.1	

CHANGE RECORD

ISSUE	DATE	Change Record Notes	Main Author
0.1	April 2013	Original	Naeije
0.2	26 May 2013	Processing rest contribs	Naeije
0.3	3 June 2013	Restructuring	Cotton
0.4	7 June 2013	Final draft edit	Naeije
1.0	12 June 2013	Review of Chapters 4,5	Cotton
1.01	14 June 2013	Additions to sections 3.2.3, 3.4.6, 3.5.3, 4.4.3	Andersen

CP4O	Preliminary Analysis Report	D2.1	

Abstract

ESA's CryoSat-2 mission is the first one to carry a radar altimeter that can operate in SAR mode. Although the primary aim is land and marine ice monitoring, the SAR mode capability of the CryoSat-2 SIRAL altimeter offers potential benefits for ocean applications. The project "CryoSat Plus for Oceans" (CP4O) exploits CryoSat-2 data over the ocean. CP4O is supported by the ESA under the Support to Science Element (STSE) Programme, and by CNES, and brings together an expert European consortium. Objective is to build a sound scientific basis for new applications of CryoSat-2 data over the open ocean, polar ocean, coastal seas and for sea-floor mapping. In addition new methods and products will be generated and evaluated that should enable the full exploitation of the capabilities of the CryoSat-2 SIRAL altimeter, and extend their application beyond the initial mission objectives. The ultimate goal is to maximise the scientific return of the CryoSat-2 mission and be prepared for the full exploitation of future SAR enabled altimeter missions like Sentinel-3 and Jason-CS.

After the first phase of the project, which dealt with the consolidation of the scientific requirements consulting the user community a preliminary analysis of the state-of-the-art has been carried out. This comprises a comprehensive review of the state-of-the-art, relevant current initiatives, algorithms, models and EO-based products and datasets that are relevant in the context of innovative ocean applications for CryoSat-2 data. This document reports on the outcome of the state-of-the-art analysis focussing on low and high-resolution open ocean altimetry, high-resolution polar ocean and coastal zone altimetry and high-resolution sea-floor altimetry. It is complemented by a risk analysis to identify the risk areas and the solutions for mitigation.

Acknowledgments

CP4O	Preliminary Analysis Report	**D2.1**	

Contents

CP4O	Preliminary Analysis Report	D2.1	

Figures

CP4O	Preliminary Analysis Report	D2.1	

Tables

CP4O	Preliminary Analysis Report	D2.1	

Abbreviations and Definitions

ADC	Analogue-to-Digital Converter
ADT	Absolute Dynamic Topography
AGC	Automatic Gain Control
AIR	Azimuth Impulse Response
ATBD	Algorithm Theoretical Basis Document
AMR	Advanced Microwave Radiometer
ADT	Absolute Dynamic Topography
BRF	Burst Repetition Frequency
BUFR	Binary Universal Form for the Representation of meteorological data
CAI	Coarse Altitude Instruction
CLS	Collecte Localisation Satellites
CNES	Centre National d'Etudes Spatiales
CNR	Consiglio Nazionale delle Ricerche
CODE	Centre for Orbit Determination in Europe (University of Bern)
COMAPI	Coastal Modelling for Altimetry Product Improvement
CP4O	CryoSat Plus 4 Oceans
CPP	Crysosat Processing Prototype
CRYMPS	CRYosat-2 Mission Performance Simulator
DAC	Dynamic Atmospheric Correction
Dcomb	An objective analysis data combination methodology
DDA	Delay-Doppler Altimeter
DEM	Digital Elevation Model
DTU	Danmarks Tekniske Universitet
DUACS	Developing Use of Altimetry for Climate Studies – CLS altimeter Processing system
ECMWF	European Centre for Medium-Range Weather Forecast
Envisat	ESA Remote Sensing Satellite (2002-2012)
EO	Earth Observation
ERA	ECMWF ReAnalysis
ERS-1	ESA Remote Sensing Satellite (1991-2000)
ERS-2	ESA Remote Sensing Satellite (1995-2011)
ESA	European Space Agency
ESOC	European Space Operations Centre
FAI	Fine Altitude Instruction
FBR	Full Bit Rate data – CryoSat Product that contains (in SAR mode) individual complex echo waveforms
FES*YYYY*	Finite Element Solution Global Tide models
FDM	(CryoSat) Fast Delivery Marine Product
FSSR	Flat Sea Surface Response
FTP	File Transfer Protocol
GDR	Geophysical Data Record
Geosat	US Altimetry Satellite Mission (1985-90)
GIM	Global Ionospheric Map
GNSS	Global Navigation Satellite System
GOCE	Gravity field and steady-state Ocean Circulation Explorer – ESA Satellite

CP4O	Preliminary Analysis Report	D2.1	

	Gravity Mission
GOT (*X.Y*)	Global Ocean Tide model derived from satellite altimetry
GPD	GNSS-derived Path Delay
GPS	Global Positioning System
GTS	Global Telecommunications System
HDF	Hierarchical Data Format
IDE	Identification (definition) for outstanding CryoSat issues
IGDR	Interim Geophysical Data Record
IMEDEA	Institut Mediterrani d'Estudis Avançats
IPF	Instrument Processing Facility
IRI95	International Reference Ionosphere, 1995
Jason	US/French Altimeter Satellite (2001-)
JPL	Jet Propulsion Laboratory
LAI	Range word from SAR pre-processor
LRM	Low Resolution Mode, sometimes also called Low Rate Mode
LUT	Look Up Table
L1B	CryoSat Product that contains (in SAR mode) multi-looked waveforms
L2	CryoSat Product that contains geophysical parameters
MDT	Mean Dynamic Topography
MLE (N)	Waveform re-tracking approach - Maximum Likelihood Estimate – providing N (3 or 4) output parameters
MOG2D	2 Dimensional gravity wave model used to model dynamic ocean response to atmospheric wind and pressure forcing
MSS	Mean Sea Surface
MWR	Micro-Wave Radiometer
NCEP	National Center for Environmental Predictions
NEA	North East Atlantic
NetCDF	Network Common Data Form
NIC09	New Ionosphere Climatology generated by Scharroo and Smith
N-ERM	Near-Exact Repeat Orbit
NOAA	National Oceanic and Atmospheric Administration
NOC	National Oceanography Centre
NRT	Near Real Time
OA	Objective Analysis
OCOG	Offset Centre-of-Gravity (retracker)
OGDR	Operational Geophysical Data Record
OPeNDAP	Open-source Project for a Network Data Access Protocol
OSTST	Ocean Surface Topography Science Team
PD	Path Delay
PDF	Probability Density Function
PLRM	Pseudo-LRM
PRF	Pulse Repetition Frequency
PTR	Point Target Response
PVR	Preliminary Validation Report
RADS	Radar Altimeter Database System (TU Delft) - http://rads.tudelft.nl/rads/rads.shtml
RB	Requirements Baseline

RDSAR	ReDuced SAR
RIM	Regional Ionospheric Maps
RIR	Range Impulse Response
RMS	Root Mean Square
RT	Real Time
SAMOSA	SAR Altimetry Mode Studies and Applications – ESA funded Project
SARIN	Synthetic Aperture Radar INterferometric mode
SAR	Synthetic Aperture Radar
SARM	SAR Mode
SI-MWR	Scanning/Imaging MWR
SIRAL	Synthetic aperture Interferometric Radar ALtimeter
S/N	Signal to Noise Ratio
SLA	Sea Level Anomaly
SPECTRE	Service and Products for ionosphere Electronic Content and Tropospheric Refractivity over Europe from GPS data – Regional Ionosphere model
SSB	Sea State Bias
SSH	Sea Surface Height
SST	Sea Surface Temperature
STSE	Support To Science Element
SWH	Significant Wave Height
TAS	Thales Alenia Space
TDS	Thredds Data Server
TEC	Total Electron Content
TOPEX	US / French Altimeter Satellite (1992-2006)
TU Delft	Technical University of Delft
UPC	Technical University of Catalonia
uTEC	Unit of TEC (10^{16} electrons/m^2).
WTC	Wet Tropospheric Corrections

1 Introduction

The ESA CryoSat-2 mission is the first space mission to carry a radar altimeter that can operate in Synthetic Aperture Radar (SAR) mode, also known as Delay-Doppler Altimeter (DDA). Although the prime objective of the CryoSat-2 mission is dedicated to monitoring land and marine ice, the SAR mode capability of the CryoSat-2 SIRAL altimeter also presents the opportunity of demonstrating significant potential benefits of SAR altimetry for ocean applications, based on expected performance enhancements which include improved range precision and finer along track spatial resolution.

The "CryoSat Plus for Oceans" (CP4O) project is supported under the ESA Support To Science Element Programme (STSE) and brings together an expert consortium comprising, CLS, DTU Space, isardSAT, NOC, Noveltis, SatOC, Starlab, TU Delft, and the University of Porto. The main objectives of CP4O are:

- to build a sound scientific basis for new scientific and operational applications of CryoSat-2 data over four different areas, which are: open ocean, polar ocean, coastal seas and sea-floor mapping.
- to generate and evaluate new methods and products that will enable the full exploitation of the capabilities of the CryoSat-2 SIRAL altimeter, and extend their application beyond the initial mission objectives.
- to ensure that the scientific return of the CryoSat-2 mission is maximised.

1.1 Purpose, Scope and Goals

This document, referred to as the Preliminary Analysis Report (PAR), provides the summary of a comprehensive review of the state-of the art, relevant current initiatives, algorithms, models and EO-based products and datasets that are relevant in the context of the investigated theme of innovative ocean applications for CryoSat-2. In particular it reports on the state-of-the-art analysis of low and high-resolution open ocean altimetry, high-resolution polar ocean and coastal zone altimetry and high-resolution sea-floor altimetry. It is complemented by a risk analysis to identify the risk areas and the solutions for mitigation. Together with the requirements baseline **[RD.3]** this document leads to the proposal of products, their development, evaluation and validation set down in writing in the Development and Validation Plan (DVP, deliverable D2.2).

1.2 Document setup

In line with the Statement of Work in the original ITT **[RD.1]** and according to our Technical Proposal for CryoSat Plus 4 Oceans (CP4O) project **[RD.2]**, this

document summarises all the outcomes of Task2 (SoW), referred to as work Package 2000 (CP4O), which includes:

- A detailed review, assessment and cross-comparison of existing products, datasets, methods, models and algorithms, as well as related range of validity limitations, drawbacks and challenges;
- A detailed analysis of the suitable models and data integration approaches as well as their related limitations, drawbacks and challenges;
- A survey of all accessible data sets associated (space, airborne and in situ) that could be of use in helping ESA to perform an adequate development and validation activity. Investigation of problems such as the lack of sufficient data and identification of practical solutions;
- A survey of current and upcoming initiatives and projects related to CryoSat-2 innovative ocean applications;
- An analysis and identification of the best candidate test areas to be used in the upcoming development and validation of products, including a complete analysis and description of the available data over those test areas.

These sub tasks have been conveniently copied one-to-one to Work Packages WP2100 up to WP2500 and these addresses the subsequent tasks as such. In performing the analysis we have considered recent scientific publications, as well as researches and operational projects funded in the last few years by ESA, the EC and R&D national programmes. Obviously the expertise and experience of the partners in the consortium have served as guidelines. It was decided to take the most recent Ocean Surface Topography Science Team (OSTST) meeting (Venice, September 2012) as reference point to define the "state of the art". Any new insights, visions, models etc. after that date are monitored closely but have not been addressed in this document. In addition we also complement the research and by this the report by a risk analysis pointing out risk areas that could affect the final success of the project measured by each objective and solutions to cope with these risks or to mitigate them.

Chapter 2 defines our proposed research and how we have organized it in terms of work breakdown and resource allocation. Chapter 3 provides the results of our studies per sub task or work package, whereas Chapter 4 relates the results to the different sub themes: open ocean, polar ocean, coastal zone, and sea floor mapping. In conclusion Chapter 5 gives conclusions and recommendations, which are direct input for the DVP.

1.3 Documents

RD.1 Support to Science Element, CryoSat+: Ocean and CryoSat+ : Land/Inland Water, Statement of Work, ESA. EOEP-STSE-EOPS-SW-11-0001, Version 2 09/08/2011

RD.2 Cryosat Plus for Oceans, Technical Proposal, SatOC, DTU Space, isardSAT, NOC, Noveltis, STARLAB, TU Delft, University of Porto and CLS, Response to ESA ITT AO/1-6827/11/I-NB, November 2011

RD.3 Cryosat Plus for Oceans - Scientific Requirements Consolidation (D1.1), STARLAB, NOC, CLS, DTU Space, SatOC, ESA Project Report, March 2013.

2 WP2000 – the work

2.1 Introduction

As stated before this task or work package entails the review of the state-of-the-art in CryoSat-2 ocean altimetry. It is led by scientists from Delft University of Technology (TUDelft), who have a long track record in altimetry research and (conventional) altimeter calibration and validation. Together with Altimetrics LLC (Remko Scharroo) and NOAA they have developed the Radar Altimeter Database System (RADS). Direct support for executing the task comes from CLS and NOC, while DTU, isardSAT, Noveltis, UPorto, SatOC, and STARLAB contributed on specific sub-themes related to their respective expertise. Altimetrics LLC has the role of adviser.

2.2 Objectives

Despite the priority of ice monitoring it is clear that CryoSat-2's ocean products be it from the conventional altimeter mode (LRM), the SAR mode or SARin mode, are indispensable for investigating small– to mesoscale ocean processes, in particular in coastal regions and high-latitudes. The large uncertainty in sea level change is at the regional scale, particularly where dynamic processes play an important role. Regional sea level changes may very well modify the patterns of ocean circulation and climate change. There is consensus that there exists a somewhat larger than average sea-level rise near the North Pole due to Arctic freshening (increased runoff and precipitation), and a relatively lesser rise south of 60° S due to balancing heat uptake and deep water upwelling. For climate and climate change assessment it is absolutely essential to quantify these regional dynamic processes at high latitudes, because they significantly contribute to the global average sea level change estimate. This is where CryoSat-2 can play a significant role. It is therefore important to choose the best available processing methodologies and the best available corrections and models. It is also very likely that some of these will need tailoring to the specific characteristics of the CryoSat-2 measurements globally and regionally, given that CryoSat-2 carries the first non-conventional altimeter instrument. In this Work Package (WP2000) we perform a detailed preliminary analysis of the state of the art in altimetry processing directly linked to the CryoSat-2 instrument and data output. We draw upon the wealth of expertise already existing among the project partners and their wide-ranging connections with the broad altimetry, sea level and climate community. All WP2000 partners have gathered, examined and proposed the latest algorithms currently available to CryoSat-2 dedicated to low and high-

resolution open ocean altimetry, high-resolution polar ocean altimetry, high-resolution coastal zone altimetry, and high-resolution sea floor altimetry. They include:

- Altimeter instrumental corrections, i.e. monitored biases and drifts of the altimeter range and timing (ultra-stable oscillator and other instrumental variations), wave height (related to aging of the altimeter) and backscatter (due to variations in instrumental gain settings);
- Altimeter- and region specific algorithms and models like the sea state bias correction, as well as the wet troposphere path delay and ionosphere path delay for which no direct (platform) measurements are available;
- Orbital ephemerides, i.e. position of the satellite, the altitude in particular, which includes the selection of an appropriate gravity field model and reference frame, also to align CryoSat-2 with other missions like Jason and Envisat;
- Tidal corrections, *i.e.* displacement of the land and ocean as a result of solar and lunar attraction, including second-order effects, like ocean loading, and complex tides;
- Dynamic atmospheric correction, i.e. the effect of atmospheric pressure on the sea level, taking into account the different responses of the sea surface to various frequencies in the atmospheric forcing.

Producing CryoSat+ ocean products and striving for the best quality not only depends on the choice of altimeter corrections, but also on choice of re-tracking algorithm, location of the altimeter data (open ocean vs. coastal), and on the degree of averaging that in turn depends on the envisioned usage (assimilation in operational models, global and local sea level change, geostrophic currents, etc.). This is especially true for the range measurement, but also other altimeter derived products like wind and waves need special attention. Where new re-tracking approaches are to be employed for SAR mode data, there is a need to validate the derived sea state measurements. Peculiarities of this mission that significantly add to its potential for oceanography are access to higher latitudes as well as the higher resolution in coastal regions and across storms. Obviously, next to the employment of the expertise of the respective contributors to this task the most recent scientific publications, as well as recent relevant researches and operational projects have been considered. WP2000 is complemented by a risk analysis focussing on those aspects that could affect the final success of the project, together with solutions or ways to mitigate these risks. All the outcomes have to be reported in the Preliminary Analysis Report (PAR, this document), one of the Task deliverables, and the implementation of remaining activities are proposed in the detailed Development and Validation Plan (DVP).

2.3   Technical requirements review

In this section we attentively consider CryoSat-2's specific problems and peculiarities:

- In contrast to previous conventional (pulse-limited) altimeter missions, CryoSat-2 is not a dedicated platform for ocean research: as a consequence there is no microwave radiometer (MWR) for wet tropospheric corrections, nor is there the capability to make a direct measurement of the first order ionospheric effect by means of a dual-frequency altimeter. Moreover, the orbit of CryoSat-2 has a rather long repetition period, unsuited for collinear tracks analyses. These three particular features have been studied to a large extent already by CLS (2004) in the HERACLES project on the eve of the first CryoSat-2 launch. We revisit the outcome of this study, update to current understanding and perception, and ultimately develop what was, is and will be proposed in these problem areas. Clearly, we question the ionosphere corrections, the wet troposphere corrections and the accuracy of the mean sea surface (MSS) underlying the accuracy of derived sea level anomalies;

- In addition, CryoSat-2 provides the first innovative altimeter with SAR and SARIn modes. This raises the direct problem of "how to process these data?" Compared to pulse-limited altimetry it is a totally different branch of sport. In our opinion trying to answer this question is one of the core activities of the CryoSat+ study. We build on the results that have come out of the SAMOSA study by SatOC, NOC, Starlab and DTU. This study was initiated in 2007 to investigate the improvements that SAR mode altimetry can offer in measurements over ocean, coastal and inland water surfaces, developing practical implementation of new theoretical models for the SAR echo waveform. It is clear that having specific processing for SAR and SARIn raises a number of new issues to be studied, such as RDSAR (reducing SAR to pseudo LRM data), sea state bias (SSB) in SAR mode, and land contamination, to name a few.

As addressing CryoSat-2's specific problem areas (inventory and evaluation) is part of the work of the task itself we will not exhaustively treat them here but leave that for the resulting report. We suffice with highlighting some of the geophysical corrections. Most of the proposed enhancements to the current CryoSat-2 data, as far as geophysical corrections are concerned, are already included in the RADS Altimeter Database System. We exploit the abilities of RADS to provide these corrections to be incorporated in CryoSat+ products in the most cost-effective way. In addition, the tools included in RADS will be employed to do most of the cross- satellite validation.

The path delay (PD) due to the presence of water vapour in the atmosphere whose correction is simply known as the wet tropospheric correction (WTC), is one of the major error sources in satellite altimetry *[Obligis et al., 2011]*. With an

absolute value less than 50 cm, it is highly variable both in space and time. Due to this high variability, the most accurate way to model this effect is through the measurements of microwave radiometers (MWR) on board the altimetric missions. However, as mentioned before, CryoSat-2 does not carry an on-board radiometer and presently relies on model corrections such as provided by ECMWF, which however are less accurate than direct measurements and lack spatial detail. Therefore, alternative methods are needed to get the highest possible accuracy for CryoSat-2, i.e., better than ECMWF. We will adopt a methodology based on the approaches described by Fernandes et al. (2010) and Stum et al. (2011). The basis of this approach is the data combination (DComb) through objective analysis of all existing path delay data sources, from MWR on board remote sensing satellites, Global Navigation Satellite Systems (GNSS) and the ECMWF model.

Also the specific problems of the retrieval of the wet tropospheric corrections in the polar regions are investigated. In these regions the water vapour content of the atmosphere is small and the corresponding path delay usually does not exceed a few centimetres (both in terms of mean and standard deviation). However, the path delay retrieval from passive microwave radiometers is hampered by the ice contamination on the radiometer measurements. Since it is anticipated that this will be the major problem to be addressed in these regions, techniques for efficient detection of ice contamination in radiometer measurements need to be investigated. Furthermore, altimeter wave forms in polar regions are difficult to re-track with existing re-trackers (UCL and SAMOSA) and therefore special re-trackers have to be developed and investigated to handle sea ice contaminated regions, for the purpose of isolating sea ice returns from reflections from open leads within the sea ice. An undesirable discontinuity in the SLA transitions going from LRM mode to SAR mode has also been noticed, and this has to be addressed properly.

Coastal regions also play a significant role in exploiting CryoSat-2 data, because here the altimeter operates in the high resolution SAR mode. Fernandes et al. (2010), Brown (2010), Desportes et al. (2007), and Obligis et al. (2010, 2011) already addressed precise computation of the wet tropospheric correction in coastal regions. However, since they rely on on-board MWR measurements, these methods cannot be applied to CryoSat-2 directly. However, we propose adaption of Fernandes et al. (2010), by replacing the measurements from the on-board MWR by data acquired by radiometers flying on other remote sensing satellites and making use of the GNSS- derived path delays from coastal and inland GNSS stations. For this we need techniques that efficiently detect land contamination in the MWR measurements.

CP4O	Preliminary Analysis Report	D2.1	

2.4 WP2000 organization and work breakdown

Considering the objectives of Work Package 2000 (Task 2) we identify the need of reviewing all existing CryoSat-2 products and availability, reviewing all suitable models for re-tracking and data integration approaches, surveying auxiliary data sources to help the development and validation of the CryoSat+ ocean products, surveying upcoming activities that could support CryoSat-2, and finally choosing the best suitable test areas for validation purposes.

In more detail, we have 5 activities (subtasks) within WP2000 of which Figure 2.1 gives the structure. In the next subsections we will subsequently discuss these sub-work packages.

CP4O	Preliminary Analysis Report	**D2.1**	
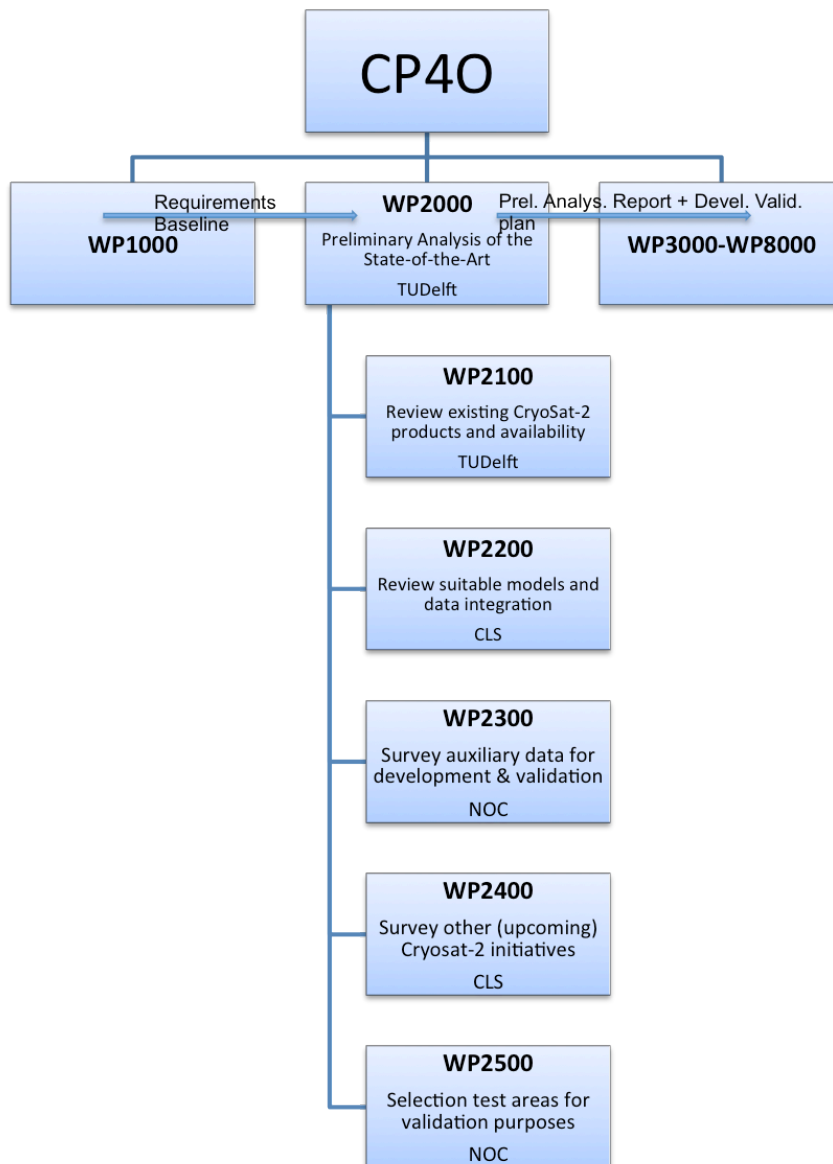
Figure 2.1 Work breakdown for WP2000

2.4.1 WP2100 – Review existing CryoSat-2 products and availability

1. Review CryoSat-2 LRM products over the ocean, among which L1B, L2, FDM, RADS, CNES RDSAR and LRM CPP products (TUDelft)
2. Review CryoSat-2 SAR products over water: L1B and L2 (NOC)
3. Review CryoSat-2 SAR products at high latitude and over sea ice: L1B and L2 (DTU)
4. Review CryoSat-2 altimeter corrections over open, coastal and polar ocean, including orbits, ionosphere, wet troposphere, tides, SSB and DAC (Uporto, Noveltis, TUDelft).

2.4.2 WP2200 – Review suitable models and data integration

1. Review SAR re-tracking open ocean, coastal ocean and sea-floor mapping: e.g. SAMOSA2 and SAMOSA3 re-tracking algorithms, numerical SAR waveform models (NOC, DTU)
2. Review SAR re-tracking over open ocean (CLS)
3. Review SAR re-tracking over sea ice: e.g. threshold, leading edge, double ramp, beta and OCOG re-trackers for polar regions (DTU)
4. Review RDSAR methodologies: SAR FBR processing to pseudo- LRM (Starlab, CLS)
5. Review improved/dedicated corrections for
    a. LRM over open ocean: e.g. SSB (TUDelft)
    b. SAR over coastal ocean: e.g. GNSS-derived wet trop (U. Porto, CLS), regional tidal models, ionosphere correction models and DAC corrections (Noveltis, CLS)
    c. SAR over polar ocean: better ionosphere (Noveltis) and tides (DTU)
6. Review sigma0 retrieval in LRM and SAR mode: identification of needed algorithms and auxiliary data sources (NOC, TUDelft)
7. Review data integration methods: optimized methods to integrate data from multiple satellite altimeters targeted to develop higher resolution products (DTU, TUDelft).

2.4.3 WP2300 – Survey auxiliary data for product development and validation

1. Survey of satellite altimeters over the oceans through RADS (TUDelft)
2. Survey of satellite data over polar regions: like SAR, ICESAT and Envisat (DTU)
3. Survey of airborne data, particularly CRYOVEX (DTU)
4. Survey of *in situ* data: tide gauges, wave measurements, including wave period and direction, datasets available through Globwave (NOC, SatOC, Noveltis).

2.4.4 WP2400 – Survey other (upcoming) CryoSat-2 initiatives

1. Survey of RADS (NOAA/Altimetrics/TUDelft)
2. Survey of eSurge (NOC)
3. Survey of REAPER (CLS, isardSAT, Altimetrics and TUDelft)
4. Survey of SAMOSA (SatOC)
5. Survey of COASTALT (NOC)
6. Survey of PISTACH (CLS)
7. Survey of LOTUS (DTU)
8. Survey of CNES CPP SAR re-tracking for Sentinel-3: CryoSat-2 experiments (CLS)
9. Survey other initiatives like CCI sea level ECV

CP4O	Preliminary Analysis Report	D2.1	

2.4.5 *WP2500 – Selection test areas for validation activities*

1. Selection of open ocean LRM areas for global comparison with other altimeters (TUDelft)
2. Selection of open ocean SAR areas: sites with in situ data, especially directional wave buoy data, if possible collocated with tide gauges (Starlab, NOC, CLS, SatOC)
3. Selection of open ocean SAR areas for sea-floor mapping: sites with high-resolution marine gravity information (DTU)
4. Selection of coastal ocean SAR areas: sites with wet tropo, iono and regional tidal corrections and *in situ* data, especially directional wave buoy data, preferably collocated with tide gauges *e.g.* English Channel, Gulf of Lion, Gulf of Cadiz, German Bight, and North Western Mediterranean Sea (Tuscany/Corsica) (NOC, Noveltis, SatOC)
5. Selection of coastal ocean SARIn areas (isardSAT)
6. Selection of polar ocean SAR areas: SSH validation data in the Arctic region, tide gauges and mean sea surfaces

3 WP2000 - The results

3.1 WP2100 - Review Existing CryoSat Products and Availability

3.1.1 *Review CryoSat-2 LRM products over water (TU Delft)*

3.1.1.1 Standard ESA products (L1B, L2, and FDM)

For a detailed overview of the standing issues with the ESA products we refer to the reports published in frame of the CryoSat-2 quality work group (QWG). The current ESA processor is producing so-called "baseline-B" product also referred to as IPF2LRM/2.4. In TUDelft's latest analysis of this Baseline-B product we provided the QWG with the following conclusions with regard to LMR L2 (RADS product is re-tracked L1b product, and ESA improved is ESA standard product augmented with improved corrections among which a new sea state bias – see also next Section on improved products):

- Timing bias in ESA product is −4.7ms (ESA recommended correction) plus −4.2 from own analyses, totalling −8.9ms
- Range bias ESA product is estimated at −23.4cm w.r.t. TOPEX frame
- ESA product SLA crossover rms 12.7cm high when compared to improved product 6.1cm and RADS product 6.5cm: this difference is also clearly visible in dual crossovers with Jason-2
- High crossover rms is greatly reduced in the improved product by introducing improved corrections for
  - *Sea state bias*: ESA product suffers from erroneous σ_0 (7 dB bias) and by that erroneous wind speed. Corrected product takes SSB from retracked level1b (similar as RADS product)
  - *Ionosphere*: ESA and RADS both implemented a GIM solution for the products but they do differ: maybe differences in the used maps: near real-time vs. interim vs. final or a difference in cut-off altitude? This is still under investigation.
- SWH is on par with RADS product, and also on par with Jason-1 and -2
- Histograms of sigma0 hint to find a solution to the sigma0 problem in the direction of taking into account the mispointing of the platform

The fast delivery marine product (FDM) originates from a different processor and by that also has a different re-tracking. Also the format differs and in contrast of the delayed LRM L2 product it does already contain the 1 Hz measurements, so there is less problem with concatenating the orbit and putting the corrections at the right place. Analyses show that applying the recommended ESA value for the

timing bias of −4.7 ms is enough for almost eliminating all of the timing bias. Also SWH and SSB fit better the RADS (retracked) product, which produces the lowest crossover rms. Though again the sigma0 shows a bias, for FDM this mounts to 2dB leading to an erroneous wind product and remaining problem with standard SSB but to a lesser extent than the original LRM product.

It is on basis of these analyses and the other findings and standing issues in the QWG that we are not further considering the level2 ESA products (both LRM and FDM), but work on own developments regarding re-tracking the Level1b products (both LRM and FDM), which seems to have the least problems. We are very pleased with the FDM product as it provides a means to produce an NRT product, much needed after the demise of Envisat in April 2012.

3.1.1.2 Improved LRM products (RADS and CPP)

Both CNES/CLS and NOAA/Altimetrics/TUDelft came to solutions to further improve the LRM product, based on the ESA L2 product (in RADS: ESA improved) and also based on the ESA L1b product (RADS product and CPP product). The CryoSat Processing Prototype was setup as a test-bed for SAR measurements coming from the upcoming Sentinel-3 mission. Though it's main purpose is the SAR processing it also provides the LRM-like reduced SAR processing and LRM processing to be able to guarantee smooth transitions between the different altimeter modes. All these CPP products start from either FBR data or Level 1b data and are re-tracked in a way similar as being done at NOAA for RADS. More information on reduced SAR can be found in Sections 3.2.2.3 and 3.2.2.4. Also more on CPP can be found in **[Boy et al., 2011].**

Due to the problems mentioned in the previous Section on the ESA products, for RADS two different approaches for improvements were investigated:

- Re-tracking the return waveforms available in the ESA L1b product, and by that computing new wave height, backscatter, and range. At the same time also determining new SSB: this is called the RADS product
- Keep the re-tracking parameters of the original product but replace a number of corrections among which the new determined SSB: this is referred to as the improved ESA product

The following steps are needed to get the original ESA data in RADS:

"Original" LRM Level 2 data

- Get delay-time LRM L2 data (Baseline B) from ESA
- Merge data files (few to tens of minutes normally) into passes and subcycles of 29 days (à la GDR) in RADS
- Contains only SSH at 20-Hz (not range or orbit)

- All corrections and orbit given at the beginning of each 1-Hz period (should be middle)
- A lot of effort to get orbit and range at the middle of the 1-Hz
- Add –4.699112 ms [Dinardo, priv. comm.] plus an additional –4.2 ms to time tags; correct orbit accordingly
- All the rest untouched

"Original" FDM Level 2 data

- Get fast-delivery FDM L2 data (Baseline B) from ESA
- Merge data files (as above)
- Already contains 1-Hz measurements
- Add –4.699112 ms to time tags; correct orbit accordingly

What steps are needed to get the re-tracked RADS product:

- Daily download FDM and LRM L1b data from ESA
- Retrack waveforms to compute own wave height, backscatter, and range using a MLE3-type retracker
- Takes approximately 1 minute per day of data
- Merge data files (few to tens of minutes normally) into passes and subcycles of 29 days (à la GDR) in RADS
- Use additional geophysical corrections from L1B
- Overwrite and add common RADS geophysical corrections
    o SSB (that we determined ourselves)
    o Latest MSS models (DTU10, CNES-CLS11), geoid
    o Tides (FES2004, GOT4.8, GOT4.9)
    o ECMWF and NCEP meteo, GPS and NIC09 iono, MOG2D IB
    o Off-line orbits from Delft, ESOC, and CNES
- Compute wind speed from backscatter (Abdalla)
- Compute sea level anomalies from orbit - range – corrections

What steps are needed to get the improved ESA product in RADS. We start with the "Original" FDM and LRM Level 2 data (see previous), and then

- Overwrite and add common RADS geophysical corrections
- SSB (that we determined ourselves from retracked L1B data)
- Latest MSS models (DTU10, CNES-CLS11), geoid
- Tides (FES2004, GOT4.8, GOT4.9)
- ECMWF and NCEP meteo, GPS and NIC09 iono, MOG2D IB
- Off-line orbits from Delft, ESOC, CNES
- Compute wind speed from backscatter (Abdalla)
- Compute sea level anomalies from (orbit – range – corrections)

CP4O	Preliminary Analysis Report	D2.1	

Now having all these different products available in RADS we can start to compare and the most easiest but also fairest comparison is computing crossover residuals, both single crossovers and dual crossovers with for instance Jason-2. Table gives an overview of crossover values for the 2013 data (January up to and including April).

Table 3-1 Crossover statistics for original, improved and RADS L2 (LRM) product. Dual crossovers are between CryoSat-2 and Jason-2. Maximum interval of crossover is half a subcycle=14.5 days.

	Original	Improved	Retracked
Residual timing bias	-0.08 ms	+0.17 ms	-0.50 ms
Single XO rms	12.7 cm	6.1 cm	6.5 cm
Dual XO rms	7.7 cm	5.6 cm	4.7 cm

Clearly the RADS product is superior and proposed as one of the candidate products in the CP4O project. In the detailed validation it will be cross-compared with the CPP products from CNES.
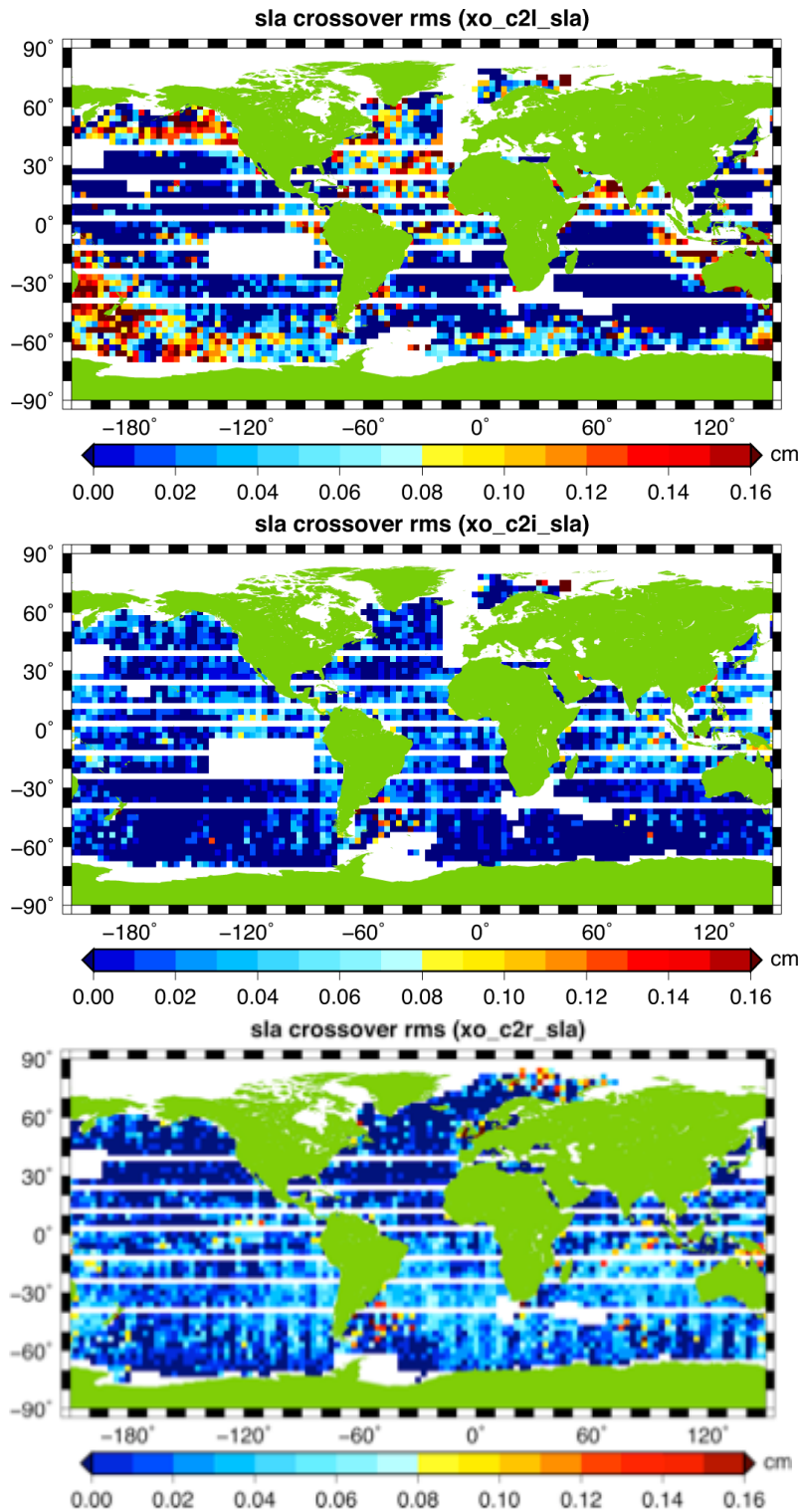
Figure 3.1 Crossover difference residual rms for 2013 data for the original ESA product (top), the improved product (middle), and the RADS product (bottom). The RADS product has the lowest rms.

CP4O	Preliminary Analysis Report	D2.1	

3.1.2 *Review CryoSat-2 SAR products over water: FBR and L1B*

This analysis focuses on the CryoSat-2 SAR FBR and L1B products distributed operationally to users by ESA. These operational products are generated by the ESA Instrument processing Facility (IPF) and are sometimes referred to as the "Kiruna" products.

In contrast to the original CP4O proposal, the analysis does not include an assessment of the quality of ESA CryoSat-2 SAR L2 products. CryoSat-2 L2 SAR products are not presently suitable for scientific exploitation over water surfaces as required by CP4O. Hence, the assessment of SAR L2 products has been replaced by an analysis of SAR FBR products (also sometimes called L1A).

CryoSat-2 SAR L1B products are currently available for two versions:

Baseline A	July 2010 – December 2012
Baseline B	February 2012 – onwards

The main difference between Baseline A and Baseline B is the use of finer gate spacing in Baseline B (half that used in Baseline A). Given that the number of gates is unchanged (128), this finer gate spacing results in a truncation of the trailing edge of the waveform.

The change to Baseline B was motivated primarily by the need to improve the performance of CryoSat-2 over sea ice.

Another reprocessing (Baseline C) is expected in late 2013/early 2014, featuring the finer gate resolution and non-truncated waveforms (hence, 256 gates in SAR mode).

Input to this task comes from anomalies reported through the CryoSat Quality Working Group (QWG) and from analyses of FBR and L1B SAR products in the SAMOSA and CP4O projects. In the next section, we simply list the anomalies relevant to CryoSat-2 SAR FBR and L1B products as reported by the QWG. Anomalies are listed below using the Anomaly Reference number used in [**CryoSat QDS, 2013**].

Finally, Table 3-2 in Section 3.1.2.2 provides an overview of the issues with an *a priori* assessment of the impact of these anomalies on the CP4O project.

3.1.2.1 <u>Reported anomalies relevant to CryoSat-2 SAR FBR and L1B products</u>

CRYO-IDE-1 & CRYO-IDE-42: Timing Error in L1B SAR data – Impact Low

The "SAR Mode Retracked Range" shows the difference to the altitude minus range, which results from the retracking correction. However, a timing error in the L1B products has been identified which is causing a 'ticking' problem. An investigation has shown that the problem appears to be solved when the L1B waveforms are doubly sampled. It appears then necessary to change the L1 processor in order to get double sampled waveforms in SAR and SIN modes.

This anomaly was closed with the release of the new IPF in February 2012. Hence, it only applies to CryoSat-2 SAR L1B Baseline A products.

CRYO-IDE-8: Bent Model for Ionospheric Correction not provided for latitudes greater than 82 degrees – Impact Medium (Polar Theme)

The Bent Model for the Ionospheric Correction is not being provided for latitudes greater than 82 degrees (north and south) in both Level 1 and Level 2 data products for each mode. The correction should be provided as input to the IPF1 post-processor. The Dip map file used was originally generated for use with Envisat and a modification for use with CryoSat latitudes is not yet available.

A solution to this problem is not foreseen yet.

The issue remains open.

CRYO-IDE-20: Incorrect conversion of the tracking parameter – Impact Low

A 2-meter jitter occasionally appears in the FBR waveforms, due to an incorrect conversion of the tracking parameter H0. This can be seen as weak power, above the surface, in the L1B waveforms. The H0 conversion for SIN and LRM is correct, while the occasional jitter of 1 LAI unit (~2 meters) is introduced by the SAR Pre-Processor algorithm.

This anomaly was closed with the release of the new IPF1 in February 2012. Hence, it only applies to CryoSat-2 SAR L1B Baseline A products.

CRYO-IDE-26: No power in L1B SAR average 1Hz waveforms – Impact Low

Zero power has been noted in the average 1Hz echoes.

This anomaly was closed with the release of the new IPF1 in February 2012. Hence, it only applies to CryoSat-2 SAR L1B Baseline A products.

CRYO-IDE-27: L1B SAR & SIN beam behaviour stack amplitude set to zero – Impact Low

The beam behaviour parameter 'stack amplitude' in Level 1B SAR and SIN products is set to zero. This parameter is used in the Level 2 SAR discrimination algorithm and should actually contain non-zero values.

This anomaly was closed with the release of the new IPF1 in February 2012. Hence, it only applies to CryoSat-2 SAR L1B Baseline A products.

CRYO-IDE-39: Incorrect CAL1 gain variation – Impact Low

The CAL1 'gain variation' compensates for small instrument power changes. It has been observed however, that the wrong power corrections are being applied to the science data products. This is most evident for LRM mode, where an incorrect gain variation of 40dB is applied. These CAL1 gain parameters are incorrectly set in the IPFDB. New corrected values have been identified and successfully tested.

This anomaly was closed with the release of the new IPF1 in February 2012. Hence, it only applies to CryoSat-2 SAR L1B Baseline A products.

CRYO-IDE-40: CAL1 path delay resolution – Impact Low

The CAL1 impulse response currently has the following resolution in current L1B products: 0.468 m (1 range bin) / 64 (zero padding) = 7.32 mm This is ~50 ps 2-way and is not considered to be enough. The path delay resolution can be improved in order to increase the path delay resolution by a factor of 128 for LRM and SAR modes and 512 for SIN mode.

This anomaly was closed with the release of the new IPF1 in February 2012. Hence, it only applies to CryoSat-2 SAR L1B Baseline A products.

CRYO-IDE-45: Missing SAR/SIN data in Arctic Ocean – Impact Low (Polar Theme)

Before the latest IPF upgrade in January 2011, it was noted that a large amount of L2 SAR mode data was missing in a strip centred approximately on the 80-degree east meridian. The missing strip is also present in the L1B data. This issue is no longer present since the end of January 2011 when the IPFs were updated, however it is required to determine what the original problem was just in case this reoccurs. It should be noted that the data is only missing at L1b and L2 and the corresponding data at L0 is not missing, therefore it seems this is an issue which was related to IPF1, and perhaps fixed 'unknowingly' in the IPF1 update provided in January 2011.

This anomaly, although not present anymore, will be tracked and monitored to ensure it is not present in the data, which is reprocessed as part of the CryoSat Reprocessing Campaign.

CRYO-IDE-54: CAL1 products not applied to science data – Impact Low

An error in the new Calibration strategy, which was implemented on the 28th February 2011, is causing the CAL1 L1b products to no longer be used for calibrating science data, but values are taken from IPFDB instead.

This anomaly was closed with the release of the new IPF1 in February 2012. Hence, it only applies to CryoSat-2 SAR L1B Baseline A products.

CRYO-IDE-55: Incorrect values for 'cycle number' in all SIRAL product header files – Impact Low

The cycle number provided in the CryoSat header files is incorrect as this number currently corresponds to approximately a cycle length of 197 days (~2853 orbits) and the correct cycle number should correspond to a cycle length of 369 days and 5344 orbits.

This anomaly was closed with the release of the new IPF in February 2012. Hence, it only applies to CryoSat-2 SAR L1B Baseline A products.

CRYO-IDE-68: Failure of EECFI interpolation with DOR_NAV – Impact Low

There is a problem with the IPF1 handing of the L0 DORIS Navigator file and also in using the EECFI. Usage of the DORIS Navigator with EECFI interpolation is currently presenting an error due to the CFI initialization. The error is relatively small (within ±2 meters), proportional to the altitude rate. Following an analysis, this error has been found to be dependent on the delta-UTC1 (difference between UTC and UTC1). The delta-UTC1 is always zero in the DOR_NAV products, but is always non-zero in the DORIS Precise and Preliminary products.

This anomaly was closed with the release of the new IPF1 in February 2012. Hence, it only applies to CryoSat-2 SAR L1B Baseline A products.

CRYO-IDE-69: Wrong use of CFI interpolation with DOR_NAV – Impact Low

There was a problem concerning the EECFI reading of the DORIS Navigator product itself, whereby a data gap was reported by EECFI, even though the gap did not actually exist within the DORIS Navigator.

This anomaly was closed in September 2012 as it did not occur anymore with the release of the new IPF1 in February 2012. Hence, it should only apply to CryoSat-2 SAR L1B Baseline A products.

CRYO-IDE-70: AGC1 and AGC2 power levels incorrect between receive chain1 and receive chain2 (L1 SAR&SIN) – Impact Low

An analysis of the stack data has shown a large discrepancy between the power levels of echoes from the two receiver chains (RX1 and RX2). The total AGC being applied to echoes is incorrect for both SAR and SIN modes. Presently, the value of corrected AGC for receiver chain1 (antenna A) is AGC1 which is extracted from chain1 calibration and the value for receiver chain2 (antenna B) is AGC2 which is also extracted from chain1. The proper handling for chain1 should be AGC1 +AGC2 from chain 1 and the handling for chain 2 should be AGC1+ AGC2 from chain 2. As a result of this, in areas where the AGC is varying significantly over sea ice and land ice margins, the power is incorrect. Over ocean,

the AGC values are quite stable and hence the problem has not been previously seen.

This anomaly was closed with the release of the new IPF1 in February 2012. Hence, it only applies to CryoSat-2 SAR L1B Baseline A products.

CRYO-IDE-74: Disagreement between L1b product specification format doc and L1b code for waveform Flags – Impact Low

The L1b product specification documentation 'CRYOSAT Ground Segment Instrument Processing Facility L1b Products Specification Format' is due to be updated regarding the 1Hz and 20Hz, SAR and SIN waveform flags.

This anomaly was closed with the release of the new IPF1 documentation in February 2012.

CRYO-IDE-75: Pitch sign mismatch and attitude biases – Impact High

Upon comparison of the angles deduced form the L1B SIN data with that from the star tracked files obtained from ESOC, there seems to be a bias in the pitch and roll angles (both<0.1 degrees). Also the sign of the pitch angle seems to be wrong.

This problem is currently under investigation, and should be refined when the datation biases are fixed.

The issue remains open.

CRYO-IDE-78: Erroneous phase difference calibration application in IPF1 – Impact Low

There is currently an issue with the handling of CAL-4 calibration, which appears to be introducing an error that has the effect of replacing the phase difference calibration with a random phase difference that is adding 23 microradians RMS of phase difference noise into the data. This is not a major problem over ocean areas where both the AGC and phase difference calibration are reasonably stable, however over ice sheet margins the issue is more significant.

This anomaly was closed with the release of the new IPF1 in February 2012. Hence, it only applies to CryoSat-2 SAR L1B Baseline A products.

CRYO-IDE-85: Wrong SAR window delay computation – Impact Medium

Rare occurrences are expected in the tracker height computation due to shifted bits in IPF1. The DPM corresponding equation performs the steps of bit shifting, division, and truncation in the wrong order. The code correction is available and will be implemented in the next IPF1 version.

The issue remains open.

CRYO-IDE-111: UT1 field in products header to be filled – Impact Medium?

The value of Delta_UT1, provided in field #8 within the CryoSat Main Product Header, is currently always filled with zero.

This problem has been fixed with the new IPF1 Vk2.0 and IPF2 Vk1.0 updates, for the FDM chain only. It will therefore be fixed for all modes with the release of Baseline C, scheduled for the end of 2013.

The issue remains open.

CRYO-IDE-112: Gain Ingestion from AutoCal products – Impact High

There is currently an error, which has been detected in the SIN Specialised Processor, which is causing the failure of the ingestion of the gain values from the AutoCal products. The fix to this anomaly is known and will be implemented with the next IPF1 update.

The issue remains open.

CRYO-IDE-116: Wrong selection rule for auxiliary USO drift file – Impact Medium

The current selection rule doesn't allow the most recent DORIS USO drift auxiliary file to be selected, but a file is still selected nonetheless and a value is always provided in L1B products. It is therefore not clear if the DORIS USO correction factor provided in the products is correct.

The issue is under investigation.

The issue remains open.

CRYO-IDE-141: Wrong code for bursts in IPF1 SAR 1 Hz – Impact Medium

Currently, the time entry for the burst centre for L1B SAR and SIN 1Hz waveforms is incorrect. For SAR only, the number of bursts shown is also incorrect.

The corrections are ready for implementation.

The issue remains open.

CRYO-IDE-142: Blurring of IPF1 SAR&SIN 1Hz waveforms with high orbit height rate – Impact High

It has been reported that there is a blurring effect visible on SAR and SIN 1Hz waveforms when the orbit altitude rate is high. The blurring is thought to be due to two causes: the misalignment of burst echoes that make up the waveform, and a shift effect on echoes within a single burst when there is a high altitude rate.

The waveforms are aligned with respect to the minimum LAI, and this assumes the altitude of the satellite is constant. Therefore to address the first cause, a better alignment of bursts that uses both LAI and altitude information will be implemented. This new processing step has already been prototyped. In the case of high altitude rates, echoes can present blur when averaged. A suggested solution is to shift all of the echoes within each burst to correct for this effect.

The solution is ready to be implemented with the release of Baseline C, which is scheduled for the end of 2013.

CP4O	Preliminary Analysis Report	D2.1	

The issue remains open.

CRYO-IDE-143: Wrong sign of CAL1 correction – Impact High

It has been discovered that in recent months that sigma-0 values have been declining by ~0.1 dB per month. The power level transmitted by CryoSat has also been declining by a few 100ths of a dB per month. Nominally the CAL mode detects this and provides a correction to the sigma-0, however it appears that this correction is being applied with the wrong sign, hence the apparent drop. This problem may impact users as it can affect wind speed and sea state bias correction values.

This problem has been fixed with the new IPF1 Vk2.0 and IPF2 Vk1.0 updates, for the FDM chain only. It will be fixed for other modes with the release of Baseline C, scheduled for the end of 2013.

The issue remains open.

CRYO-IDE-151: SAR/SIN power calibration error in IPF1 SP – Impact High

In the current L1B SAR and SIN products the gain correction does not include the CAL1 component that takes into account the instrument ageing (power decrease of about 0.3dB per year).

The solution is ready to be implemented with the release of Baseline C which is scheduled for the end of 2013.

The issue remains open.

CRYO-IDE-155: Intra-burst alignment for IPF1 SAR&SIN 20-Hz waveforms – Impact High

Similar to the 1 Hz waveforms in CRYO-IDE-142, the 20Hz SAR&SIN 64 waveforms in the burst are not aligned with respect to the satellite altitude change rate. A fine alignment is required for the 64 waveforms in each burst. Again, this should be performed with a fine shift to each of the waveforms before the azimuth FFT.

The solution is ready to be implemented with the release of Baseline C which is scheduled for the end of 2013. The issue remains open.

CRYO-IDE-161: Bad DAC over ocean – Impact High

Some orbits have bad DAC values (default) in the L2 products. The DAC is not extracted at L2, it is extracted at L1, so a bad flag at L2 indicates that the data is already flagged as bad in L1B.

The problem is under investigation.

The issue remains open.

CRYO-IDE-162: UTC-UT1 in microseconds instead of milliseconds – Impact High

Both in the XML (field#11) and in the DBL MPH (field#18), the field Delta_UT1 for UTC-UT1 should be provided in microseconds instead of milliseconds.

This problem has been fixed with the new IPF1 Vk2.0 and IPF2 Vk1.0 updates, for the FDM chain only. It will therefore be fixed for all modes with the release of Baseline C, scheduled for the end of 2013.

The issue remains open.

CRYO-IDE-167: Datation bias in SAR and SIN modes – Impact High

A few sources of datation bias (total amount of about 0.5 ms) have been identified in the new IPF1 Vk2.0 release for SAR and SIN modes:

- The sign of the datation event offset parameter is wrong
- PIND_SAR_INDEX / PIND_SIN_INDEX vales in the PCONF
- DORIS datation is referenced to the Centre of Mass, when it should be referenced to the Antenna Centre

The solution is ready for implementation.

The issue remains open.

CRYO-IDE-170: Integrated power in L1B product – Impact Low

The need of integrated power information in L1B products was agreed at the latest QWG meeting. The information about the integrated power of the Range Impulse Response can be computed in the CAL1 processors and then propagated up to level 1b, to be used by the level-2 processors in the future.

The solution will be implemented with the release of Baseline-C, which is scheduled for the end of 2013. The issue remains open.

CRYO-IDE-171: LRM one range gate shift – Impact Medium

The problem is one range gate shift in LRM, with respect to SAR. This is incorrect for LRM and creates a couple of problems regarding calibration and L2 retracking. A known correction will modify the LRM waveform the way it should be and align SAR and LRM L1B waveforms in terms of window-middle point.

This solution will be implemented with the release of Baseline-C, which is scheduled for the end of 2013.

The issue remains open.

CRYO-IDE-176: Range error due to CoM reference – Impact High

A source of range error has been identified in both IPF1 versions K1.0 & 2.0 for all modes.

Satellite location, based on DORIS, is given on the platform Centre of Mass (CoM). FBR/L1B waveforms are referenced (IPF1 K1.0 & 2.0) on the centre of the baseline of the interferometer. The waveform window delay is based on DORIS, while the waveforms are referenced on the centre of the baseline. A range

error thus occurs depending on the difference in z-axis between CoM and centre of interferometric baseline.

The problem is under investigation.

The issue remains open.

3.1.2.2 Summary of issues and relevance to the objectives of CP4O

Table 3-2 provides a summary of issues affecting CryoSat-2 SAR FBR and L1B products together with some assessment of the impact of the CP4O project's ability to deliver its objectives.

The impact on CP4O of issues affecting only CryoSat-2 SAR Baseline A products is deemed low, given that enough data is now available with Baseline B to allow necessary scientific exploitation.

CP4O	Preliminary Analysis Report	D2.1	

Table 3-2 Summary of reported anomalies relevant to CryoSat-2 SAR FBR and SAR products and impact on objectives of CP4O project

Anomaly Reference #	Description	Status	SAR products affected	Impact on CP4O
CRYO-IDE-1 & 42	Timing Error in L1B SAR data	Closed	L1B Baseline A	Low
CRYO-IDE-8	Bent Model Ionospheric Correction not provided for lat > 82 deg	Open	L1 & L2 Baseline A & B	Medium (Polar theme)
CRYO-IDE-20	Incorrect conversion of the tracking parameter	Closed	FBR & L1B Baseline A	Low
CRYO-IDE-26	No power in L1B SAR 1Hz waveforms	Closed	L1B Baseline A	Low
CRYO-IDE-27	L1B SAR & SIN beam behaviour stack amplitude set to zero	Closed	L1B Baseline A	Low
CRYO-IDE-39	Incorrect CAL1 gain variation	Closed	All levels Baseline A	Low
CRYO-IDE-40	CAL1 path delay resolution	Closed	All levels Baseline A	Low
CRYO-IDE-45	Missing SAR/SIN data in Arctic Ocean	Open	L1B before Jan 2011	Low (Polar theme)
CRYO-IDE-54	CAL1 products not applied to science data	Closed	L1B Baseline A	Low
CRYO-IDE-55	Incorrect values for 'cycle number' in all SIRAL product header files	Closed	All levels Baseline A	Low
CRYO-IDE-68	Failure of EECFI interpolation with DOR_NAV	Closed	All levels Baseline A	Low
CRYO-IDE-69	Wrong use of CFI interpolation with DOR_NAV	Closed	All levels Baseline A	Low
CRYO-IDE-70	AGC1 and AGC2 power levels incorrect between Rx chain1 and Rx chain2	Closed	All levels Baseline A	Low
CRYO-IDE-74	Disagreement between L1b product specification doc and L1b code	Closed	Documentation	Low
CRYO-IDE-75	Pitch sign mismatch and attitude biases	Open	All levels Baseline A & B	**High**

CRYO-IDE-78	Erroneous phase difference calibration application in IPF1	Closed	All levels Baseline A	Low
CRYO-IDE-85	Wrong SAR window delay computation (rare)	Open	All levels Baseline A & B	Medium
CRYO-IDE-111	UT1 field in products header to be filled	Open	All levels Baseline A & B	Medium ?
CRYO-IDE-112	Gain Ingestion from AutoCal products	Open	All levels Baseline A & B	**High**
CRYO-IDE-116	Wrong selection rule for auxiliary USO drift file	Open	All levels Baseline A & B	Medium
CRYO-IDE-141	Wrong code for bursts in IPF1 SAR 1 Hz	Open	L1B Baseline A & B	Medium
CRYO-IDE-142	Blurring of IPF1 SAR&SIN 1Hz waveforms with high orbit height rate	Open	L1B Baseline A & B	**High**
CRYO-IDE-143	Wrong sign of CAL1 correction	Open	All levels Baseline A & B	**High**
CRYO-IDE-151	SAR/SIN power calibration error	Open	L1B Baseline A & B	**High**
CRYO-IDE-155	Intraburst alignment for IPF1 SAR&SIN 20-Hz waveforms	Open	L1B Baseline A & B	**High**
CRYO-IDE-161	Bad DAC over ocean	Open	L1B Baseline A & B	**High**
CRYO-IDE-162	UTC-UT1 in microseconds instead of milliseconds	Open	All levels Baseline A & B	**High**
CRYO-IDE-167	Datation bias in SAR and SIN modes	Open	All levels Baseline A & B	**High**
CRYO-IDE-170	Integrated power in L1B product	Open	L1B Baseline A & B	Low
CRYO-IDE-171	LRM one range gate shift (wrt SAR)	Open	L1B Baseline A & B	Medium
CRYO-IDE-176	Range error due to CoM reference	Open	All levels Baseline A & B	**High**

CP4O	Preliminary Analysis Report	D2.1	

3.1.3   Review CryoSat-2 SAR Products at High Latitude and over Sea Ice

3.1.3.1   <u>L2</u>

To evaluate the SAR L2 product in the Arctic Ocean, all 2012 SAR data from the region was extracted and then compared with the UCL04 MSS, which is part of the L2 product. For the generation of a MSS the accuracy is of greater importance than the precision an therefore it was decided to calculate the mean difference of the height observations with respect to an existing MSS for each track and evaluate on the distribution of the mean track offset instead of looking at the individual observations in the tracks. The histogram of the mean track offset is shown in Figure 3.2 (left).

It is first observed that both the mode and the mean of the distribution is around −0.9 m to −1.0 m clearly indicating a problem with absolute height reference in either the L2 elevations, UCL04 or both. Secondly it is noticed that the distribution is skewed toward lower elevations indicating a bias between the L2 sea-ice lead retracker and the L2 ocean retracker.

To further investigate the height reference offset the L2 observations was compared with the DTU10 MSS, see Figure 3.2 (right). It should be noticed that DTU10 is referenced to the TOPEX ellipsoid where CryoSat-2 is referenced to the WGS84 ellipsoid, which result in a vertical offset of 70 cm at the poles. The DTU10 distribution is sharper and smoother than UCL04, thus DTU10 is a better mean representation of the SAR observation in the Arctic Ocean.
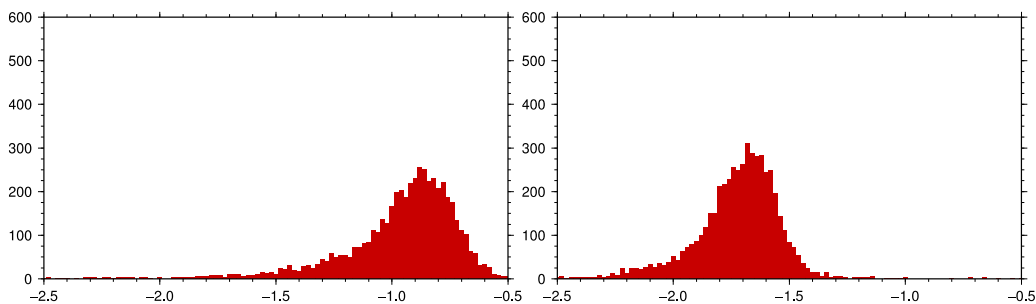
Figure 3.2 Histograms of mean offset per CS-2 track relative to UCL04 (left) and DTU10 (right). Note that DTU10 is using the TOPEX ellipsoid and is therefore offset by -70 cm.

Next the mean difference between L2 observations and DTU10 was calculated in a 50 km by 50 km grid to investigate possible spatial patterns in the difference between the L2 observations and the MSS models. From Figure 3.3 (left) is clearly seen that UCL04 and the L2 heights have several areas with differences exceeding 40 cm above 80º of latitude, again indicating that UCL04 doesn't give a useful representation of the Arctic Ocean as observed by CryoSat-2. The

comparison with DTU10 in Figure 3.3 (right) is good in the sea-ice covered part of the Arctic Ocean. In both the UCL04 and the DTU10 an offset of around 50 cm is found between the sea-ice covered area and the open ocean area above Iceland, Norway, Finland and, parts of Russia, where sea-ice debris must be expected.

Finally, in both the comparison with UCL04 and DTU10 a large upward offset going from the Russian coast at 165º longitude towards the polar gap is noticed. This is believed to be two or several orbits with either an orbit error or a SIRAL altimeter anomaly.
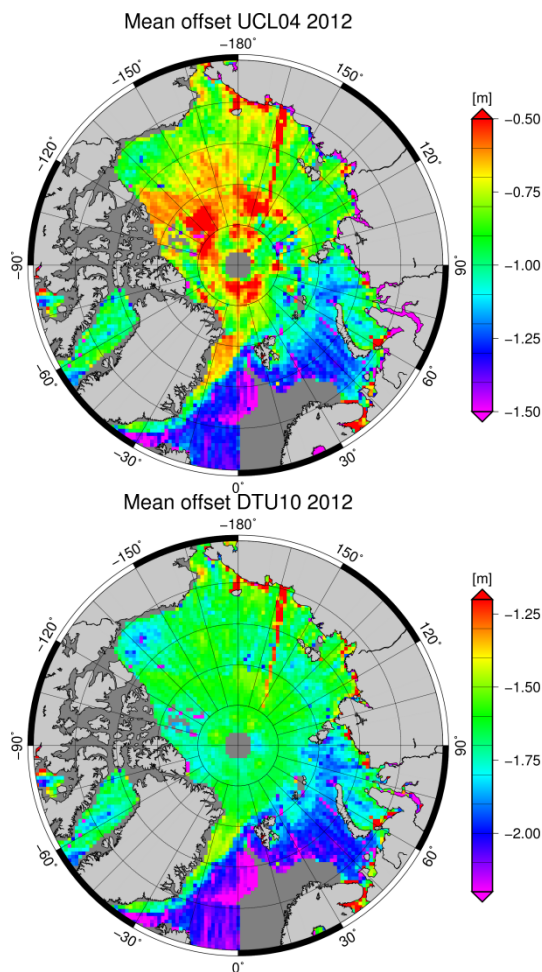
Figure 3.3 Difference between CryoSat-2 L2 observations and UCL04 (left) and DTU10, averaged over 50 km by 50 km square boxes. Note that the DTU10 color-coding is shifted 70 cm to make the colours comparable in the two figures.

3.1.3.2 L1b

Return echoes from leads in sea-ice covered regions are characterized by very high peakiness, in some cases the returns almost behave like a delta function. With only a few samples representing the return from the surface it is not possible to fit a complex model to the echo so a more simple approach must be taken when retracking the waveforms.

One of the major challenges is to recreate the magnitude of the peak and to aid this task the SAR processor has been updated with a range oversampling factor of two resulting in a doubling of the range cell resolution. Figure 3.4 shows an example of an echo from a sea-ice lead that has been processed with both the baseline A and the baseline B processor.

Using the same approach as for L2, the L1b data is investigated by applying various retrackers on the L1b waveforms and comparing the derived heights with DTU10. The retrackers are described in details in 3.2.1.7, except the DTU prototype threshold retracker, which is currently under development.
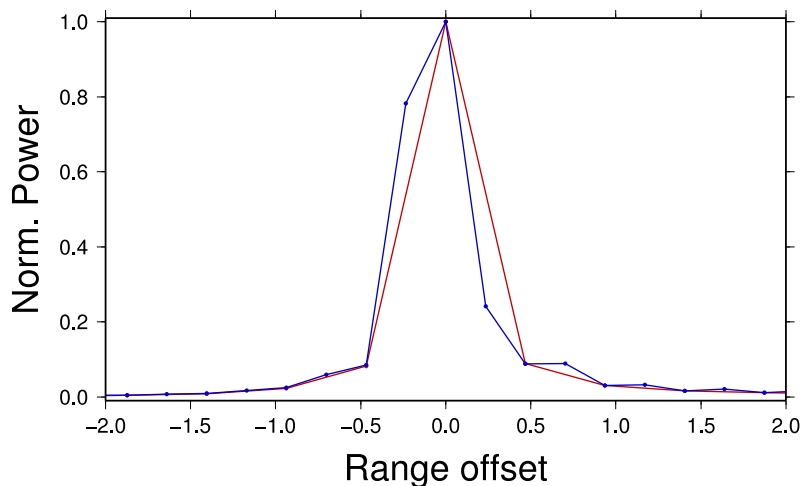
Figure 3.4 An echo from a lead in sea-ice processed with baseline A (red) and baseline B (blue).

Comparing the three retrackers in Figure 3.5 with the L2 retracker in Figure 3.2 (right) it is seen that significant improvement can be gained by choosing a new optimized retracker over the L2.

However, even with the increased range resolution and the improved DTU prototype retracker, the mean track offset (Figure 3.5 bottom) indicates that before a MSS can be derived from the SAR data work is needed before the absolute level can be established.
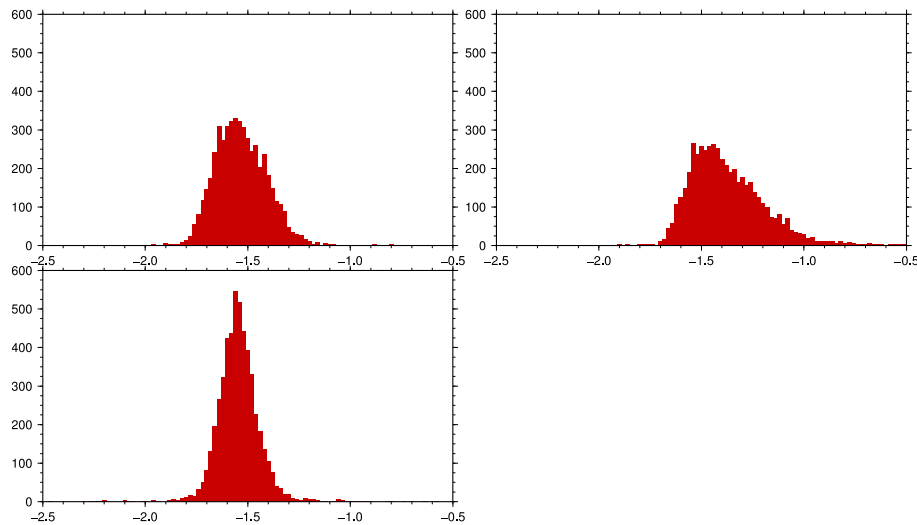
Figure 3.5 Distribution of mean track offset relative to DTU10 for three retrackers (from left: standard threshold retracker, leading edge threshold retracker, and the new DTU prototype threshold retracker (bottom)). Recall that the DTU10 is related to the TOPEX ellipsoid, which give rise to a -70 cm offset.

3.1.4   Review CryoSat-2 Altimeter Corrections

For the QWG DEOS (TUDelft) has been reviewing the altimeter corrections as found on the original L1b and L2 ESA LRM products. In Section 3.1.1 we already presented the details on the TUDelft analyses of the original data products and explained how we come to 2 different improved products, one only updating the corrections/models and one also using retracking. Recipes are given to put the original product in RADS, to put the improved product in RADS, and to put the retracked product in RADS. Having everything in RADS it is quite simple to do the (inter)comparisons. From this comparison we conclude that the dynamic atmosphere correction (MOG2D), the dry troposphere and wet troposphere corrections (ECMWF and NCEP meteo data) are the same for each of the products, meaning that original and RADS already use the latest correction models globally and that improvements only should be sought in local and regional areas, like the coastal zones. In summary for global products for open ocean altimetry we can suffice with the DAC and troposphere corrections, as they are available on the original product.

Concerning the different available orbits; in RADS the original CNES orbit is complemented with available offline products from DEOS, ESOC and CNES. As part of a calibration/validation contract DEOS has been calculating alternative orbits since the launch of CryoSat, basically to show that the orbit in the original product is good enough. Though it is academically interesting to look at differences between these orbit solutions the comparison merely shows the differences in data editing, software accuracy, and parameter estimation details, most of the used models is the same. In an overall comparison ESOC found rms differences between the different solutions in the order of 1.5cm. As this falls

within the absolute accuracy of the measurement we are not making a definitive choice now what orbit to choose; it will be part of the validation and verification of the CP4O end products.

Figure 3.6 shows a comparison between the DEOS solution and the CNES POE orbit in the three directions cross-track (top), radial (middle) and along-track (bottom). The dashed red line gives the mean of the daily standard deviation between the two solutions. In brackets both the mean average offset is given and the mean rms offset. In the along track direction the DEOS solution shows an unexplained difference of -1.10 cm to the POE orbits which could be interpreted as a bias of approximately 1.5 µs between the used time systems. The MOE orbits are a clear improvement over the DIODE navigator product and they are available within one or two days, the POE orbits have a latency of a month, the POE orbits show more than 10% improvement in the three-dimensional residuals compared to the MOE orbits.
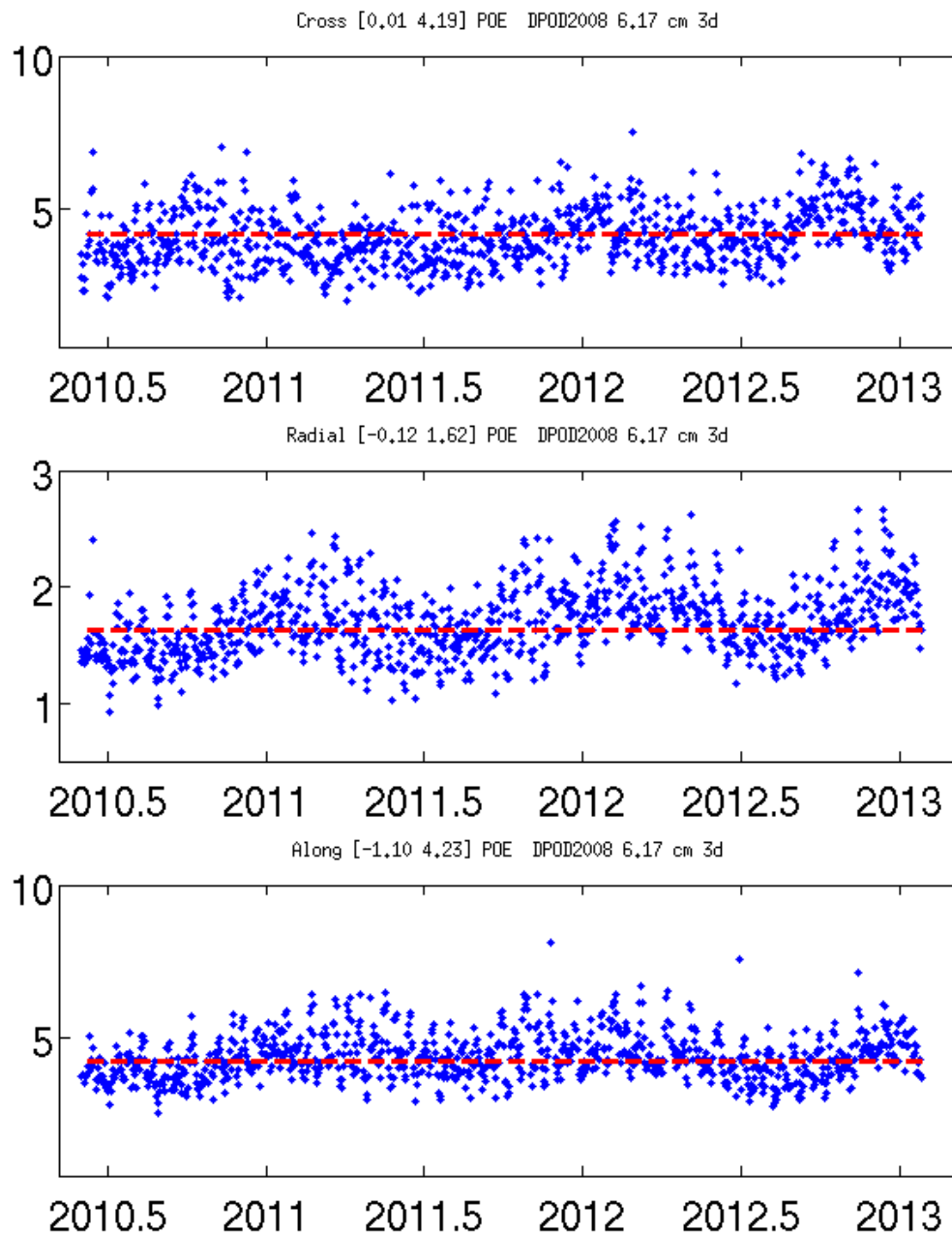
Figure 3.6 DEOS orbit comparison with CNES POE solution: daily mean standard deviations for the cross– (top), radial– (middle) and along track component (bottom). In brackets the average offset and the average standard deviation.

CP4O	Preliminary Analysis Report	D2.1	

The ionosphere correction is a different story. Both original ESA product and RADS improved products make use of the JPL Global Ionosphere Maps (GIM). This is undoubtedly the best solution globally (also see Section 3.2.4.3). However when we compare the RADS products with the original product we do see a remaining difference in ionosphere correction. Figure 3.7 provides an example of a typical ionosphere correction differences for baseline-B data from subcycle 37, pass 520 (February 2013). This pass, often used as reference track, is a long stretch of data not interrupted by land/islands along a track in the pacific hitting the American coast near the border of Alaska with Canada. The red curve represents the RADS implementation and the green curve the ESA implementation (the improved not-retracked product, blue curve, has the RADS implementation and is therefore completely hidden behind the red curve). The differences might hint to a scaling difference stemming from not taking the orbital height of CryoSat-2 correctly into account, or a difference in choice of maps: so either fast, interim or final ionosphere maps. This is currently under investigation by DEOS. It will be clear that these differences could lead to slightly higher crossover rms, though cannot entirely explain the high crossover rms in the original product (see also Section 3.1.1.2)
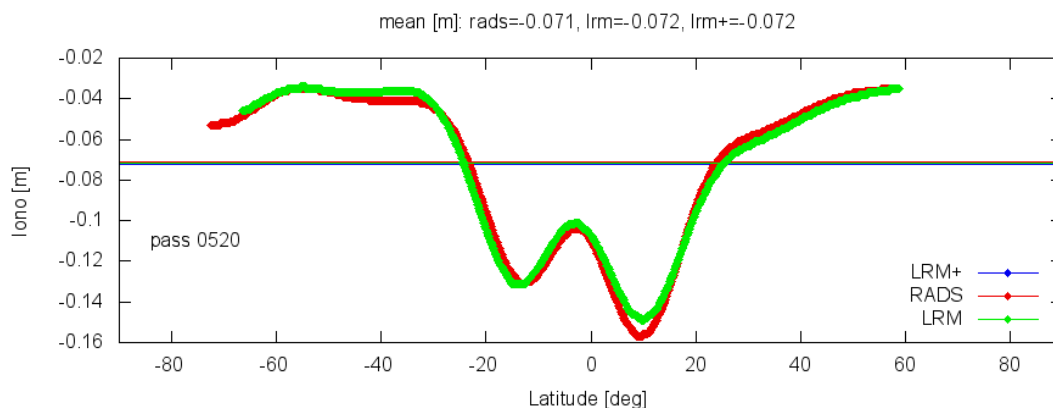
Figure 3.7 GIM ionosphere corrections for LRM track 520, February 2013: RADS implementation in red (and blue), and original product implementation in green.

For that we have to take a closer look at the sea state bias; this is one of the other corrections that have substantial differences when compared with the improved products in RADS. Now SSB is directly related to SWH and wind speed, which in turn is related to the sigma0. Sigma0 is dealt with in Section 3.2.1.6, from which we conclude that it has a bias of 7dB in the ESA product and some other problems and that the computed wind is therefore unusable. This means that we have to make our own tailored SSB correction. The SWH in the original product seems on par with the improved products so we are not concerned with (small) differences in SWH. Besides we take the SWH from the re-tracked product anyway.

The sea-state bias correction compensates for the bias of the altimeter range measurement toward the troughs of ocean waves. This bias originates from an electromagnetic (EM) bias, a skewness bias, and an instrument tracker bias. The EM bias is physically related to the distribution of the specular facets, the skewness bias comes from the altimeter median tracker, while mean is what we need, and the instrument tracker bias is related to the chosen tracker to deduce the SWH from the radar echo. In the simplest representation SSB is modelled by a simple percentage of SWH (usually 4%). However, the SSB also depends on the wind field and the type of waves. Therefore, a more advanced parametric model, also known as BM4, is proposed (**[Gaspar et al., 1994]**):

$$SSB = a0 + SWH \times (a1 + a2 \times SWH + a3 \times U + a4 \times U^2),$$

where U is the wind speed derived from the backscatter coefficient. This equation estimates the total combined SSB correction because all SSB components depend on SWH. The in RADS adopted method for estimating SSB follows the recipe known as hybrid method as presented in **[Scharroo and Lillibridge, 2004]**. This hybrid method combines the direct estimation of sea-state bias (SSB) from sea height residuals with the parametric fitting process and a successive smoothing of the remaining residuals. This hybrid method essentially produces a nonparametric SSB model in the form of a smooth grid in a 2- dimensional space determined by significant wave height and backscatter coefficient. The sensitivity to external geophysical corrections is small. The impact of trends in significant wave height and backscatter through the sea-sate bias on sea level change estimates is troubling though: it is important to investigate whether these trends are real, or merely a result of aging of the altimeter.

In a nutshell: in RADS for CryoSat we calculate the sea level anomalies (with no SSB applied), taking sigma0 and SWH from the retracked L1B product. Then we bin the anomalies in sigma0-SWH space, which means averaging them in 0.1dB by 0.25m sigma0/wave bins. The anomaly or height residual field then directly shows the true underlying SSB (direct estimate). The parametric field or BM4 model (5 parameters, including an overall bias to take care of SSB=0 when SWH=0) is fitted through the anomalies in a weighted least squares scheme (weight depending on bin rms and number of points). Then the direct estimate and the parametric field are blended to form the hybrid model. Removing the BM4 smooth fit from the direct estimate subsequently forms SSB residuals. Then the residuals are smoothed using a Gaussian smoother with a scale of 0.1 dB in backscatter and 0.25m in wave height. Again, the number of points and the rms in each bin is used as a weight. The final hybrid model is then formed by the sum of BM4 and the smoothed residuals. In the normal operation window (data rich regime) the differences between direct and hybrid model are small. Outside this window the SSB is hardly used. Figure 3.8 presents our RADS hybrid state bias model: the direct estimate in the top panel and the hybrid SSB model in the bottom panel. On average this amounts to 4% of SWH, which is in agreement with the expectations.
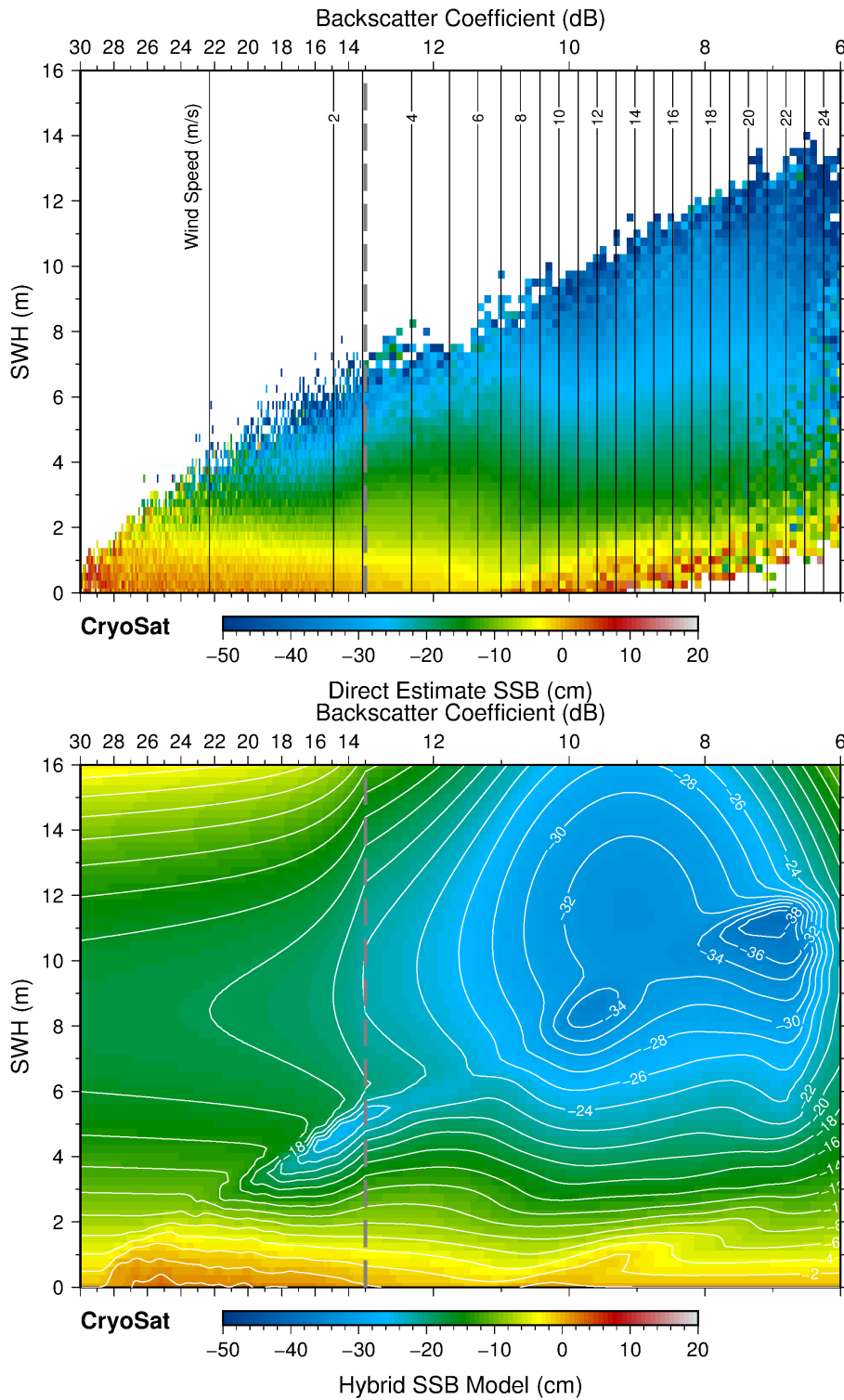
Figure 3.8 RADS hybrid sea state bias model based on sea level anomalies gridded in sigma0-SWH space, a BM4 model fitted and smoothed residuals blended in. Direct estimate in top panel and smoothed hybrid model in bottom panel.

Figure 3.9 shows an example of SSB differences when we compare the ESA original values (green curve) with the values for our improved product (blue curve) and the values for the RADS retracked product (red curve) for our reference track pass 520 (February, 2013). Clearly these differences can go up to 10cm and give rise to high crossover rms in the original product. The crossover analyses shown in Section 3.1.1.2 demonstrate the need for a tailored SSB model. The retracked RADS product incorporating the described tailor-made hybrid SSB model exhibits the lowest crossover rms, both internally (single crossovers) and externally (crossovers with Jason 1 and -2). Also for the improved product (not retracked) we used a custom made SSB model fit to these data; that's why the blue curve is slightly different from the red curve.
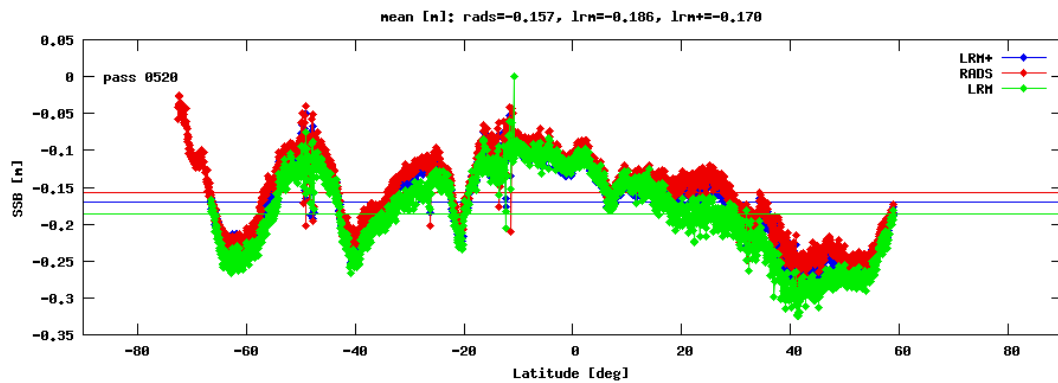
Figure 3.9 Sea state bias (SSB) corrections for LRM track 520, February 2013: RADS solution in red, the original product solution in green, and for the improved but not retracked product in blue.

3.2 WP2200 Review Suitable Models and Data Integration Methodologies

3.2.1 Review SAR Re-tracking

3.2.1.1 Review SAR retracking for open ocean and coastal zone & sea floor mapping

As for conventional altimetry, the mean power of the SAR waveforms over the ocean can be represented as the triple convolution of three terms: the response of the radar to a flat surface (P_{flat}), the point target response function (PTR) and the sea surface height probability density function (PDF_{sea}).

$$P_{f,t} \propto \sigma_0 \, G^2_{f,t} \, P_{flat\,f,t} * PTR_{f,t} * PDF_{sea} \qquad \text{Eq. 3-1}$$

where σ^0 is the backscatter coefficient and G is the antenna gain pattern.

SAR altimeters are characterized by a bi-dimensional PTR, which is the product of the range impulse response (RIR) and the azimuth impulse response (AIR). For SAR altimetry, the mean waveform is a two-dimensional function of time (delay) and distance along-track (Doppler frequency), which depends on ocean geophysical parameters of interest (range, significant wave height and backscatter coefficient from which one derives wind speed) and other parameters linked to geometry, satellite orbit parameters, platform attitude, etc…

To date, there exist several solutions to compute the mean SAR altimeter waveforms, which are reviewed briefly here.

3.2.1.2 Numerical SAR waveform models

Here, the triple convolution in Eq. 3.1 is computed numerically to provide an exact solution for the SAR waveform. This is the method adopted by TAS **[Phalippou & Enjolras, 2007], [Phalippou & Demeestere, 2011]** and by CNES **[Boy *et al.*, 2012].** The method offers an exact solution to the problem and makes it possible to account for complex forms of the various terms, for example the antenna gain pattern or the PTR, without the need for approximations.

In **[Phalippou & Enjolras, 2007],** both the RIR and the AIR are approximated by sinc[2] functions, while the antenna gain is simulated with a Bessel function associated with a circular aperture. The PDF of the sea surface height is taken to be Gaussian, although this method would make it equally possible to use a non-Gaussian sea surface PDF to account for non-linear wave effects.

CNES and CLS have developed two numerical approaches:

A numerical retracking algorithm (CryoSat Processing Prototype, CNES/Toulouse)

Over the past 3 years CNES has developed a processing chain (CPP) for the CryoSat-2 ocean data acquired in both LRM and SAR mode. This prototype aims at contributing to expertise studies for the future Sentinel-3 mission. Regarding the SAR-mode processing, a numerical retracking algorithm based on simulation of Doppler echoes model is implemented. This method is considered to be more robust than alternatives, particularly when faced with atypical observations (e.g., elliptical antenna pattern, off-nadir mispointing angles, point target response). It was used to evaluate the Halimi semi-analytical approach by model comparison.

The proposed numerical method consists in fitting a Doppler waveform with a pre-computed echo model (generated off-line by a simulator) that is described by known instrumental and geophysical parameters. This method may require huge data storage and, inevitably, long processing times to generate an echo model database with varying sets of sensitive parameter values (sea-state, satellite parameters) and with small sampling intervals. In implementing this strategy, the goal is to build a database in a way that ensures the accuracy and precision of the estimates. However, this may highlight some difficulties that should be considered in future or related work.

Multi-looked echo models are computed by using a simulator that mimics the CryoSat-2 altimeter response in SAR mode. This simulator consists of several components: 1) a scene generator module that generates a flat sea surface with high-resolution 1mx1m, 2) a power returns simulation: radar equation is applied to each point of the surface to compute the backscatter power taking into account the real elliptical antenna pattern. Signals in amplitude are then sorted by Doppler band and accumulated in the appropriate range gates of the waveforms. 3) The resulting model of the FSSR is convolved with the PTRs (in along-track and distance) of the radar. The Doppler bands corrected in range are then summed (multi-looking) to finally form the Doppler echo model for a flat sea surface (the sea wave height is applied "on the fly" in the retracking process). This simulator has been validated by exhaustive testing (i.e., comparison between the estimated surface parameters and the initial ones with an LRM maximum likelihood estimator).

As for conventional altimetry, the ocean parameters estimated from the numerical SAR retracking are expressed as:

$$\theta_n = \theta_{n-1} - g\left(BB^T\right)^{-1}_{\theta_{n-1}} (BD)_{\theta_{n-1}}$$

Where θ_n is the estimated parameter at iteration n; B,D are the partial derivatives and residuals matrix, and g is the loop gain (between 0 and 1).

For unsolved analytical model, derivatives of the mean return power can be computed numerically. The method consists in approximating the derivatives by a finite difference involving the database of pre-computed echo models. At each

iteration n, models using the current estimation vector θ_{n-1} are directly taken from the database. The performances of this method have been evaluated theoretically using simulated LRM waveforms and, have been statistically validated on real data by applying it on J2 raw measurements. The results are found to be consistent with those obtained from a classical MLE4 retracking.

The numerical SAR retracking is based currently on a 3-parameters model that accounts for varying off-nadir mispointing angles provided by the star trackers. First results (focusing on the range and so on the epoch) have been assessed through Cal/Val process and recently communicated to scientific meetings. Analyses of sensitivities of this solution are still under study.

A numerical retracking algorithm (CLS/Toulouse)

CLS has been conducting different studies, on CNES funding, to better understand the principle of the SAR processing and to develop simulation tools that are able to exactly reproduce the raw echoes acquired by a SAR mode altimeter and to process them, accounting for all corrections up to the final retracking algorithm. Based on an end-to-end SAR radar altimeter simulator, CLS has developed its own SAR numerical retracking. The proposed technique slightly differs from the CPP one. The main difference resides in the construction of the echo model database. On CNES side the database is generated by an amplitude numerical simulator method and on CLS side by a complex numerical simulator method that applies the usual Doppler processing scheme and the multi-looking step. The present Doppler/SAR echo model does not into account mispointing angles in the solution process.

The SAR numerical retracking algorithm is similar to the CPP one as discussed previously. However extra computing effort is done to simulate all pulses contributing to a Doppler echo and to average hundreds of incoherent Doppler/SAR waveforms to remove the speckle noise and obtain proper smoothed model echo. This makes the method time-consuming and more complicated to implement.

This algorithm including the true Doppler processing serves as a reference, and has already provided a substantial support to the development of the operating CNES CryoSat Processing Prototype (CPP). Some evolutions of the model are already planned to better account for the effects of new parameters (radial velocity, altitude and antenna mispointing angles) and lead to a model, which will therefore be more representative of CryoSat-2 SAR altimeter measurements.

Figure 3.10 Formulation of the numerical SAR waveform model used by TAS (from Phalippou & Demeestere, 2011)

3.2.1.3   Semi-analytical SAR waveform model

Wingham *et al.*, 2004 proposed a semi-analytical solution to Eq. 3.1. The model has been implemented at UCL and the expression of the model is summarized in Figure 3.11 **(Giles *et al.*, 2012).**

Model

$$p_r(\tau) = p_t(\tau) * p_z(\tau) * I(\tau)$$ General expression for the mean each power (Brown, 1977)

$$p_t = p_0 g_p \text{sinc}^2(\pi B\tau)$$ Transmitted power pulse from CryoSat-2 $$p_z = \frac{1}{\sqrt{2\pi}\sigma} e^{-\frac{1}{2}(\tau/\sigma)^2}$$ Surface elevation pdf

I depends on the backscatter (σ^0), antenna gain and range from the radar to the surface

One-way gain of a synthetic beam

$$I(\tau) \sim \frac{\lambda^2 G_0^2 D_0 c\sigma^0}{32\pi^2 h^3 \eta} \sum_{k=-\frac{(N_b-1)}{2}}^{\frac{(N_b-1)}{2}} H\left(\tau + \frac{\eta h \xi_k^2}{c}\right)$$

Integration around a range ring

Summation over N_b looks

The pattern of a synthetic beam at an angle ($\rho_k\cos\vartheta - \xi_k$) from its boresight in the along track direction.

$$\cdot \int_0^{2\pi} d\vartheta\, d(\rho_k \cos\vartheta - \xi_k)$$

$$\cdot \exp\left[-2\left(\frac{(\rho_k \cos\vartheta - \mu)^2}{\gamma_1^2} + \frac{(\rho_k \sin\vartheta - \chi)^2}{\gamma_2^2}\right)\right]$$

pitch   Elliptical antenna pattern   roll

Wingham et al., 2004

Figure 3.11: Formulation of the semi-analytical SAR waveform model developed by UCL (from Giles et al., 2012)

The model accounts for the slight ellipticity of the CryoSat-2 antenna beam and shows explicit dependence of the SAR waveforms on platform roll and pitch mispointing angles.

CNES/CLS have also developed a semi-analytic approach **(Halimi, ENSEEIHT/Toulouse)**

In the frame of a research project directed by CNES, CLS and the University of Toulouse, Halimi thesis study aims at developing an analytical modelling of the SAR altimeter ocean power-waveform, and an associated retracking algorithm to infer the sea surface parameters (i.e. epoch, wave height and amplitude).

Starting from the same hypotheses made by Brown, but using a different geometrical approach, an analytical formula for the FSSR associated with Doppler altimetry has been derived. The proposed FSSR model includes earth roundness, considers a Gaussian approximation for the antenna gain as it is used in the classical Brown model, and it doesn't contain antenna mispointing angles. The double convolution defining the mean power is then computed numerically. In this operation a cardinal sine function is used to model the PTRs in along-track and across-track directions. In some situation, the use of the real shape of the PTRs may be preferred to handle distortions. In this way, the power waveform

avoids analytical approximation, minimizing the geophysical dependent biases in the retrieval parameters. The resulting single-look model depends on three parameters: the epoch, the sea surface wave height and the amplitude. A multi-look model is obtained by summing all the reflected power from the along track beam surface of interest after applying appropriate delay compensation. A least squares approach based on the Levenberg-Marquardt algorithm is then applied to estimate the 3 parameters (i.e., epoch, the sea surface wave height and the amplitude) associated with the multi-look Doppler model.

Simulation results performed on synthetic data clearly show the potential of the SAR altimetry when compared to conventional altimetry in terms of error reduction. The analysis of real CryoSat-2 waveforms has confirmed the effective performance of the proposed Doppler model since a better estimate is obtained than with the usual conventional method. However, when dealing with antenna mispointing angles as encountered on-board CryoSat-2, this no-mispointing solution model is no longer well suited. The sensitivity of the SAR-mode altimeter data to off-nadir mispointing (mainly across-track) angle is known. It leads notably to errors in the retrieval. A new formulation of the SAR echo model with 5-parameters, including mispointing angles in across and along-track directions is currently under investigation in order to improve the consistency between the SAR altimeter waveform and model at varying parameters (particularly in different pointing scenarios).

3.2.1.4   Fully-analytical physically-based SAR waveform model: SAMOSA

Several physically-based SAR waveform models were developed by Starlab within the ESA-funded SAMOSA project **[Cotton, 2011].** There are three versions of the SAMOSA models, offering different levels of complexity (see Figure 3.12). Both numerical and analytical forms of the models were developed, and tested against simulated SAR waveforms from the CryoSat Mission simulator and against measured waveforms as provided in the ESA CryoSat-2 L1B SAR products.

	SAMOSA1	SAMOSA2	SAMOSA3
Non-linear wave statistics	N	Y	N
Asymmetric antenna	N	Y	Y
Earth ellipticity effects	N	Y	Y
Across-track mispointing	N	Y	Y
Correct response to mispointing	N	Y	Y
Fully analytical	Y	N	Y
Computationally efficient	Y	N	Y

National Oceanography Centre
NATURAL ENVIRONMENT RESEARCH COUNCIL

OSTST 2011 San Diego 19-21 Oct 2011

Figure 3.12: Effects accounted for in the various versions of the SAMOSA models for SAR waveforms developed in the ESA SAMOSA project (from [Gommenginger et al., 2011a]).

While providing satisfactory fit against CryoSat-2 SAR waveforms, the SAMOSA1 model was not able to account for CryoSat-2's asymmetric antenna beam pattern or accurately represent the effect of platform mispointing on the SAR waveforms. SAMOSA1 is no longer in use after the more advanced SAMOSA2 and SAMOSA3 models superseded it.

SAMOSA 2 is an entirely new physically based formulation developed by Starlab, starting from the original radar equation. It accounts for various additional effects, including the asymmetricity of the antenna beam, the ellipticity of the Earth, along- AND across-track mispointing and non-linear ocean surface statistics. It is based on the PDF of sea surface height proposed by [**Rodriguez, 1988].** SAMOSA2 offers a physically correct response to mispointing and improved fit against ESA CryoSat-2 L1B SAR waveforms. Full details about the derivation and expression of SAMOSA2 are given **in [Ray *et al.*, 2013]**

SAMOSA3 is a simplified form of SAMOSA2 obtained after neglecting the non-linear ocean surface effects and some second-order terms **[Gommenginger *et al.*, 2012]**. SAMOSA3 is a fully analytical model that provides a simple and computationally efficient solution to compute the two-dimensional delay-Doppler maps of the SAR echo power as a function of range, significant wave height and backscatter coefficient, while retaining the advanced features of SAMOSA2.

3.2.1.5   Empirical SAR waveform model

An empirical fully-analytical model was proposed by **[Sandwell *et al.*, 2011]** for the purpose of retracking CryoSat-2 SAR waveforms for improved marine gravity. The proposed formulation is shown in Figure 3.13
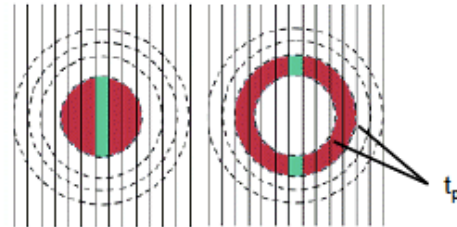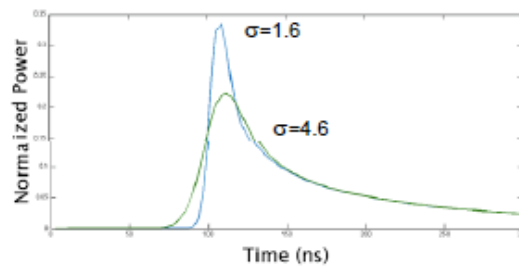
Figure 3.13: Formulation of the empirical SAR waveform model proposed by Sandwell et al., 2011 (from Sandwell et al., 2011).

While the formulation is indeed simple, it is not clear how/whether the empirical model captures the effect of the asymmetric antenna pattern and the influence of mispointing. The 20Hz range noise obtained for CryoSat-2 SAR data with this empirical model was found to be larger than that observed by other groups, leading the authors to conclude that this "fully-analytic retracking model is suboptimal" **[Sandwell *et al.*, 2011].**

Limitations, drawbacks and challenges (from CNES/CLS)

Although considerable progress has been made, there is still a large amount of work to make SAR mode fully operational for the oceanographic community and to ensure continuity of high precision altimeter measurements after Jason-3 with subsequent missions (Sentinel-3 and Jason CS). In comparison with the

experience the scientific community has been developing on LRM altimetry for decades (20 years since the first TP and ERS waveforms and much more since Skylab, Seasat and Geosat), SAR mode processors are still in their infancy. Recent investigations led by agencies and research groups concerned by SAR mode technology (e.g., ESA, SAMOSA group, Thales Alenia Space, UCL, CNES, CLS, NOAA, …) have already produced very good preliminary results for CryoSat-2 SAR waveforms, with the development of robust retrackers (based on analytical or numerical algorithm consideration) that are suited to the SAR echoes. However, this work is still on going, as retrackers have not yet achieved a successful retrieval of all three parameters, i.e. sea surface heights, wave heights and wind speeds from SAR-mode data.

Some remaining issues that may impact the SAR-mode performance still need to be analysed and worked out, namely:

- the inconsistent behaviour of SAR retracker at low wave heights (below 1m) currently observed by all the teams involved in SAR processing,
- the sensitivity of the SAR mode retrievals to varying orbital and instrumental parameters, such as the platform mispointing angles, the altitude, the spacecraft velocity,
- the potential impact of the long-wavelength swell waves (close to the along-track SAR resolution) on the estimates,
- the lack of SSB solution suitable to SAR mode measurement geometry. Similarly to the conventional altimeter approach, the SSB for the SAR mode should be empirically evaluated from altimeter itself, as function of wave height and backscatter coefficient measurements, since theoretical electromagnetic bias models are not accurate enough. At this moment, one limitation of this method may reside in the difficulty to estimate SAR mode sigma-naught for peaky waveforms and then to derive any SAR SSB correction (unless RDSAR estimate is used in the absence of SAR sigma-naught). Ne further complication is that an empirical SSB correction must be constructed over many cycles (allowing to account for seasonal variations) to make the model consistent throughout a mission.

3.2.1.6   Review Sigma0 retrieval in LRM and SAR mode (TuDelft, NOC)

Sigma0 retrieval in LRM mode

From the TUDelft analyses in frame of reporting to the QWG it became clear that both the L2 baseline A and the baseline B products suffer from problems with the sigma0. This quantity, also referred to as backscatter coefficient, is a function of the radar frequency, polarisation and incidence angle and the target surface roughness, geometric shape and dielectric properties. It is computed from the

power (amplitude) of the return pulse of the altimeter, and can be directly related to wind speed. The sea state bias then is computed from empirical models combining wind speed (backscatter) and significant wave height. So, an error in the sigma0 results in an error in the wind speed and so also in the sea state bias. In baseline A the mode of the sigma0 histogram seemed ok but the sigma0 was reversed, however in baseline B though it was reversed back a bias was introduced along with other peculiarities. In Figure 3.14 sigma0 histograms are plotted based on subcycle 23 (January 2012, baseline B product). We compare the original ESA L2 product (left) with the RADS re-tracked L1b product (right). The bias is at 7dB, but more importantly the RADS result is more symmetric around the mode (10.8db), and smoother. It also compares well with other satellites like the Jasons and Envisat. The CryoSat-2 original product shows 2 typical bumps in the histogram indicated by the red arrows.
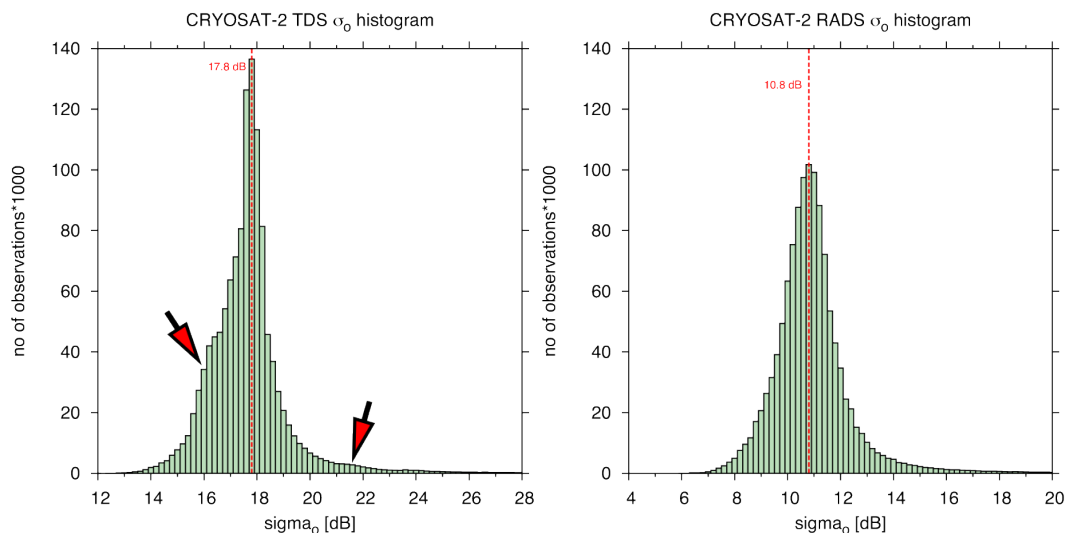
Figure 3.14 CryoSat-2 sigma0 histograms for the original ESA baseline B product (left panel) and the equivalent retracked RADS data set (right panel). In red the modes of the histograms are given.

This is very likely caused by wrong AGC values originating from the wrong integer to float transition and a scaling problem with the estimation of the power in the waveform. On top of that, there is a difference in treatment of the mispointing of the platform (off-nadir angle). Both ESA and RADS apply a 3-parameter estimation to the waveforms (radar echoes), sc. range (epoch), swh (width/gradient), and wind (amplitude). This is also referred to as MLE3. However, in RADS we compensate for the mispointing, whereas this seems neglected in the ESA implementation. This makes the RADS implementation similar to an MLE4, only that the 4th parameter is not estimated from the waveform (decay) but comes directly from the attitude information from the on-

board star trackers (off-nadir angle). Mispointing can have a significant influence on the performance of the altimeter instrument. If the off-nadir angle is zero or very small a straightforward MLE3 would be the preferred re-tracker for open ocean, but for CryoSat-2 platform it can not be neglected. We already recommend this to be implemented in the next update of the ESA ground processor, and will be using the applied approach in RADS also for the CP4O products**. [Smith and Scharroo, 2011]** provides more detail on the retracking of range, SWH, sigma0, and attitude in CryoSat-2 LRM altimetry and how it is done for RADS: the CS2's waveforms from the ESA L1b FDM and LRM products are retracked based on circular beam theory using the azimuthally averaged Half Power Beam Width. This seems to work pretty well as an approximation for the LRM waveforms (in fact the antenna pattern is slightly elliptical). Parameters that are re-tracked are epoch, width, amplitude, mispointing and noise. Basically the system allows for choice of parameters to be fit and parameters to held fixed, but the MLE4 approach, as mentioned before, where the 4th parameter (mispointing) does not actually come from the fit but from the given off-nadir angle in the L1b product, is highly favoured.

As an example what the impact is of an erroneous sigma0 estimate, we plotted for subcycle 37, pass 520 (February 2013) the along-track values of the sigma0 (top) and wind speed (bottom). Pass 520 is long stretch of data along a track in the pacific hitting the American coast near the border of Alaska with Canada. LRM stands for original ESA product, LRM+ for the improved (but not retracked) product, and RADS for the retracked product. To get to comparable power in the wind speed the original wind speed curve has to be multiplied by 6 to 7, but still would lack the detail present in the properly retracked product.

mean [dB]: rads=11.086, lrm=17.075, lrm+=10.720
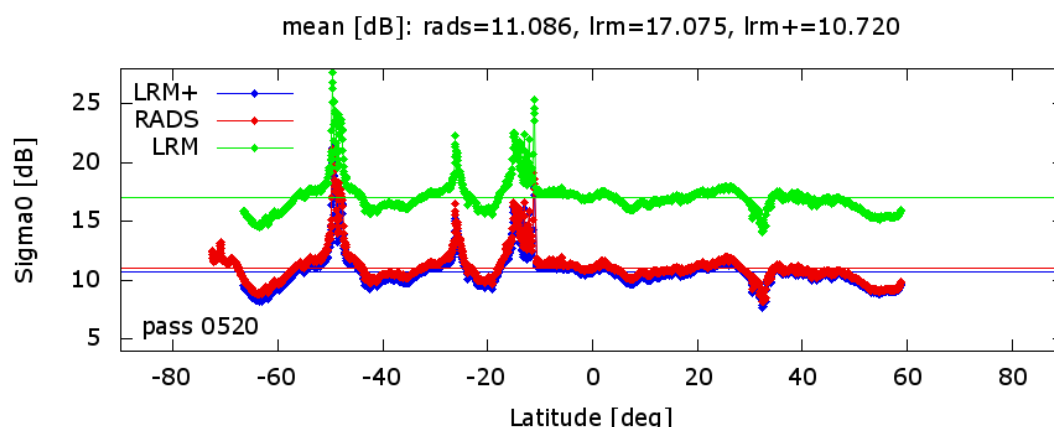
CP4O Preliminary Analysis Report
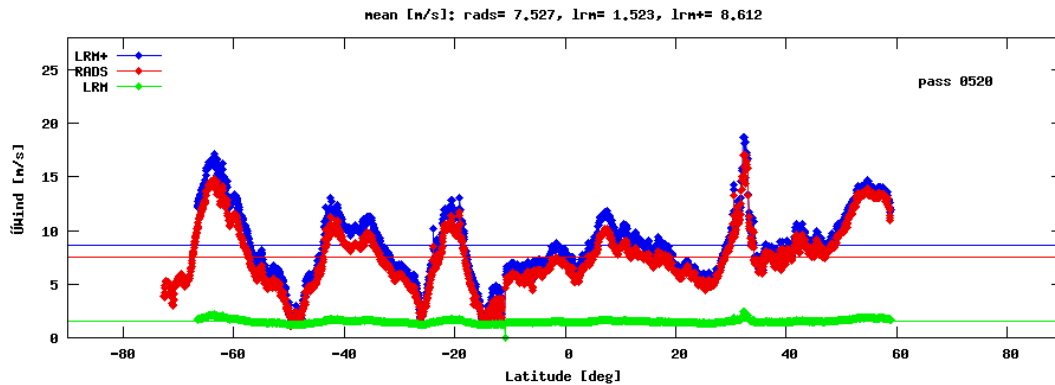
Figure 3.15 Sigma naught (top) and wind speed (bottom) for track 520 (February 2013) comparing original ESA LRM L2 product with improved product and RADS retracked.

Sigma0 retrieval in SAR mode

As in LRM, Sigma0 refers to the Normalized Radar Cross Section at nadir and gives a measure of the reflectivity of the surface. Over the ocean and in the absence of rain, Sigma0 decreases with ocean surface roughness and is typically used to derive information about wind speed.

Sigma0 is related to the peak power of the received echo, Pu, in which it appears as a multiplicative factor. Pu is estimated by retracking the SAR altimeter waveforms with a suitable model. The exact relation between Sigma0 and Pu will depend on the SAR waveform model used for retracking.

For CryoSat-2, the power echo sample values are scaled to fit between 0 and 65535. The scaling factors can change for each waveform (20Hz). To convert these back to values in Watts, the following equation should be used:

*Power in Watts = scaled value * (scale_factor*10^9) * 2^scale_power*   Eq. 3-2

where scale_factor and scale_power are given as fields 77 and 78 in the Waveform SAR group structure of the CryoSat-2 L1B products.

For both SAR and LRM, it is common practice to normalize waveforms prior to retracking. The power echo samples are scaled by the maximum value, so that waveform samples take values between 0 and 1. However, even for multi-looked waveforms, the maximum value in successive 20Hz waveforms shows rapid fluctuations, and this would introduce unwanted noise in other retrieved parameters (e.g. SSH). Thus, the maximum value is estimated with a running window (typically 5 gate samples wide) to provide a more stable value of the maximum with which to normalize waveforms.

By construction, the values of Pu retrieved by retracking normalized waveforms will be around 1. To recover the value of Pu in physical units (Watts), one has to

first reverse the normalization, and then convert the retrieved maximum amplitude to real power units using the scaling factors provided in the L1B products.

3.2.1.7   Review SAR re-tracking over sea ice: e.g. threshold, leading edge, double ramp, beta and OCOG re-trackers for polar regions (DTU)

CryoSat2 Level 1B SAR data is processed using various empirical retrackers to determine the sea surface height and its variation in the Arctic Region. Improved retracking based on the combination of OCOG (Offset Centre of Gravity) **[Wingham et al., 1986]**, Threshold method **[Davis, 1995]**, **[Davis, 1997]** and Leading Edge Retrieval **[Lee et al., 2008]**, **[Bao et al., 2009]** is used to estimate the sea surface height. This sea surface height determination is to be compared with the ESA sea surface heights available in the CryoSat2 Level 2 data. A comparison is done with marine gravity field (obtained by experiments done on board ships) for retracker performance evaluation. Traditional empirical retrackers work on the complete power waveform of the echo. The retrackers intend to find the correct location in the power waveform that is corresponding to the point where the reflection occurs. Two traditional empirical methods are the application of the OCOG and Threshold method, which work on the statistics of the complete power waveform in order to locate the reflection point. Contrary to traditional empirical retrackers, the methods used do not work on the complete power waveform. The customized retrackers are applied just on the leading edge of the power waveform. This leading edge is the part of the waveform where the reflection has occurred. Hence focusing on this leading edge rather than the complete waveform will reveal better reflection locations. The novelty of the project lies in the extraction of the leading edge and using it for processing rather than applying the OCOG and Threshold retrackers on the complete waveform. This improves the sea surface height determination as the leading edge contains the information about the reflecting surface, its physical properties and its location in the direction of EM wave propagation.

Extraction of Leading Edge

This retracker uses the statistical properties of the echo waveform to compute two difference thresholds (start and stop) for the neighbouring power bins. These start and stop thresholds are based on the standard deviation of the consecutive and alternate power difference in the bins. Next, a loop is run to check the power differences throughout the waveform for neighbouring bins. If this power difference is greater than the start threshold, the system records the beginning of a subwaveform. Further when the power difference of neighbouring bins of this subwaveform is less than the stop threshold, this is recorded as the end of the subwaveform. As a result the power waveform is divided into various subwaveforms each having one peak. The first subwaveform corresponds to the peak for the leading edge. The retracking algorithms are applied on this leading edge.

CP4O	Preliminary Analysis Report	D2.1	

Leading Edge – OCOG Method

The Offset Centre of Gravity (OCOG) method finds the centre of gravity of the leading edge of the waveform based on the power levels in the bins. A rectangle about the centre of gravity is developed defining an amplitude (A) and width (W). The Centre of Gravity (COG) is hence calculated and used to find the Leading Edge Position (LEP). In the Leading Edge – OCOG method the centre of gravity of just the leading edge is obtained rather than the centre of gravity of the complete waveform.

Leading Edge – Threshold Method

This retracker compares the leading edge power bins with a threshold determined from the statistics of the waveform. The Threshold retracker makes use of the Amplitude (A) determined in the (OCOG) method. The threshold is chosen to be 75% of the Amplitude (A). The required power bin is obtained by linear interpolation between the 2 adjacent bins where the threshold crossing occurs on the steep part of the leading edge of the power waveform. The threshold level of 75% needs to be modified as per the composition of the satellite data and should be different for (LRM), (SAR) and (SARIN) components. This distinguishing procedure would be applied in the forthcoming versions of the waveform retrackers.

Retracker performance w.r.t. gravity field

In order to evaluate the performance of the two waveform-retrackers, comparison is done with the sea surface heights as available in the Level 2 components of CryoSat2 data. There is a one to one correspondence with sea surface height and gravity field because the gravity field is obtained by taking the derivative of the sea surface height anomaly along the track. Gravity fields are computed using the heights obtained in the two methods as well as for the Level2 components. The standard deviation of the difference between the marine gravity field and the gravity field obtained via the sea surface heights works as an indicator of the performance of the retracker. The smaller the value of this standard deviation, the better the retracker is. The standard deviation in mgal of the gravity field differences between the marine gravity field and the retracked gravity field is computed and displayed month-wise in Table 3-3 for the year 2011. The table includes results of the two traditional (OCOG, Threshold) methods, the two leading edge methods and the ESA – determined CryoSat2 Level 2 data. It is noted that the LE + THRES method performs the best, concluding that focusing just on the Leading Edge improves the results.

Table 3-3 Standard Deviation (mgal) of difference in retracked and marine gravity field.

	OCOG	THRES	LE + OCOG	LE + THRES	Level 2
FEB	10,275	10,152	7,632	7,026	11,170
MAR	8,058	8,587	6,689	6,701	8,870
APR	8,579	8,587	6,294	5,940	6,338
MAY	9,806	9,859	8,905	8,882	12,851
JUN	9,555	9,574	9,099	7,470	9,336
JUL	10,461	10,607	10,395	7,799	9,326
AUG	6,206	6,241	6,208	6,010	6,235
SEP	4,968	4,968	4,980	5,047	4,840
OCT	5,336	5,327	5,375	4,924	5,332
NOV	8,593	8,540	8,173	7,683	9,843

Retracker performance w.r.t. sea surface height

Once the sea surface height is obtained using the various retrackers, the mean sea surface and all other corrections are removed which leaves a sea surface height anomaly. The 20 Hz sea surface height anomaly is converted to 1 Hz and the standard deviation of the 20 values for each second is recorded. At the end, the mean of this standard deviation is obtained. A lower value of the mean standard deviation reflects a better retracking procedure. The 7 retrackers thus compared are the traditional OCOG Retracker (R1), the traditional Threshold Retracker (R2), the 5 parameter Beta Retracker (R3), the Leading Edge + OCOG Retracker (R4), the Leading Edge + Threshold Retracker (R5), the Maxima as Threshold Retracker (R6), and the ESA Retracker used in the CryoSat2 Level2 Product (R7).

Table 3-4 shows the mean standard deviation for SAR and SARIN data for the 7 retrackers. The customized leading edge retrackers are R4 and R5 and they show considerably better performance as compared to other retrackers. Figure 3.17 show the sea surface height anomaly for the two leading edge retrackers for summer and winter months. Figure 3.18 shows the waveform processing for leading edge extraction and the application of the leading edge retrackers.

Table 3-4 Mean standard deviation (sea surface height anomaly in meters) for the 7 retrackers for SAR/SARIN Data.

Retracker	SAR Summer	SAR Winter	SIN Summer	SIN Winter
R1	0,104	0,092	0,116	0,128
R2	0,104	0,092	0,116	0,128
R3	0,086	0,087	0,107	0,097
R4	0,071	0,067	0,087	0,100
R5	0,069	0,066	0,083	0,094
R6	0,069	0,064	0,083	0,044
R7	0,091	0,075	0,114	0,121

Conclusion

CryoSat-2 Level 1B data was processed using the two improved waveform retrackers. The statistics so obtained reveal that the customized/improved retrackers show a better performance as compared to the CryoSat2 Level2 products or the traditional retrackers that work on the complete waveform. This proves the assumption that applying retracking just on the leading edge of the power waveform results in improved sea surface height determination.
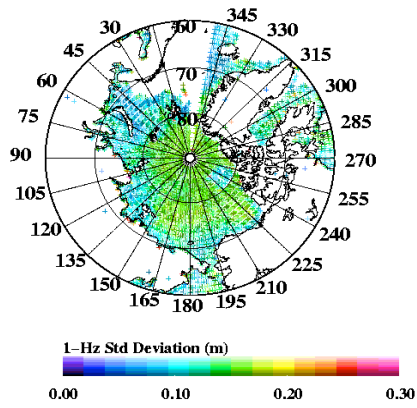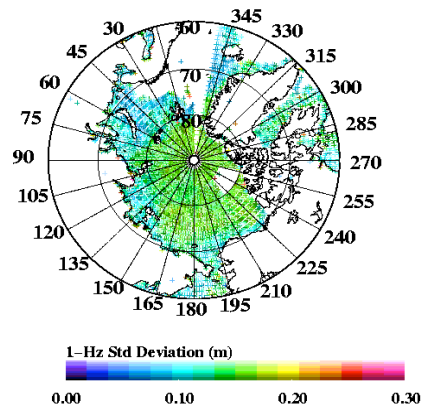
SAR R4S

SAR R5S

SAR R4W
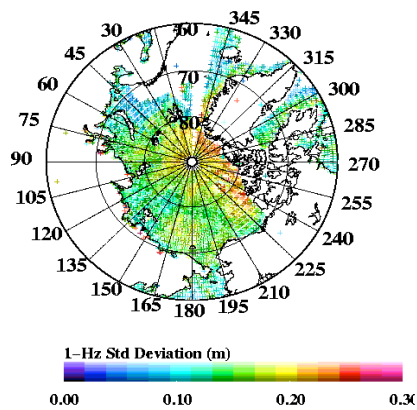
SAR R5W
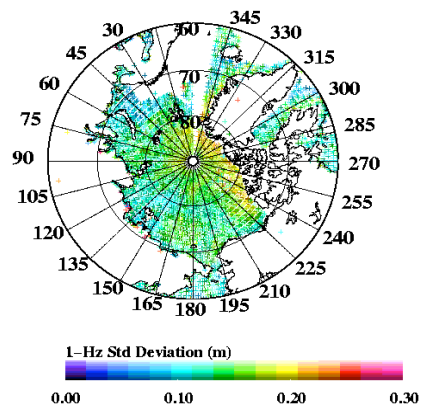
Figure 3.16 Sea surface height for R4 and R5 retrackers during Summer (S) and Winter(W).
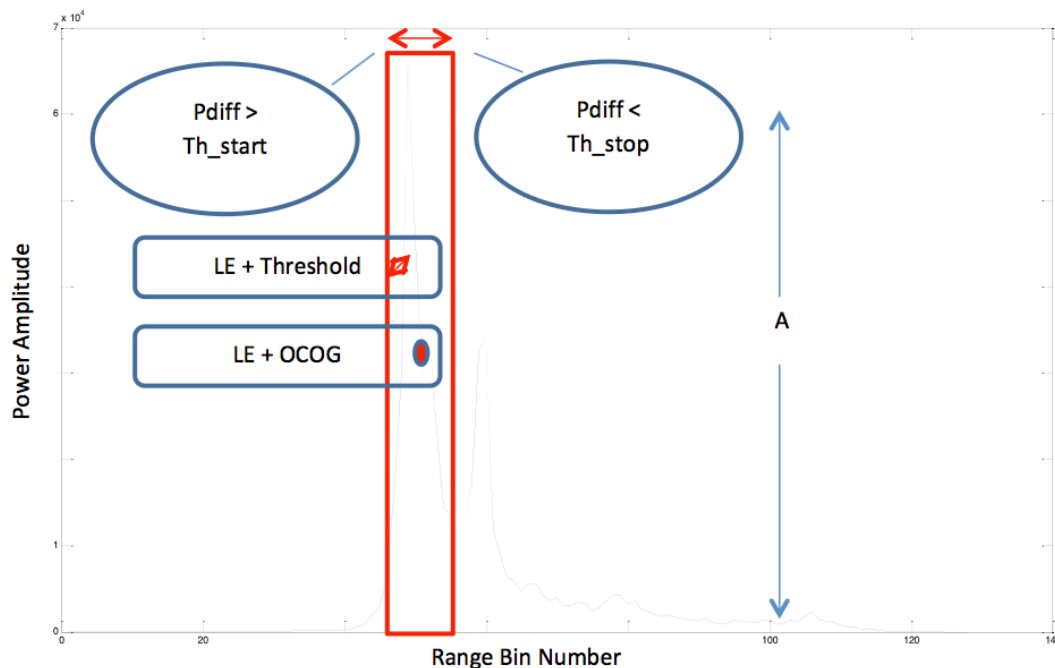
Figure 3.18 Application of Leading Edge Extraction, OCOG Method and Threshold method.

3.2.2 Review RDSAR methodologies

In this section, we review the existing methodologies to process SAR Full Bit Rate (FBR data) to derive Low Resolution Mode (LRM) waveforms from SAR Mode (SARM) data. Henceforth such techniques are known as ReDuced-SAR (RDSAR) techniques, and the resulting waveforms Pseudo-LRM (or PLRM) waveforms.

We will present a review of the three techniques that have been independently developed and implemented by three different institutions and companies. These are:

1. The SAMOSA RDSAR methodology, developed in the framework of the SAMOSA project;
2. The CNES RDSAR methodology, embedded in the CNES CryoSat Processing Prototype (CPP);
3. The NOAA/Altimetrics RDSAR methodology.

Here we provide an overview of these techniques. Further details about specific algorithms are envisioned to be made and available in other subsequent deliverables of the CP4O project.

The various strategies to ensure a fair comparison of PLRM and LRM L2 data performances as well as the extensive validation activities are not in the scope of this document and will be addressed in WP4000.

3.2.2.1   LRM and SARM

The SIRAL altimeter on board CryoSat-2 (and therefore also its simulator, CRYMPS) has three acquisition modes:

- Low Resolution Mode (LRM) – conventional altimeter mode, where pulses are transmitted at a rate of 1970Hz. The mode performance is equivalent to a conventional altimeter.
- SAR Mode (SARM), where pulses are transmitted in the form of burst. Each burst consists of 64 pulses transmitted at a rate of 17.8KHz. The duration of a single burst is 3.6 ms, and bursts are transmitted every 11.7ms.
- InSAR Mode (inSARM), not of interest for this section.

The two modes of interest in this document are the SAR Mode and the Low Resolution Mode. While both LRM and SARM transmit identical pulses at a frequency of 13.575GHz, their main difference is the Pulse Repetition Frequency (PRF), and its associated effects. In the LRM, the relatively low PRF implies that subsequent echoes are not correlated, therefore allowing reducing their noise by incoherent averaging. Pulse-to-pulse correlation is instead requested in the SAR mode, to enable the coherent processing of the synthetic antenna: such correlation is achieved using a relatively high PRF (some 9 times the LRM one). On top of this, in SARM pulses are transmitted in burst (64 pulses per burst) while in LRM pulses are transmitted continuously.

Provided that SIRAL's LR and SAR modes are mutually exclusive, the possibility of reducing the high-PRF SARM echoes to the low-PRF LRM ones is the only way to compare the two modes and their performances in a direct way.

In the following sections we focus on three RDSAR techniques, independently developed and implemented by different groups/institutions/companies. In all RDSAR methodologies, SAR FBR echoes are combined coherently and/or incoherently in such a way that SARM PRF is effectively reduced from 17.8KHz to a value close to the LRM PRF (1970Hz). The different steps needed to reduce the data are strongly related with the various processing stage of the two modes and therefore, in the following sections an overview of the various processing modules needed for SAR and LR modes is provided.

The main difference between the LRM and SARM modes is the Doppler processing, which is the basis of any synthetic aperture approach. Figure 3.19 shows the main processing block for the LRM while Figure 3.20 shows the same for the SAR mode.

 SARM FBR data corresponds to individual complex (I and Q) components. Therefore, data is telemetered after the A/D block shown in Figure 3.21. In this same figure is it easy to identify the typical processing steps of a synthetic aperture radar, with the deramping module, the 2-dimensional FFTs, the range cell migration, etc.
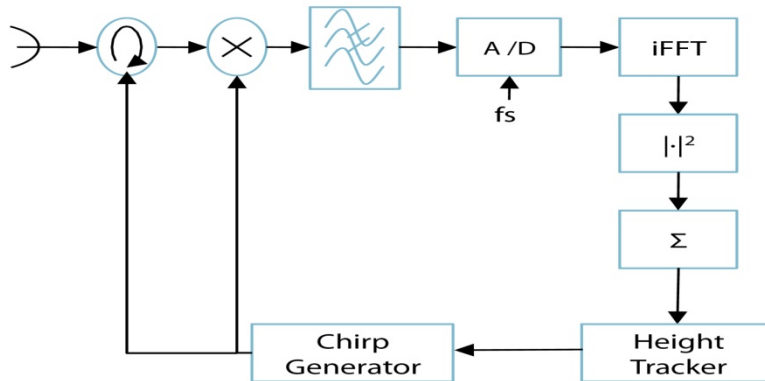
Figure 3.19 LRM processing block diagram.
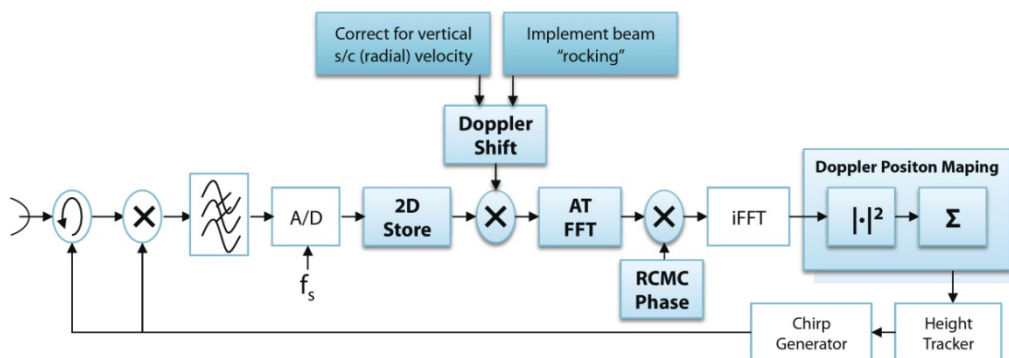
Figure 3.20 SARM processing block diagram.

The main characteristics of CryoSat LRM, as reported in [CryoSat MDD, 2007] are:

- Data is delivered in frequency domain
- PRF = 1970Hz
- Echoes are multi-looked incoherently on-board (reduction of Speckle)
- It is assumed that the echoes are averaged at a rate of ca. 20Hz. This corresponds to ca. 92 echoes.

The main characteristics of CryoSat SARM, as reported in [CryoSat MDD, 2007] are:

- Data is delivered in time domain prior to on-board Fourier transform. The IF anti-aliasing filter is already applied on-board. Only the corrections of

the effects of this filter (amplitude ripples in the spectral domain) have to be applied to the FBR data.

- Data delivered in I, Q samples
- 64 pulse per burst
- PRF = 17.8kHz
- Burst length = 3.6ms
- Burst repetition interval = 11.7ms
- The data have not been multi-looked

3.2.2.2 SAMOSA RDSAR

This RDSAR software was developed within the framework of SAMOSA CCN1 contract, and documented in one of its deliverables [Marquez et al., 2010], which has been used as one of the source for this document. RDSAR algorithm processes and transforms SAR altimeter mode (SARM) Full Bit Rate (FBR) acquisitions in such a way that they emulate conventional altimeter data (Low Resolution Mode data - LRM), which are called pseudo-LRM (or PLRM).

As requested in the SAMOSA original contract, the software reads SARM FBR data (or SARM L1a data) as generated by CRYoSat-2 Mission Performance Simulator (CRYMPS), reduces it to emulate LRM data, and outputs the resulting sequence (pseudo-LRM sequence), also propagating along-track position information from CRYMPS.

The reduction of SARM data to LRM does not consider the tracker compensation by window delay correction and Gain (Automatic Gain Control – AGC, and fixed gain) compensation.

This RDSAR algorithm has so far only been used with simulated data from CRYMPS, and not with real data. In the context of WP4000 of the CP4O project, RDSAR will be tested using real FBR data from CryoSat-2. Its performances with respect to real data will be assessed, particularly by retracking the RDSAR pseudo-LRM waveforms, and by comparing the estimated parameters with both estimations from SAR-mode data, and with in-situ ground-truth data (whenever available).

Comparing Figure 3.19 and Figure 3.20 above, it is easy to identify that the processing steps to reduce SARM FBR data to pseudo-LRM will have to include at least:

- A transformation of data from frequency domain (IFFT)
- A transformation of data to power
- An incoherently integration of waveforms at a rate of approximately 20Hz

All this to be applied to SARM FBR after A/D.

These three steps are essential for the reduction to LRM, but not sufficient. Previous to the transformation of data to the frequency domain, SARM FBR

CP4O	Preliminary Analysis Report	D2.1	

waveforms must be combined and/or selected in such a way to cancel pulse-to-pulse correlation. In addition, the different in transmission patterns of LRM and SARM (continuous or burst) results into an unequal number of waveforms for equal-duration time sequences. Therefore, to enable a fair comparison of the two modes, it is necessary to adjust variances of data to account for the difference in number of pulses of each statistics.

Within SAMOSA, two different approaches have been studied and proposed:

- Methodology A
- Methodology B

The two methodologies are described in the next subsections.

3.2.2.2.1 Methodology A

This methodology has been reported, for example, in [RDSAR SD, 2012]. SARM and LRM mode transmit identical pulses. As already pointed out, the main difference of these two modes is their PRF and its associated effects (pulse-to-pulse correlation or decorrelation). The most straightforward way to achieve for the PLRM waveforms a PRF similar to the one of LRM is obviously to conveniently select SARM echoes, such that the sequence achieved has the requested pulse-to-pulse PRF. In other words, we select one every m SARM echoes such that the resulting sequence has a PRF equivalent to LRM. This will also ensure the requested pulse-to-pulse decorrelation, at least for sea states with SWH $> 2m$, as shown, for example, in [Dinardo, 2008].

For such solution, the calculation of m is achieved as:

$$m = \frac{PRF_{SARM}}{PRF_{LRM}}$$

If this is calculated with CryoSat-2 specifications, the resulting value of m is 9. Considering that each burst in SARM contains 64 pulses, we can extract 8 decorrelated waveforms per burst. Unfortunately, choosing one every nine complex SARM waveforms results into a sequence with a minor number of waveforms with respect to its equivalent LRM sequence for an identical time interval. This is due to the receiving gaps between bursts in SARM as described, for example, in [CryoSat MDD, 2007] and represented in Figure 3.21. While in LRM the altimeter is constantly transmitting and receiving pulses at a PRF of 1970Hz, this is not the case for SARM, in which a set of 64 pulses (referred as burst) is transmitted and the altimeter turns into reception mode until the next burst is transmitted.
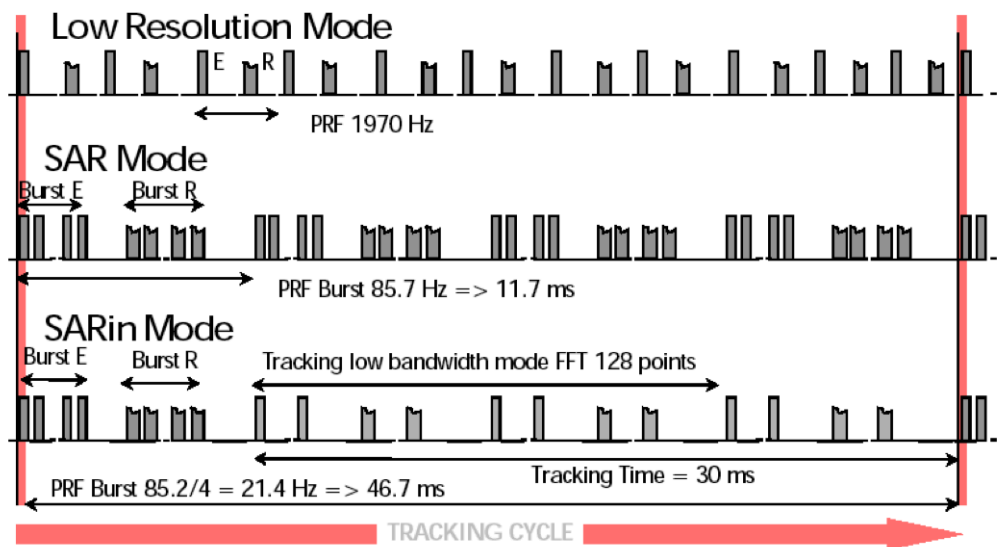
Figure 3.21 Timing of transmitted (E) and received (R) pulses in each of the three SIRAL modes (from [CryoSat MDD, 2007]).

To account for this difference, given a time interval t_LRM with a certain deterministic number of LRM pulses, we must calculate a time interval t_SARM, in which we can select an equal number of pseudo-LRM waveforms. To allow the exploitation of full bursts, t_SARM should be a multiple of Tb or burst repetition interval. We will refer hereafter to Nb as the number of bursts during t_SARM seconds. Therefore, t_SARM shall be calculated as:

$$t\_SARM = T_b * N_b$$

As said, Methodology A is based on selecting one every nine waveforms, thus obtaining 8 pseudo-LRM echoes per burst. Therefore, the total number of pseudo-LRM echoes for t_SAR seconds shall be expressed as:

$$N_{PLRM} = N_b * 8$$

To achieve an equal number of pulses from the pseudo-LRM sequence and the LRM sequence we must force

$$N_{LRM} = N_{PLRM}$$

Knowing the PRF of LRM, the previous can be calculated in the form of time as:

$$t_{LRM} = N_{LRM}/PRF_{LRM}$$

From the previous it can be easily derived that in order to have the same number of accumulated echoes for LRM and pseudo-LRM sequence we need to have t_SARM almost three times longer than the t_LRM (using T_b=11.7ms and PRF_{LRM}=1970Hz the result is t_SARM=2.88 t_LRM).

Provided the right duration of the SARM data to process, one every nine SARM FBR echoes during t_SARM must be selected. As said, this will result into eight pseudo-LRM complex waveforms per burst.

Subsequently, data is transformed from frequency domain, as follows:

$$X_{IFFT}(k,l)=IFFT_k[X_{tc}(n,l)]$$

where k = 1 to N_F.

Finally, data is converted to power:

$$P(k,l)=|X_{IFFT}(k,l)|^2$$

and corrected for a number of gains, to be taken into account (see, for example, [Dinardo, 2008]):

1. a static fixed gain G_{RF} which depends on the RF instrument;
2. a dynamic gain G_{AGC} depending on the Automatic Gain Control (AGC);
3. a gain G_{ADC} dependent upon the Analogue-to-Digital Converter (ADC), and finally
4. a processing gain of the different echoes G_S.

Hence, the L1b power waveform, PL1b can be computed as follows:

$$P_{L1b}(k,l)=P(k,l)-G_{RF}-G_{AGC}-G_{ADC}-G_S$$

where $P(k,l)$ is the frequency domain processed power echo generated by mode dependent methods, and all units are in dB.

Finally data is incoherently integrated at a rate of approximately 20Hz.

$$W(k,m) = \frac{1}{N}\sum_{l=1}^{N} P_{L1b}(k,l)$$

where M = *1:N:NSARM - N*, and *N* is the total number of waveforms during the incoherent integration time, which for CryoSat-2 is approximately 0.05 seconds.

N is therefore calculated from the number of LRM complex echoes incoherently integrated to generate one L1b LRM waveform. From [CryoSat MDD, 2007], the number of LRM waveforms incoherently summed is 91. Knowing that every burst is equivalent to 8 pseudo-LRM echoes, in order to build the L1b PLRM we will incoherently integrate 88 waveforms. The rationale behind this choice is the need to approximate the 91 waveforms of the L1b LRM and, at the same time, to use an integer number of bursts – namely 11. This technique allows to fairly compare L1b LRM waveforms and L1b pseudo-LRM since they are derived from the incoherent integration of an almost equal number of complex waveforms (i.e., the L1b SNR for both sequences is improved in the same way by the averaging). Note that this technique results into a L1b pseudo-LRM sequence with an approx 7Hz posting rate, while the LRM L1b sequence posting rate is approximately 20Hz. This lower posting rate might have an impact in the performance of the final 1Hz products (final products at same posting space-step than the radar resolution).

3.2.2.2.2 Methodology B

Methodology B, proposed by the European Space Agency (ESA), resembles Methodology A in that it aims at obtaining one SARM echo out of nine. The difference lies in that the echoes in between are not disregarded. Here, one every eight echo is obtained by incoherent averaging eight subsequent echoes. Actually, the algorithm foresees that the number of single echoes to be averaged can vary from 1 (which is equivalent to Methodology A) to 8. Therefore, the difference with respect Methodology A is that all the waveforms of SARM FBR dataset are subjected to IFFT and transformed into power. After this an incoherent pre-summing of waveforms is performed, as follows:

$$P_{presum}(k,l) = \sum_{m=1}^{n} P(k+m,l)$$
$$k = 1:8:K$$
$$n = [1,8]$$

Starting from this pre-summed waveform, the remaining part of the processing is the same as for the Methodology A. Note that the resulting sequence will still be a 7Hz posting rate L1b pseudo-LRM sequence, as achieved in methodology A, but the SNR improvement in the trailing edge will be better than for Methodology A.

Considering that the echoes at SARM PRF are coherent, their incoherent summation will not improve the SNR in the leading edge (which is the most coherent area of the waveform) while it results in a certain improvement of the SNR in the trailing edge.

3.2.2.3 CryoSat Processing Prototype RDSAR

In preparation to the Sentinel-3 mission, CNES has set up a CryoSat Processing Prototype (CPP) to facilitate the development and testing of CNES innovative methods for processing SAR mode data over ocean. This was implemented in an attempt to provide very accurate and valuable data products that would permit the full exploitation of the capabilities of the CryoSat-2 SIRAL radar altimeter, and more globally assess the benefits of the SAR mode whose improvements have only been predicted in theory up to now. This investigation is also relevant for the specification of the SAR mode to be embarked on-board the Jason-CS mission. In addition, it addresses a number of questions relating to the SAR mode, such as the performance of the various retracking algorithms, the altimeter technologies (closed burst mode vs. interleaved), the SAR mode retrievals sensitivity (to satellite pointing and directional waves), the Sea Surface Bias (SSB), and land contamination, to name a few. It is part of a challenging program led by operational and research agencies (ESA, EUMETSAT, NOAA, CNES and NASA) that are primarily concerned with meeting the future expectations of the

scientists and operational users from the ocean community and other scientists interested in the remote sensing of sea-ice, land ice and hydrology.

Although the along-track improvement in sampling resolution is straightforward, some uncertainties still remain in the retrieved elevations as well in the accuracies of the other surface parameters. For example, one of the main issues is to demonstrate whether, in practice, the SAR mode height is actually better or worse than the LRM one. To allow the assessment of the in-orbit performances of the SAR mode data and in the same manner the quality of the processing method, CNES has designed the CPP with the ability to generate and/or process two other sets of CryoSat-2 waveforms:

- the Reduced SAR (RDSAR) mode data, aka LRM look-like or pseudo-LRM, that provide a LRM reference over the same ground tracks during SAR mode (enabling direct comparisons of their retrievals performance);
- the LRM mode data to ensure that the data quality continuity between SAR and LRM measurement modes can be achieved.

Both are processed separately on-ground by the CPP facility then retracked using a conventional Brown ocean retracker, but different geographical regions are covered from each other, one corresponding to the SAR mode locations and the other corresponding to the LRM mode areas which spread over wide ocean-regions.

On-board the CryoSat-2 mission, SAR mode data are processed in a closed burst mode providing 4 bursts per 20-Hz tracking cycle (64 pulses at 18 kHz rhythm used in one burst). Thus when SAR data are processed in a pulse-width limited manner, the timing and number of pulses (FBR echoes) per unit time is different to the LRM sequence of a conventional altimeter (90 independent pulses regularly spaced per tracking cycle). The RDSAR method implemented in CPP consists of averaging all pulses from 4 successive SAR bursts (i.e. 4*64 = 256 FBR echoes) to form a 20 Hz Brown echo. However a much smaller number of pulses are contributing to the range noise reduction of the resulting waveform, since significant pulse-to-pulse correlations occurs at the PRF of 18 kHz [Boy et al., 2011]. Only 32 pulses, corresponding to a ~2 kHz frequency, are contributing to the speckle de-correlation instead of 90 for CryoSat-2 LRM for weak SWH, which leads to a noisy RDSAR waveforms and, thereby, a retrieved range error multiplied by a factor of sqrt(90/32) for comparison with LRM one. In practice the overall noise performance is slightly further improved since de-correlation of thermal noise occurs at higher PRF.

Prior to be averaged, each individual pulse must be shifted in the range window to be aligned on the first pulse of the cycle. The shift is computed from the vertical velocity (extracted from the COR2 altimeter command or from the orbit information). For each pulse, the range shift must be calculated taking into account the on-board altitude command already applied by the altimeter (equal to the Coarse Altitude Instruction, CAI, of the 1st pulse of each burst). So, only the

Fine Altitude Instruction (FAI) must be on-ground calculated and applied to each pulse to generate the pseudo-LRM echo.

3.2.2.4 Pseudo-LRM techniques at NOAA

Since October 2011 NOAA has been producing CryoSat-2 products similar to the Interim Geophysical Data Records (IGDR) as we know them from the Jason-1 and Jason-2 projects. These "IGDR" products first featured only the Low Resolution Mode (LRM) data, retracked and enhanced from the CryoSat-2 Level 1B products. In October 2012, NOAA added so-called Pseudo-LRM data, created out of the CryoSat-2 Level 1A SAR data, providing a nearly global coverage. After retracking, the RADS (Radar Altimeter Database System) is used to add or update all the commonly used geophysical corrections and then distributed to a multitude of users. This work is also extensively discussed in **[Scharroo et al., 2013]** including cross-calibration and validation. Here we suffice with describing the method and assumptions, whereas validation will be discussed in WP4000 of the project.

In order to extend the CryoSat-2 data products to the coastal zone and fill other gaps in LRM coverage, NOAA developed a process in which the SAR data are first combined into "Pseudo-LRM" (PLRM) or "reduced SAR" waveforms, which are similar to the conventional pulse-limited waveforms. The reduced SAR waveforms are retracked and combined with the LRM data to form a harmonised product. Although this sounds relatively straightforward, many steps were needed to get this done 20 times per second:

1. Gather 4 bursts of 64 echoes.
2. Align them to a common range by phase shifting the complex power for each of the bins for each echo by a phase shift equivalent to the change of range compared to the middle one. The change of range is based on the altitude rate rather than the on-board tracker information.
3. Apply a 1-dimensional FFT to the data in the frequency direction (128 bins). This creates 256 complex and very noisy "waveforms".
4. Incoherently average (i.e. average the power) of each of the 128 bins across the 256 individual waveforms to form a single Pseudo-LRM waveform at 20-Hz.
5. Apply the low-pass filter correction.
6. Construct range, significant wave height and backscatter in a meaningful way, consistent with low-rate data.
7. Cross-calibrate the conventional and Pseudo-LRM data.

These Pseudo-LRM data have been merged with LRM data and have been available via RADS since October 2012. The status presented here is that of early 2013. Various newer developments are under implementation but have not been assessed yet.

The next sections will describe each of the 7 steps discussed above. See for a schematic illustration Figure 3.22
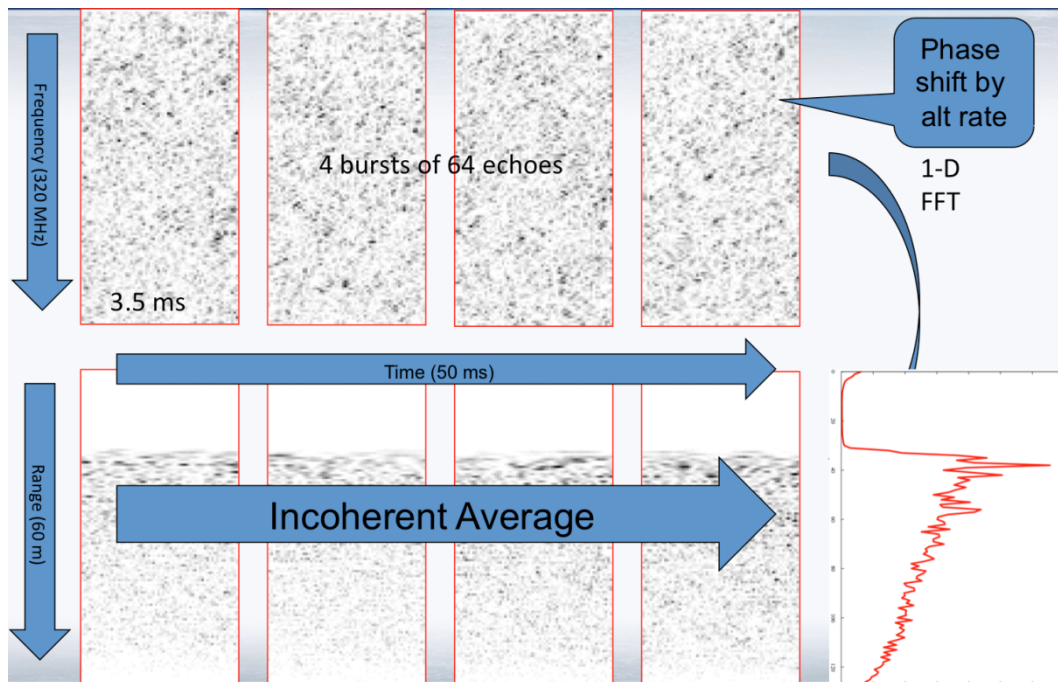
Figure 3.22 Schematic illustration of the conversion from 256 SAR mode echoes to one Pseudo-LRM waveform

3.2.2.4.1 Gather echoes

Every 50 ms, the CryoSat-2 altimeter sends 4 bursts, each with a duration of only 3.5 ms. Each burst contains 64 pulses and is followed by 9 ms of "silence" while waiting for the echoes of those pulses to return. During those pulses the power level (AGC setting) remains the same, but the range window will move at the beginning of each burst to keep the leading edge at roughly one quarter of the range window.

The Level 1A product is blocked in chunks of 64 echoes. In order to eventually match the usual 20-Hz repetition frequency of the LRM products we process 4 bursts of 64 echoes, 256 echoes in total, simultaneously.

3.2.2.4.2 Align the echoes

During the period of 0.5 ms the range window is adjusted four times. The coarse and fine height word, also referred to as LAI and FAI, describe the total time (and hence) range delay before the echoes are being captured. This positioning of the range window is based on the on-board tracker and will not provide an accurate range measurement. Moreover the *rate* of change of the range window may not be precise enough to keep the leading edge at a consistent place during the 0.5 ms period.

In order to make their power profiles coincide, we replace the height rate as determined by the course and fine height word by the altitude rate as determined by precise orbit determination. The difference between the two determines a correction of the phase of each bin of the received echo. In other words,

$$p_{kj}=(I_{kj}+iQ_{kj})\cdot e^{i\phi_{kj}}$$

The phase shift ϕ_{kj} to be added to the complex amplitude values I_{kj} and Q_{kj} for bin k in echo j becomes:

$$\phi_{kj}=k-63.5\Delta\phi_{kj}$$

where the phase shift per bin equals

$$\Delta\phi_{kj}=2_{j}-63\Delta\tau_{j}+\tau_{FAI}\omega_{k},$$

the range delay between echoes and the fine window delay (expressed in time) are

$$\Delta\tau_{j}=h_{c}\cdot 55\text{ns}$$

$$\tau_{FAI}=FAI256\cdot 12.5\text{ ns}$$

and the phase rate ω_{k} is $-2\pi400$ ns .

3.2.2.4.3 Apply 1-D FFT

In the next step we convert each echo from the frequency domain to the time domain by performing a one-dimensional Fast Fourier Transform over the 128 frequency bins. This creates 128 bins (or gates) of complex amplitudes P_{kj} in the time domain.

$$p_{kj}FF\ P_{kj}$$

This step can be performed differently following the suggestion by Jensen et al. (2001). The argued that since we are squaring the power (in the next step), some power gets aliased, and we in fact lose some of the resolution (particularly at low sea states). To solve that, Jensen et al. suggest to extended the frequency domain to 256 bins by padding the 128 existing ones with zeros, and then do the FFT to obtain 256 complex gates (with twice the resolution) in time domain.

3.2.2.4.4 Incoherently average

We are now compute the power P_k in each of the 128 gates (i.e. compute the absolute value of the complex numbers) and average those numbers across the 4 bursts. In other words

$$P_k=j|P_{kj}|$$

This creates a pseudo-LRM waveform: 128 gates of power per 20-Hz interval.

3.2.2.4.5 Apply low-pass filter correction

Just as is the case for LRM waveforms, the low-pass filter correction needs to still be applied to the just achieved waveform. This correction accounts for the fact that the low-pass filter (LPF) applied in the altimeter to determine the intermediate frequency signal is not perfect and creates more power in some gates than in others. The correction is based the echo returned from just receiving white noise. Each waveform sample *Pk* needs to be multiplied by the LPF correction factor *ck* is a function of the gate number and stored in the IPF database.

3.2.2.4.6 Construct range, significant wave height and backscatter

The method of deriving measurements of range, significant wave height, and backscatter is more or less the same as would be done from conventional LRM data. We simply apply the same 3-parameter maximum likelihood retracker (MLE3) as we do for conventional altimetry (e.g. Amarouche et al., 2004). The only key points of differences between the two are:

- The power level differs between LRM and SAR, which affects the computation of the backscatter coefficient.
- The gain in the on-board processing of the LRM echoes and the gain in the reduced SAR processing is different. Theoretically they are 82.533 dB and 126.227 dB, respectively, but NOAA and Altimetrics LLC found 82.356 and 125.8 dB instead.
- Because in SAR mode the instrument pulses only about 3.5 ms out of 12.5 ms, there are fewer independent measurements than in LRM mode. This increases the noise in the eventual 20-Hz measurements of range, significant wave height, and backscatter.

3.2.3 *Review data integration methods: optimized methods to integrate data from multiple satellite altimeters*

Data integration methods concern optimized methods to integrate data from multiple satellite altimeters targeted to develop higher resolution products, in time and space. Especially spatial resolution is of importance in areas where high detail is sought like in the coastal areas. SAR resolution might already provide the necessary spatial sampling but it might also be beneficial to merge datasets from different satellites. For one satellite the chosen orbit is always a compromise between spatial and temporal sampling: choice for high repetition means giving in in cross-track resolution and vice versa choice for denser spatial sampling means giving in on repeatability. Merging different datasets or data sources always means some form of interpolation of the data. There are several methods that start with simple binning the combined data, to some form of weighing the distance from measurement to the interpolation point, and to some form of optimal interpolation of data incorporating a priori information, or even data assimilation

into (simple) models (dynamic interpolation). The choice is very dependent on the final purpose of the higher resolution product, e.g. is it a sea level anomaly, an absolute dynamic height, a mean sea surface field or bathymetry. The latter would call for specialized methods like the direct method and the stochastic method.

[LeTraon et al., 1998] proposed an improved method based on conventional objective analysis and taking into account the along-track correlated long-wavelength error. This method could take care of the orbit error, which otherwise would corrupt the SLA field and by that the deduced geostrophic currents, especially in low-energetic areas. Later on this method was adopted and adapted in the SSALTO/DUACS system from AVISO [**Ducet et al., 2000**]. Here they use a combination of crossover minimization and optimal interpolation to arrive at combined SLA fields and absolute dynamic height (ADT) fields. For the results on the ENSO and Gulfstream pages at the RADS server also altimeter data from several missions are combined using crossover minimization in combination with an iterative distance weighted gridding method that applies decreasing e-fold parameter on the residuals in each of the iterative steps (usually 2 or 3 steps).

[Andersen and Knudsen, 1997] proposed an alternative/supplementary optimum interpolation/collocation method to the orbital adjustment method by LeTraon to handle along track signal in altimeter data in the interpolation of these. This interpolation method can be used in association with or independent from the method by LeTraon as the orbit error reduction method by LeTraon is performed prior to interpolation. However, when altimetry observations covering a temporal period like days or weeks must be interpolated to create a grid, there will always be residual along-track signal due to the natural ocean variability. This is i.e. shown in Figure X.1 in which DUACS data from the month of October 2008 are shown after the orbit adjustment by LeTraon has been applied. Obviously there is along-track residual signal that will create along-track signals in the interpolated product unless this is overly smoothed.

In this interpolation scheme by Andersen and Knudsen residual along-track errors can be modelled and taken into account in the collocation/optimum interpolation method by modelling this in the covariance function. Here a separate covariance function for the along-track error is introduced to model this signal and this covariance is added to the signal covariance covariance signal for observations on the same track to model this.

In CP4O we will apply these data integration methods to see how existing products benefit from the inclusion of the CP4O CryoSat-2 products.
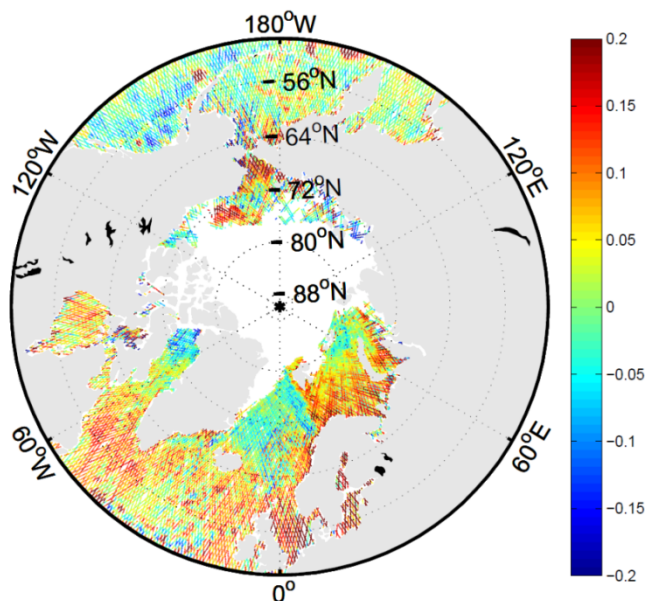
Figure 3.23 Residual along-track signal seen in the DUACS V3.0 Envisat data after orbit adjustment by LeTraon for the month of October 2008. Along track signal (as expected as data for one month is used) due is to ocean variability is clearly seen.

3.2.4 Review improved corrections

3.2.4.1 Wet tropospheric correction for CryoSat

The path delay (PD) due to the presence of water vapour in the atmosphere, the wet tropospheric correction (WTC), is one of the major error sources in satellite altimetry. With an absolute value less than 50 cm, it is highly variable both in space and time.

The mean value (Figure 3.24) shows a near zonal variation with very small values (< 5 cm) at high latitudes and maximum values (up to 35 cm) near the equator and the tropics. Figure 3.25 shows the standard deviation of the WTC, ranging from only 1-5 cm in the polar regions up to 10-15 cm in the tropics.

Due to this high variability, the most accurate way to model this effect is through the measurements of microwave radiometers (MWR) on board the altimetric missions. Two-band radiometers have been used in ERS-1, ERS-2 and Envisat and three band radiometers in Topex/Poseidon, Jason-1 and Jason-2. However, some altimetric missions such as CryoSat 2 (CS-2) do not carry an on-board radiometer, relying on model corrections such as the one provided by the European Centre for Medium-range Weather Forecasts (ECMWF), which is intrinsically less accurate than the direct measurements and tends to lack spatial detail. Therefore, alternative methods need to be pursued to tackle this problem.

CP4O	Preliminary Analysis Report	D2.1	

In the scope of CP4O a new methodology, based on the approaches described by **[Fernandes et al., 2010]** and **[Stum et al., 2011]** shall be developed. The basis of this approach is the data combination (DComb) through objective analysis of all existing data sources.

The ultimate aim of this study is the development of a wet tropospheric correction for CryoSat 2, with improved accuracy with respect to the current correction provided by ECMWF. This will be achieved by implementing a data combination methodology whereby, at each along-track location, the WTC is estimated, by objective analysis, using all available wet PD data sources.

For this purpose, the following main data sets have been identified and collected, globally, for the period of the CS-2 mission (since April 2010):

1. Water vapour products (Total column water vapour, TCWV) from passive microwave imaging radiometers on board remote sensing (RS) satellites;
2. Zenith total delays (ZTD) available online from coastal Global Navigation Satellite Systems (GNSS) stations;
3. Global grids at 0.75º×0.75º and 6-hour interval, from the ERA (ECMWF Reanalysis) Interim model.

The computation will be performed globally, therefore covering all open ocean, polar regions and coastal zones.

In this task the state-of-the-art on the computation of the wet tropospheric correction is reviewed, aiming to identify the best approach to derive the correction for CryoSat-2 with the highest possible accuracy, better than the one currently provided by the ECMWF model.
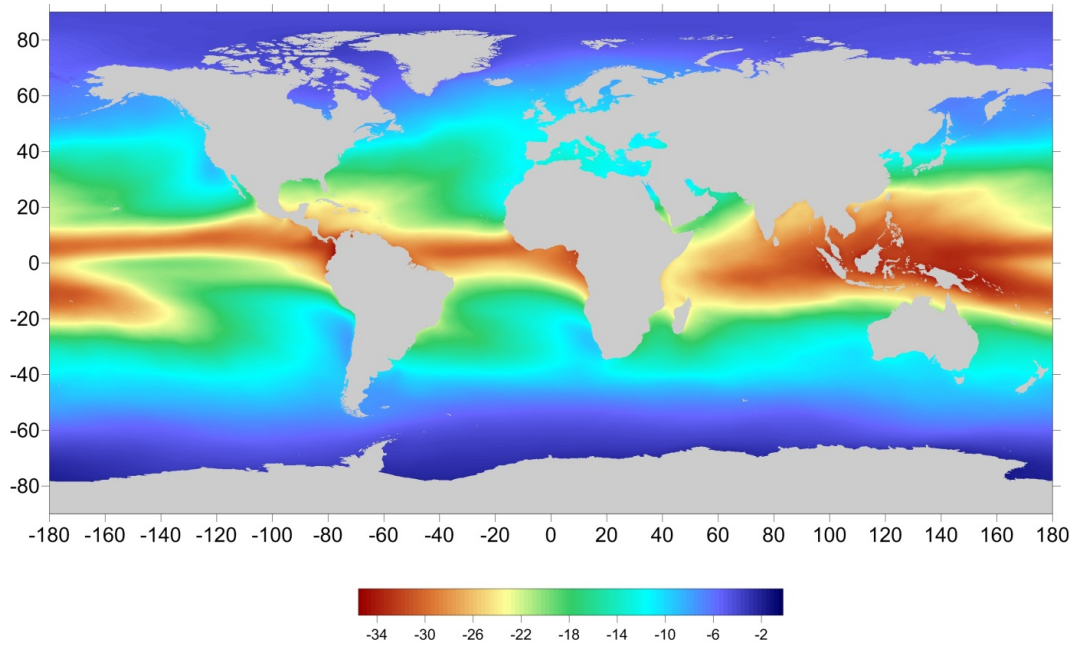
Figure 3.24 Mean value of the wet path delay field (cm).
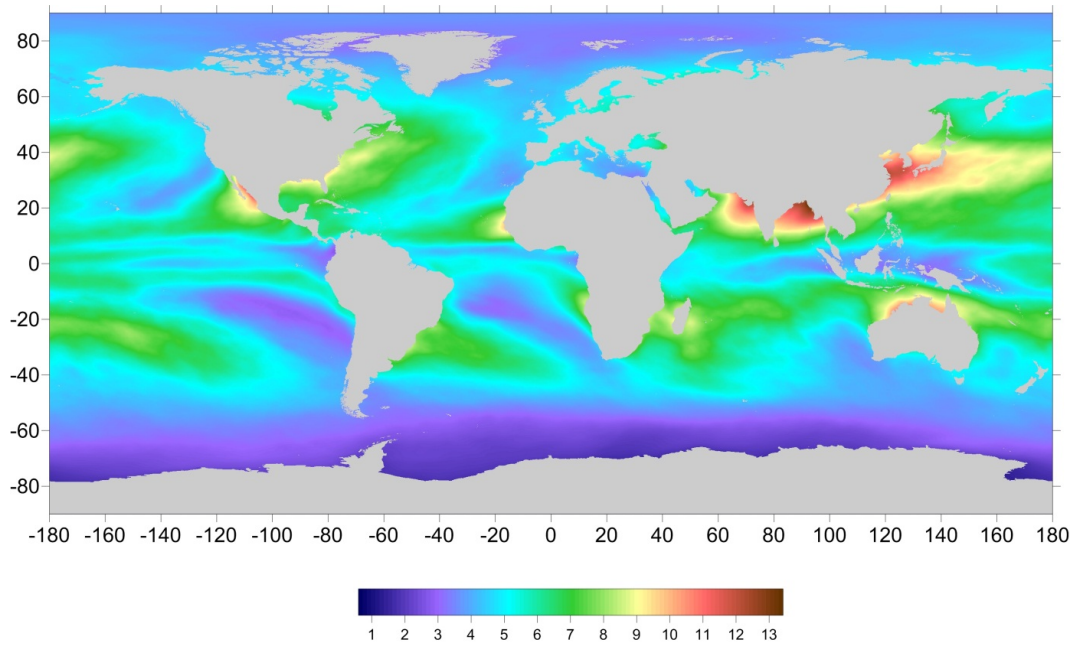
Figure 3.25 Standard deviation of the wet path delay field (cm).

3.2.4.1.1 From TCWV to WTC

The total column water vapour (TCWV), also referred as precipitable water (PW) or integrated water vapour (IWV), is the total water vapour contained in an air

column from the Earth's surface to the top of the atmosphere and is usually expressed in kg/m^2 or millimetres (mm), as the length of an equivalent column of liquid water.

The TCWV in millimetres is given by

$$W = \int_0^H \rho_w \, dz$$

Eq. 3-3

where ρ_w is the water vapour density in kilograms per cubic metre, z is the altitude (in m) , and H is the altitude above which the water vapour density is considered to be negligible.

The path delay due to the water vapour in the atmosphere, the WTC, can be estimated from TCWV and atmospheric temperature T by (e.g. **[Keihm et al., 1995]**:

$$WTC = 1.763 \int_0^H \frac{\rho_w}{T} \, dz$$

Eq. 3-4

where WTC is in metres and T is the temperature in Kelvin.

According to **[Bevis et al., 1994]** the WTC can be estimated from TCWV and T using the following expression:

$$WTC = -\left(0.101995 + \frac{1725.55}{T_m}\right)\frac{W}{1000}$$

Eq. 3-5

where W stands here for TCWV and T_m is the mean temperature of the troposphere, which may be in turn modelled from the surface temperature T_0) according to e.g. **[Mendes, 2000]**:

$$T_m = 50.440 + 0.789 \, T_0$$

Eq. 3-6

In Eq. 3-5 and Eq. 3-6, T_0 and T_m are in Kelvin, W in millimetres and WTC results in meters.

These two equations are appropriate to derive WTC from numerical weather model (NWM) fields, since these models provide both parameters: W and T_0 (2-metre temperature, 2T, in ECMWF models).

Alternatively, the direct dependence of the water vapour density on the temperature can be avoided by establishing a direct relationship between WTC and TCWV (e.g. **[Keihm et al., 1995]**, **[Keihm et al., 2000]**, **[Stum, 2011]**, since the ratio between WTC and TCWV can be described by a decreasing function of water vapour content, which partly expresses the WTC temperature dependence.

For example, in **[Stum, 2011]** the following relationship was deduced from temperature and humidity profiles from the ECMWF model fields:

$$\frac{WTC}{W} = -(a_0 + a_1 W + a_2 W^2 + a_3 W^3) \cdot 10^{-3}$$

Eq. 3-7

with a_0=6.8544, a_1=−0.4377, a_2=0.0714, a_3=−0.0038, W is in mm and WTC results in metres.

[Keihm et al., 2000] provide a similar expression which gives WTC values about 1% larger than those given by Eq. 3-7 **[Stum et al., 2011]**.

For less accurate studies, WTC can be considered approximately proportional to W by

$$WTC\ (m) = -0.0067\ W(mm)$$

Eq. 3-8

In this study, both expressions Eq. 3-5 and Eq. 3-7 will be considered in order to identify the most suitable for use with each data set. Preliminary results not shown here (comparison of wet PD computed using both procedures with wet PD from ERA Interim) indicate that the first procedure (Eq. 3-5) is the one that provides the best accuracy.

3.2.4.1.2 WTC from GNSS data

GNSS data from over 300 coastal stations are available online (Figure 3.26). These include zenith total delays (ZTD) at a set of IGS (International GNSS Service) and EPN (EUREF Permanent Network) stations. Only stations up to 50 km from the coast and with an orthometric height < 1000 m are considered.
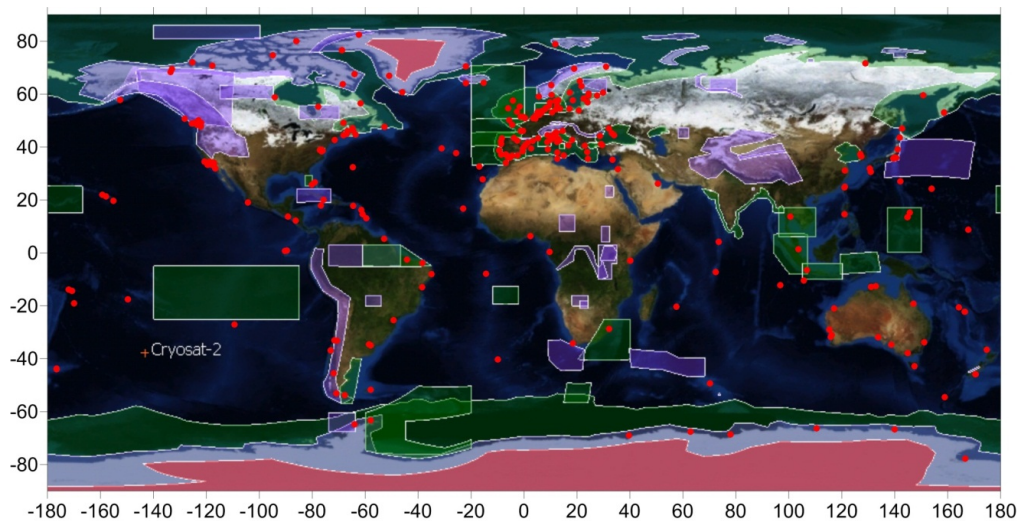
Figure 3.26 CryoSat-2 modes mask 3.4 and GNSS coastal stations

The quantity estimated at each GNSS station is the total tropospheric delay (ZTD) at station level. The quantity used in coastal altimetry is the zenith wet delay (ZWD) at sea level. This is obtained from the ZTD at station level by computing the dry correction or zenith hydrostatic delay (ZHD) from the ECMWF sea level pressure (SLP) field using the Saastamoinen model **[Davis et al., 1985]** and reducing ZHD and ZWD fields to sea level using the procedure by **[Kouba, 2008]**. Details of this processing can be found in **[Fernandes et al., 2010]** and **[Fernandes et al., 2012]**.

The development and implementation of the GNSS-derived Path Delay (GPD) wet tropospheric correction has been one of the main achievements of the COASTALT project, as discussed below in Section 3.4. GNSS data will continue to play a major role in the improvement of the WTC in the coastal regions.

3.2.4.1.3 WTC from ERA Interim

The ERA Interim model provides global grids of TCWV and 2-metre Temperature (2T) at 0.75°x0.75° spacing, every 6 hours. From these fields, at each grid node, the wet path delay caused by the troposphere in the altimeter measurement can be computed from TCWV and the surface temperature 2T using Eq. 3-5 and Eq. 3-6.

Studies (not presented here), have shown that, since about 2004, the accuracy of ERA Interim model is similar to present ECMWF operational model and has the advantage of being homogeneous through time. Therefore, ERA Interim has been identified as the most appropriate model for use in this study.

CP4O	Preliminary Analysis Report	D2.1	

3.2.4.1.4 WTC from microwave radiometers

Passive microwave radiometers on board remote sensing (RS) satellites make measurements in various water vapour absorption bands of the microwave spectrum. These measurements are converted into Brightness Temperatures (TB). From the measured TBs (usually in two or three channels), the TCWV is computed.

As shown in Section 3.2.4.1.1, the WTC can then be derived from TCWV and atmospheric temperature using Eq. 3-5 and Eq. 3-6, where the values of *T0* can be taken from a NWM such as ECMWF (either the operational model or ERA Interim), or from a direct relationship such as Eq. 3-7.

Water vapour products from scanning imaging MWR

For use in this project a database of water vapour images from all scanning MWR sensors on board RS satellites, for the period of the CryoSat-2 mission (since April 2010, until present) was set up.

Two types of water vapour products containing the TCWV field have been used: 1) Level-2 swath products, whenever available; 2) Level 2 gridded products, otherwise. Swath products are available in HDF-EOS2 format, while gridded products are available in binary format.

The existing products and their main characteristics are summarised below and in Table 3-5 and Table 3-6 (status as in February 2013).

Scanning MWR sensors on board RS satellites providing water vapour images:

1. Advanced Microwave Sounding Unit A (AMSU-A) on board the National Oceanic and Atmospheric Administration (NOAA) satellite series (NOAA-15, -16, -17, -18, -19) and on board the European Organisation for the Exploitation of Meteorological Satellites (EUMETSAT) MetOp-A satellite;
2. Advanced Microwave Scanning Radiometer-Earth Observing System (AMSR-E) on board the National Aeronautics Space Administration (NASA) Aqua satellite   unfortunately the AMSR-E antenna stopped spinning on October 4 2011;
3. Tropical Rain Measuring Mission (TRMM) Microwave Imager (TMI) on board the joint NASA and Japan Aerospace Exploration Agency TRMM satellite;
4. Special Sensor Microwave Imager (SSM/I) and Special Sensor Microwave Imager/Sounder (SSMIS) on board the Defense Meteorological Satellite Program (DMSP) satellite series (F15, F16, F17 and F18,). SSMIS is an instrument similar to the SSM/I, but with additional sounding capabilities. The SSMIS data have been carefully inter-calibrated on the brightness temperature level with the previous SSM/I, therefore extending this important time series of water vapour products;

5. WindSat Polarimetric Radiometer developed by the Naval Research Laboratory (NRL) aboard the Department of Defense Coriolis satellite;
6. NPP/ATMS - National Polar-orbiting Operational Environmental Satellite System (NPOESS) Preparatory Project/Advanced Technology Microwave Sounder.

Data access:

1. AMSU-A level-2 swath products are made available by NOAA through its Comprehensive Large Array-Data Stewardship System (CLASS): http://www.class.ngdc.noaa.gov. The Microwave Surface and Precipitation Products System (MSPPS) Orbital Global Data products (MSPPS_ORB) have been used. CLASS also provides similar products for SSM/I (F15).
2. For the AMSR-E, the Level-2B ocean swath (AE_Ocean) data set was downloaded from the National Snow and Ice Data Center (ftp://n4ftl01u.ecs.nasa.gov/SAN/AMSA/AE_Ocean.002/)
3. For TMI, the level-2 product swath data set was acquired from the Global Hydrology Resource Center (ftp://ghrc.nsstc.nasa.gov/pub/data/tmi-op/)
4. SSM/I and SSMIS data are available through Remote Sensing Systems (RSS) (http://www.ssmi.com/ssmi/ssmi_browse.html), which provide ocean data products for the DSMP satellites from F08 to F18. According to information on December 2012, products for F18 were not yet available. After August 2006, F15 products are affected by RADCAL beacon interference. The release F15 version 7 products have been corrected for this effect. In spite of this, RSS recommends that after August 2006 F15 products should not be used for climate studies. Due to required calibration and correction, F15 V7 products are provided with some delay, at present until end of 2011.

   For this study, data for F15 (SSM/I), F16 and F17 (SSMIS) were downloaded from ftp://ftp.ssmi.com/ssmi/, although F15 data shall be used with care. These data are provided in the form of daily binary files, two global grids at 0.25°x 0.25°, one containing data for all ascending and another for all descending passes. For all RSS SSM/I and SSMIS satellite products, when adjacent passes overlap at high latitudes, daily maps are created by overwriting earlier observations when the time difference between the observations is greater than 50 minutes. For WindSat the early observations are used and are not overwritten unless an observation is missing.
5. WindSat data are available through Remote Sensing Systems (RSS) (ftp://ftp.remss.com/windsat) also in the form of grid binary files - see point 4) above; Windsat version 7 products are being generated with some delay. At present they are only available until the end of 2011. For the remaining period the near real time products are available. RSS also provides similar gridded products for AMSR-E.

6. For NPP/ATMS, data can be acquired from the NOAA CLASS system (http://www.class.ngdc.noaa.gov) by selecting the "NPP Advanced Technology Microwave Sounder – ATMS" product. This is still BETA data and therefore it was not yet used in this study.

Table 3-5 Main orbital characteristics, compared with CryoSat-2, of the satellites with scanning MWR images of TCWV available for this study. Light grey cells refer to swath products while dark grey cells refer to gridded products. LTAN is the Local Time of the Ascending Node. (*) According to RSS, due to RADCAL beacon interference F15 data shall not be used for climate studies after August 2006. (**) WindSat Version 7 of RSS products are only available until the end of 2011.

Satellite	Sensor	h (km)	Inc. (º)	Per. (min)	Sun-syn. orbit	LTAN Jan 2011 hh:mm	LTAN Jan 2012 hh:mm	Data avail For CS2
CryoSat-2	-	717	92.0	93.2	NO	N/A	N/A	since April 2010
AQUA	AMSR-E	705	98.0	99.0	YES	13:36	-	until Oct 04 2011
NOAA-19	AMSU-A	870	98.7	102.1	YES	13:32	13:32	until present
NOAA-18	AMSU-A	854	98.7	102.1	YES	14:07	14:30	until present
DMSP-F15	SSMI	850	98.8	102.0	YES	16:44	16:05	(*)
NOAA-15	AMSU-A	807	98.5	101.1	YES	16:35	16:35	until present
Coriolis	WindSat	830	98.8	101.6	YES	17:54	17:54	(**)
DMSP-F17	SSMIS	850	98.8	102.0	YES	17:30	18:06	until present
DMSP-F16	SSM/IS	845	98.9	101.8	YES	19:12	18:30	until present
NOAA-17	AMSU-A	810	98.7	101.2	YES	20:20	19:40	until present

NOAA-16	AMSU-A	849	99.0	102.1	YES	19:16	20:00	until present
MetOp-A	AMSU-A	817	98.7	101.4	YES	21:26	21:27	until present
TRMM	TMI	402	35.0	93.0	NO	N/A	N/A	until present

Table 3-6 Main characteristics of the sensors with scanning MWR images of TCWV available for this study. The scale factor is the value required to multiply the original product value to get the TCWV in mm. (*) – Swath product from CLASS. (**) Grid product from Remote Sensing Systems. (***) For AMSU-A the value provided is the central pixel size; the maximum pixel size is 130 km.

SENSOR	PIXEL SIZE (km)	SWATH WIDTH (km)	N. OF (LINES,PIXELS)	NAME OF PRODUCT	SCALE FACTOR	DATA TYPE
AMSR-E	9 km	1625	(variable,243)	Med_res_vapor	0.01	SWATH
AMSU-A	50 km (***)	2200	(variable,30)	TPW	0.1	SWATH
TMI	10 km	878	(variable,104)	Columnar_water_vapor	0.01	SWATH
SSM/I (*)	25 km	1420	(variable,64)	TPW	0.1	SWATH
SSM/I, SSMIS (**)	0.25°	1790 - 1850	(720,1440)	VAPOR	0.3	GRID
WINDSAT	0.25°	1400	(720,1440)	VAPOR	0.3	GRID

Creation of a database of TCWV image products

To facilitate the data access and selection by the data combination (DComb) algorithm, all images were organised in a database, where all files were renamed according to the following code name:

"sss_iii_Dyyyyddd_Shhmm_Ehhmm_Onnnnnn_x_LLLL_CCC.eee"

CP4O	Preliminary Analysis Report	D2.1	

Each field is described in Table 3-7, Table 3-8, and Table 3-9.

On a second step, for all products, new image files were created containing only the required fields: time, latitude, longitude and TCWV. In addition, gridded products were also sorted by ascending time order.

Table 3-7 Names adopted for each sensor

Sensor Name	File Name
AMSR-E	AME
AMSU-A	AMA
SSMI/SSMIS	SSM
TMI	TMI
WindSat	WSA

Table 3-8 Names adopted for each satellite

Satellite Name	File Name
Aqua	AQU
NOAA-15	N15
NOAA-16	N16
NOAA-17	N17
NOAA-18	N18
NOAA-19	N19
MetOp-A	MTA
DMSP-F15	F15
TRMM	TRM

Coriolis	COR

Table 3-9 Format code used in files. X can have the values: A (ascending), D (descending), T (total orbit) or G(grid). eee can be 'he2' or 'bin'

Format	Meaning
sss	Satellite Name (Table 3)
iii	Sensor Name (Table 4)
Dyyyyddd	Year and day of year
Shhmm	Hours and minutes at beginning of data collection
Ehhmm	Hours and minutes at end of data collection
Onnnnnn	Orbit number of the start of data collection
X	Orbit direction
LLLL	Number of lines
ppp	Number of pixels
eee	File extension

Analysis of spatial and temporal coverage of MWR images with respect to CS-2

In this section we present an analysis of the type of coverage of MWR images that can be expected for CryoSat-2. The first remark is that, except for TMI, all sensors are on board satellites with sun-synchronous orbits with an inclination close to that of CS-2. This means that the local time of ascending node (LTAN) of each satellite remains constant all over the year. On the contrary, since CryoSat-2 orbit is not sun-synchronous, and with a very long repetition period (369 days), every day the satellite will have a pass over a different location and the corresponding LTAN will vary all over the year. This means that the set of RS satellites which provide good space-time coverage for CS-2 at a given epoch, or, say, are in phase with CS 2, a few months later will be out of phase, with a large time difference between the acquisition time of the corresponding images and the CS-2 passage. According to Table 3-5, leaving out the AQUA satellite since it stopped working in October 2011, there are 10 missions in near polar sun-synchronous orbits providing water vapour products (short names according to Table 3-8): N15, N16, N17, N18, N19, MTA, F15 (with some restrictions), F16,

F17 and COR. In summary, since October 2011 there is a total of 11/12 satellites, with 4 different sensors with variable pixel size: 50 km, 25 km and 10 km (see Table 3-6).

To have an idea of the space-time coverage of these images with respect to CS-2 passages all over the year, the longitude of equator crossings (ascending and descending), here referred as Lon_Node, and corresponding epochs were determined for CS 2 and all 10 sun-synchronous satellites mentioned above. Figure 3.27 shows Lon_Node versus time, at middle of CS-2 sub-cycle 17 (July 2011), for a period of two days. It can be observed that the time distribution of the MWR images is not uniform throughout the day, the maximum time difference between two images being around 4 hours (between an ascending MTA and a descending N19 image or vice-versa). Overall, the whole set of images constitutes a large and valuable data-set of TCWV products available for the WTC computation of CS-2.

Figure 3.28 to Figure 3.31 illustrate how different the space-time coverage of the MWR images is for four different CS 2 sub-cycles separated approximately 3 months, for different times of the year and therefore of the CS 2 369-day cycle. For example, it can be observed that for sub-cycle 23 the coverage is poorer than for any of the other three cases. It can be shown (proof not presented here) that the CS-2 orbital configuration repeats with respect to a pure sun-synchronous orbit with a period of 482 days. Therefore, the configuration presented in Figure 3.28 to Figure 3.31 repeats every 482 days. In addition to the fact that CS 2 orbit varies with respect to the corresponding orbits of the sun-synchronous satellites, the LTAN of the latter may also drift in time, in particular for the oldest missions (e.g. Ignatov and Laszlo 2004). This is illustrated in Table 3-5, where the approximate LTAN of the various satellites is given for two epochs one year apart.

Finally, the most favourable conditions exist when an ascending CS 2 pass is in phase with an ascending pass of the RS satellite which is collecting the MWR images, since both passes are nearly parallel. When an ascending CS 2 pass is in phase with a descending pass of the RS satellite, only a fraction of the MWR images for that descending pass will be within an acceptable range and therefore usable for the WTC computation.
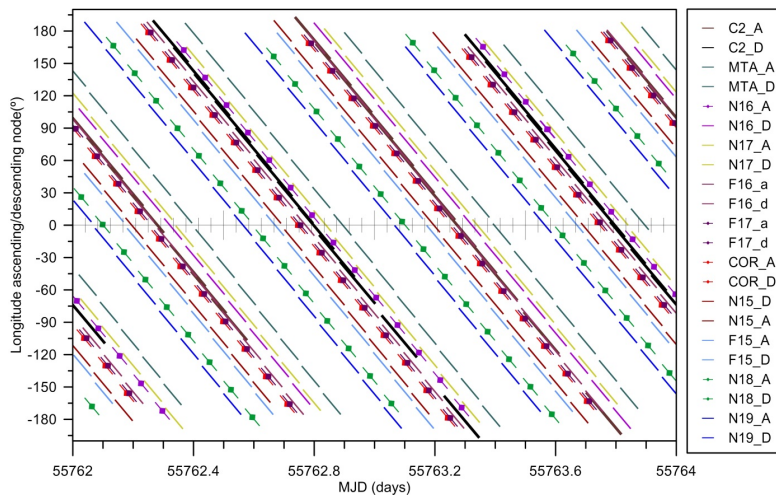
Figure 3.27 Longitude of equator crossings (ascending and descending) versus time, at middle of CS-2 sub-cycle 17 (July 2011), for 10 RS satellites (all presented in Table 1 except AQU and TRM).
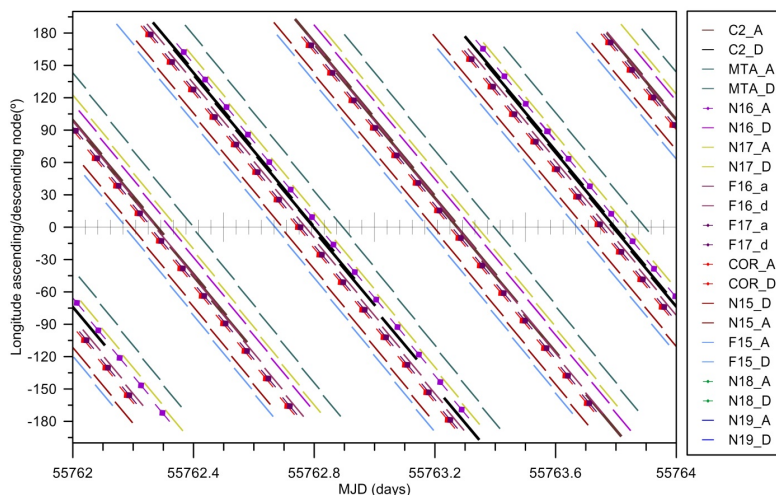
Figure 3.28 Longitude of equator crossings (ascending and descending) versus time, at middle of CS-2 sub-cycle 17 (July 2011), for the satellites with equator time differences less than 4 hours). AQU and TRM have not been considered.
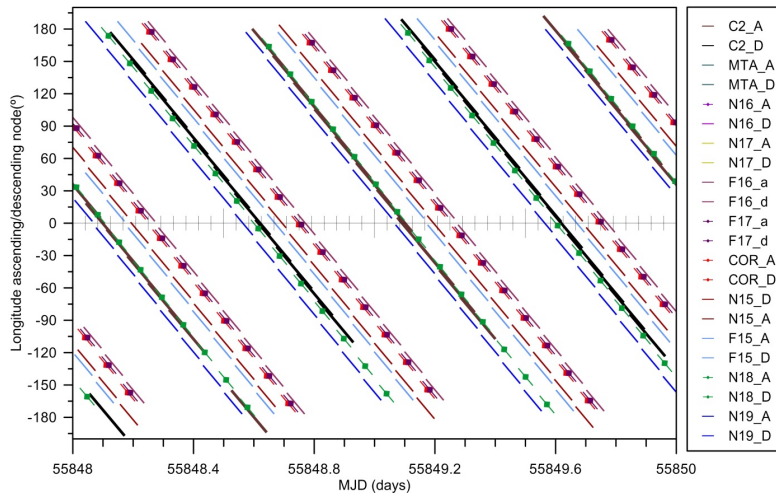
Figure 3.29 Same as on Figure 5 for CS-2 sub-cycle 20 (October 2011).
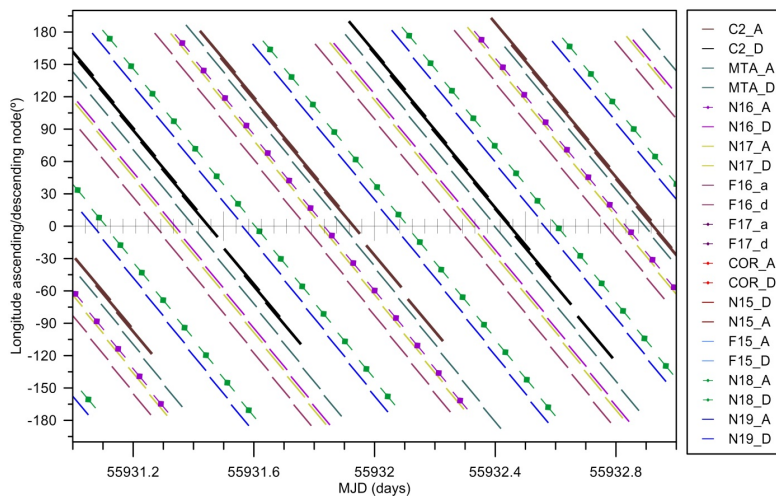
Figure 3.30 Same as on Figure 5 for CS-2 sub-cycle 23 (January 2012).
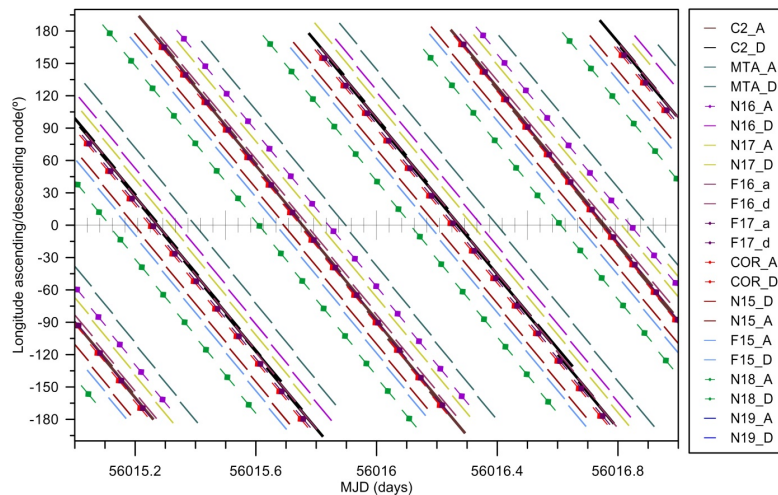
Figure 3.31 Same as on Figure 5 for CS-2 sub-cycle 26 (March-April 2012).

Figure 3.32 illustrates the two NOAA-17 and TRM images closest in time to the ascending pass 3 of CS 2 sub-cycle 26. Figure 3.33 shows all ascending passes of the Coriolis (WindSat) grid images for the day of pass 3, sub-cycle 26 passage (March 16, 2012). These two figures are representative examples of the swath and grid products used in this study.

In order to estimate the number of images available for the computation of the WTC for each CS 2 sub-cycle, the number of different images available for each CS-2 point along the satellite track was computed, considering different values for the time difference (ΔT) and distance (ΔD) between each CS 2 point and each image satisfying these conditions. This is illustrated in Figure 3.34 and Figure 3.35 for sub-cycles 23 and 26 respectively. In this analysis, only one every 30 CS-2 points were analysed (to save computation time) and various values were considered for ΔT and ΔD. For each MWR image, only points with valid TCWV values were considered. F15 images were not considered. The results are summarised in Table 3-10 and Table 3-11, for sub-cycles 23 and 26 respectively. In this analysis, Figure 3.34 and Figure 3.35 show that, as expected, the number of images available for the computation of the WTC increases with latitude, in the same way as the percentage of image overlaps (see Figure 3.32 and Figure 3.33). Due to its low inclination, TRM has a clear impact in the coverage of the low latitudes, in the band ±40°.
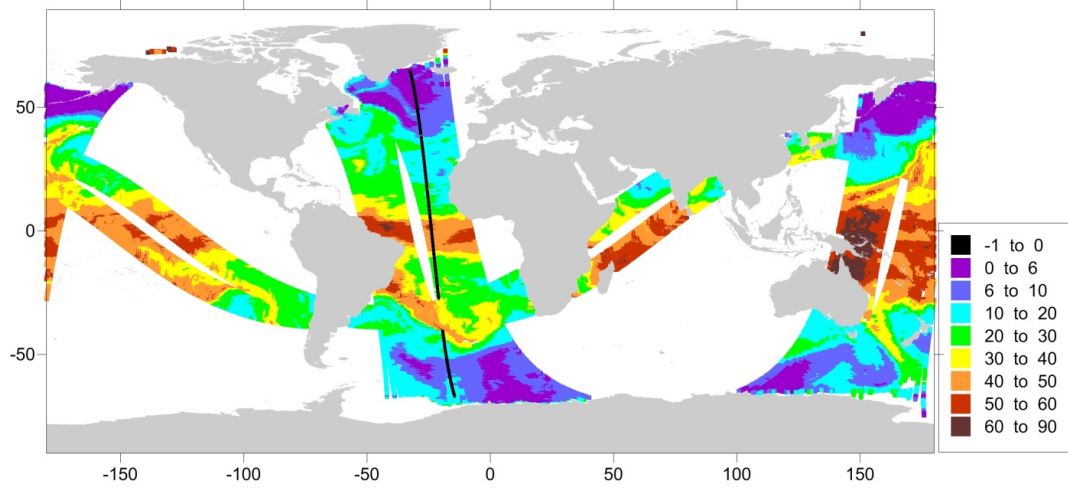
Figure 3.32 NOAA-17 (AMSU-A) and TRM (TMI) images closest in time to CS-2 ascending pass 3, sub-cycle 26. Colour scale is TCWV in mm.
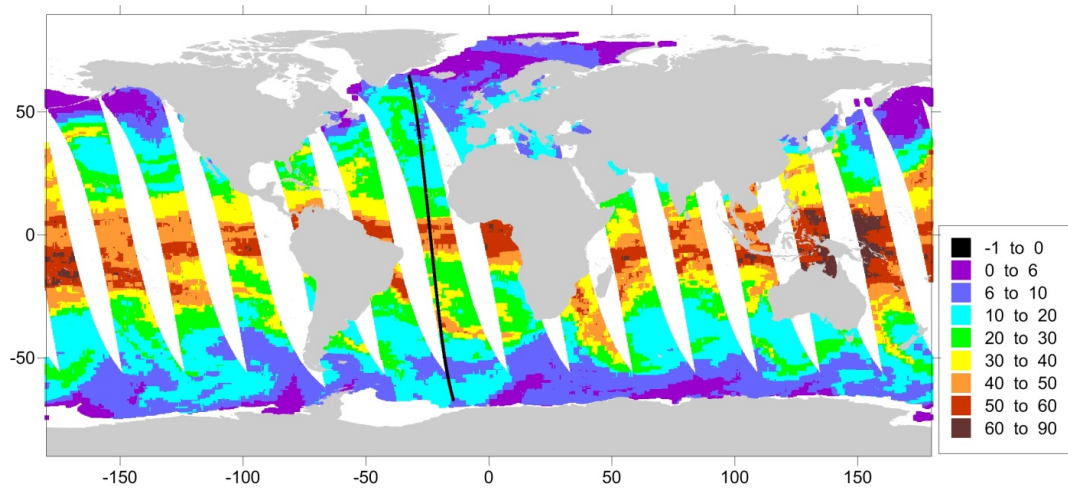
Figure 3.33 Coriolis (WindSat) ascending images for the same day of CS-2 ascending pass 3, sub-cycle 26 (March 16, 2012). Colour scale is TCWV in mm.
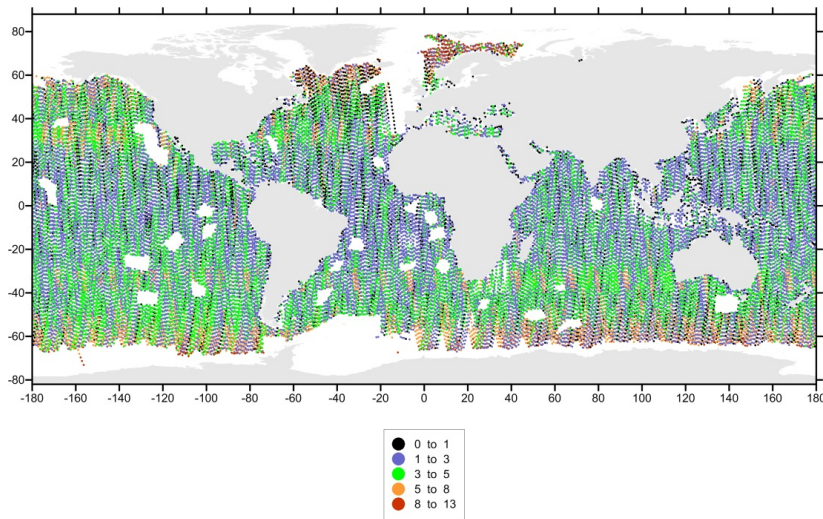
Figure 3.34 Number of images available for each CS-2 point, for sub-cycle 23, using ΔT = 180 min and ΔD = 75 km. The points with N=0 (10.2 %) are shown in black. F15 images were not considered.
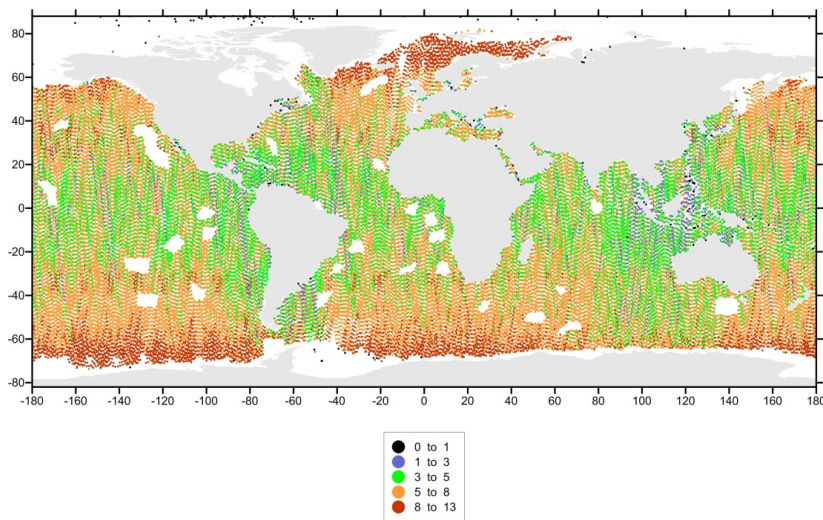
Figure 3.35 Number of images available for each CS-2 point, for sub-cycle 26 using ΔT = 180 min and ΔD = 75 km. The points with N=0 (0.3 %) are shown in black. F15 images were not considered.

Table 3-10 Percentage of points with zero available images (N0) for CryoSat-2 sub-cycle 23. The main contribution is from 5 different satellites: MTA, N16, N17, N19 and TRM.

ΔT \ ΔD	50 km	75 km	100 km

	50 km	75 km	100 km
60 MIN	65.2	62.5	61.3
90 MIN	54.0	50.7	49.2
120 MIN	39.9	36.2	34.6
150 MIN	24.9	21.3	19.8
180 MIN	13.6	10.2	9.0

Table 3-11 Percentage of points with zero available images (N0) for CryoSat-2 sub-cycle 26 as function of ΔT and ΔD. The main contribution is from 8 different satellites: N15, N16, N17, N19, COR, F16, F17 and TRM.

ΔT \ ΔD	50 km	75 km	100 km
60 MIN	8.9	7.2	6.6
90 MIN	2.9	2.0	1.6
120 MIN	1.0	0.5	0.3
150 MIN	0.9	0.4	0.3
180 MIN	0.8	0.3	0.2

As the previous analysis presented in Figure 3.27 to Figure 3.31 has shown, the number of images available within a certain time interval is not uniform throughout the year. Sub-cycle 23 is representative of one of the less favourable conditions while sub-cycle 26 is representative of one of the most favourable periods.

Considering these results, the time difference ΔT has a larger effect in the coverage than the distance ΔD. For sub-cycle 26 most of the points with the number of available images equal to zero (N0) are either at coastal areas or at high latitudes. Apart from these regions, for this sub-cycle full coverage is obtained within 2 hours. It can be observed that the distance ΔD has a clear impact in the coastal regions: decreasing ΔD increases the number of coastal points with no MWR images available. For sub-cycle 23, considering a time difference of 3 hours there are still about 10% of the points without any image within range. This stresses the importance of the remaining data sets to be used in the data combination algorithm: GNSS and ERA Interim model.

Considering the time difference, the critical value for ΔT is about 120 min, since the period of each satellite is about 100 minutes (see Table 1). However, for periods such as for sub cycle 23, increasing ΔT from 120 minutes to 180 minutes considerably increases the number of images available, reducing N0 from 36% to 10%, for $\Delta D = 75$ km.

3.2.4.1.5 Relation with CP4O sub-themes

The algorithm shall be implemented globally. This means that the correction will be available continuously, for each CS-2 location along the satellite track, for all mask modes. However, some regions deserve special attention: the polar and the coastal regions.

The specific problems of the retrieval of the wet tropospheric correction in the polar regions shall be investigated. In these regions the water vapour content of the atmosphere is small and the corresponding path delay usually does not exceed a few centimetres, both in terms of mean and standard deviation (see Figure 3.24 and Figure 3.25). However, the path delay retrieval from passive microwave radiometers is hampered by the ice contamination on the radiometer measurements. Since it is anticipated that this shall be the major problem to be addressed in these regions, techniques for efficient detection of ice contamination in MWR measurements shall be investigated.

Coastal regions play a major role in the exploitation of CryoSat-2 data since it is in these regions that the altimeter is operating in the higher resolution in the along-track direction SAR mode.

The problems associated with the computation of the wet tropospheric correction in the coastal regions, in the context of altimetric missions possessing an on-board MWR, have been addressed by several authors: **[Desportes et al., 2007]**, **[Fernandes et al., 2010]**, **[Brown, 2010]**, **[Obligis et al., 2010]**, and **[Obligis et al., 2011]**. These approaches cannot be directly applied to CS 2, since all of them rely on onboard MWR measurements. However, the approach followed by **[Fernandes et al., 2010]** and **[Fernandes et al., 2012]** can be adapted for the computation of the WTC to CS 2, by replacing the measurements from the on-board MWR by data acquired by the imaging radiometers flying on other remote sensing satellites, as described in the previous section, and still making use of the GNSS-derived path delays from coastal inland GNSS stations. A major problem associated with this approach is land contamination in the MWR measurements. Therefore, there is a need for a proper identification of the land-contaminated pixels in the remote sensing images. Techniques for efficient detection of land contamination in MWR measurements shall be investigated.

3.2.4.2   Ocean tide correction for CryoSat

With amplitudes ranging from a few centimetres to several meters in some continental shelf regions, the ocean tides contribute strongly to the ocean

topography variability observed by the satellite altimeters, and more particularly in the coastal areas. In most scientific applications using altimetry data, global models are used to correct the altimeter sea surface heights from the tide in order to focus on other signals of the ocean dynamics. The accuracy of these models is generally at the centimetre level in the open ocean (Ray et al, 2011). The main error sources are principally located in the coastal areas and in the polar regions, where the tidal signal is amplified and more difficult to comprehend because of the complex and often not well-documented bathymetry. Another issue is the strongly non-linear dynamics of the tide in the shelf seas.

3.2.4.2.1 Tide correction available in the CryoSat products

The CryoSat Products Handbook gives the list of the various corrections available in the products. The ocean tide correction distributed in the ESA CryoSat products is based on the **FES2004 model [Lyard et al., 2006]**, with a resolution of 0.125 degrees in latitude and longitude. This ocean tide model was developed at LEGOS. It is build on a hydrodynamic barotropic simulation computed on a dense finite-element grid and assimilated with tidal harmonic constants computed at altimeter crossover points (337 points from the Topex mission and 1254 points from the ERS-1 mission) and 671 tide gauges. The FES2004 model is classically used as ocean tide correction for the altimetry sea surface heights (cf. Envisat Handbook, Jason-1 Handbook, Jason-2 Handbook).

3.2.4.2.2 Other current and upcoming suitable global tide models

3.2.4.2.2.1 Empirical tide models

The other classical tide model usually provided in the recent altimetry products to correct the sea surface heights from the ocean tide is the **GOT model** (GOT00.2 in the Envisat GDR-C v2.1 and Jason-1 GDR-C products, GOT4.8 in the Jason-2 GDR-D products, which are successive updates of **[Ray, 1999]**). This empirical model is based on the FES model as a prior hydrodynamic solution and is strongly constrained with altimetry data (TOPEX, ERS-1, ERS-2 and GFO) and tide gauges. The GOT models are provided on a 0.5 degrees grid, which is hardly adequate for most shallow seas.

The **DTU10 model** (by Andersen at DTU) and the **EOT10a model** (by Bosch at DGFI) are recent empirical ocean tide models. They both use the FES2004 model as a prior solution and are highly constrained with altimetry data. They are distributed on the FES2004 model grid, with a resolution of 0.125 degrees in latitude and longitude. They are not provided as altimetry ocean tide corrections in the official products.

3.2.4.2.2.2 Hydrodynamic tide models

As well as the FES2004 model, the **TPXO7.2 model** (by Egbert at COAS/OSU) is built on a prior hydrodynamic solution assimilated with altimetry and tide

gauge data, using the OSU Tidal Inversion Software (OTIS). This global model is distributed on a 0.25 degrees grid. Regional models computed with the same tools also exist in a number of regions, at various resolutions. None of these models are provided as altimetry ocean tide corrections in the official products.

The **FES2012 model** was recently developed in the framework of a CNES project, in order to update the FES2004 model **[Carrère et al., 2012]**. In addition to many improvements made to the hydrodynamic model used to compute the prior barotropic solution, the FES2012 tidal atlas benefits from a refined finite element grid, recent bathymetry data and longer altimetry time series (TOPEX/Jason-1/Jason-2, TOPEX and Jason-1 on the interleaved orbit, ERS1/ERS2/Envisat). More than 12 000 observations have been assimilated (nearly 6 times the number of observations in FES2004) and the model will be distributed on a 1/16° grid (0.0625 degrees). It will be released to the scientific community in the coming months and is supposed to be included in the Jason-1 and Jason-2 official products.

3.2.4.2.2.3   Assessment of the various models

As it was described in the previous sections, there are two main groups of ocean tide models. Nevertheless, the empirical models are based on a hydrodynamic model (a FES model in all the cases detailed above), as prior solution. Consequently, except TPXO, they are all more or less linked and it is difficult to find independent databases of observations to assess the quality of all these models, because some of the observations may have been assimilated in the FES2004 model or in one of the others.

However, an assessment exercise was done by **[Ray et al., 2011]**, in shelf and coastal regions, where the differences between the models are the largest, due to the amplification of the tidal signal - and consequently the model errors - in the shallow waters. The conclusions of this study show that the GOT4.7 and the EOT08a (previous version of EOT10a) models are close competitors in most of the shelf regions tested for this work and give better results than the FES2004 model. The validation of the FES2012 model has shown that this new model is equivalent to the other global models in the open ocean, but gives better results than all the other global models tested in the coastal and shelf regions **[Carrère et al., 2012].**

Easier to evaluate, the resolution of the grid of the model is not of prime importance in the open ocean, where the tidal structures reach several hundreds of kilometres. On the contrary, it becomes a crucial point in the coastal and shelf regions where the ocean tide signal is more difficult to model due to the non-linear interactions of the tidal waves. On the shelves, these interactions generate tidal structures of a few tens of kilometres, which are smoothed and under-estimated with coarse grid resolutions.

Finally, another important point is the spectrum provided for each model. In Table 3-12 we synthesised the spectra of the most recent global models and some

regional models. Obviously, the richer the spectrum, the better defined the tide, if the supplementary waves are of good quality.

Table 3-12 Available spectra of the most recent global models and the COMAPI regional models

Models	Main components	Long-period tides	Non-linear components
FES2004	M2, S2, K1, O1, N2, K2, P1, Q1, S1, 2N2, Ssa	Mf, Mm, MSqm, Mtm	M4
TPXO7.2	M2, S2, K1, O1, N2, K2, P1, Q1	Mf, Mm	M4, MS4, MN4
GOT4.8	M2, S2, K1, O1, N2, K2, P1, Q1, S1	/	M4
DTU10	M2, S2, K1, O1, N2, K2, P1, Q1 + S1 from GOT4.7	/	M4 from GOT4.7
EOT10a	M2, S2, K1, O1, N2, K2, P1, Q1, S1, 2N2	Mf, Mm	M4
COMAPI regional atlases	M2, S2, K1, O1, N2, K2, P1, Q1, S1, 2N2 **+ Minor components:** E2, J1, L2, La2, Mu2, Nu2, R2, Ro1, Sig1, T2	Mf, Mm, MSqm, Mtm	M4, MS4, MN4, S4, M6, MK4, SN4, SK4, 2Q1, MP1, 2MK6, 2MN6, 2MS6, 2SM2, 2SM6, KJ2, MK3, MKS2, MO3, MSK6, MSN2, MSN6

3.2.4.2.3 COMAPI regional model

The COMAPI (Coastal Modelling for Altimetry Product Improvement) regional tide atlas in the North East Atlantic ocean was developed in the framework of a CNES project in 2009. It is based on the same methodology as the FES2004 and FES2012 models, using the same hydrodynamic barotropic model and assimilation scheme **[Lux et al., 2010]**. It benefited from a close quality checking of the bathymetry, especially in complex regions such as the Norwegian fjords.

Moreover, because of the restricted size of the zone of interest, compared to a global model, the grid resolution of a regional model can be refined in order to be able to model the non-linear structures with a good accuracy **[Cancet et al., 2012]**. Once on a regular grid, the resolution of the NEA COMAPI regional model is 1/60° (~2 km), to be compared with the classical grid resolutions of the global models (1/2°, 1/4°, 1/8° or 1/16°).

In addition, the model physical parameters (bottom friction coefficient and wave drag coefficient) were specially tuned for the area in order to give a realistic picture of the tidal energy dissipation. In the case of a global model, the same value of parameter is generally used for the entire world ocean or for large oceanic basins, which means that it is a compromise between what happens in the deep ocean and in the shelf seas, where the friction is supposed to be stronger.

The quantity of assimilated observations is also a major factor in the construction of a tidal model and highly depends on the computing resources. Because of its

spatial cover, the selection of the assimilated data is obviously stricter for a global model than for a regional one. In the case of the FES2012 model, for example, only crossover points of the TOPEX/Jason-1/Jason-2 missions were assimilated in the deep ocean, whereas along-track data were used in the shelf seas in order to better constraint the model (Figure 3.37, left panel). In contrast, the NEA COMAPI regional atlas benefited from all the TOPEX/Jason-1 along-track data, with a point every 20 km (Figure 3.37, right panel).
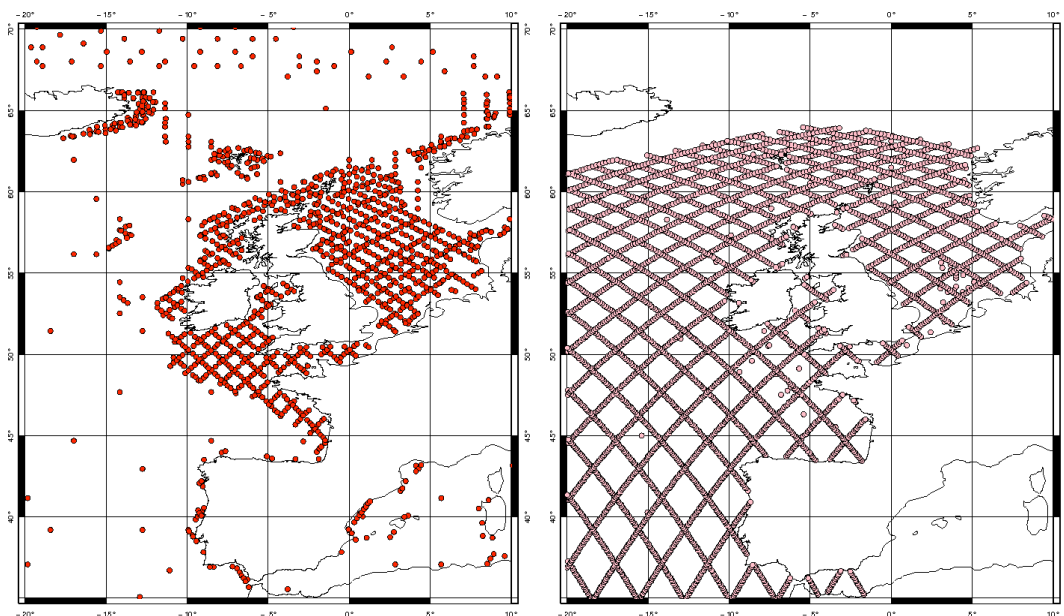
Figure 3.36 Altimetry data assimilated in FES2012 (left) and in the COMAPI NEA regional model (right), from [Cancet et al., 2012].

It should be noticed that the COMAPI NEA regional atlas was implemented in 2009, when the TOPEX/Jason-1 time series on the interleaved orbit was not long enough to compute accurate tidal constituents. Today, with three additional years of measurements, i.e. a 6-year long time series, it is possible to add this mission in the assimilated dataset, as it was recently done for the FES2012 model **[Carrère et al, 2012]**.

The COMAPI regional tidal atlas was validated using two different methods. First, the harmonic components (amplitude and phase) of each modelled tidal wave were compared to the tidal harmonic components extracted from tide gauge data time series. Then, the regional model was compared to the global models used to correct the altimetry data (FES2004 and GOT4.7), using a criterion of altimetry SLA variability reduction. The NEA regional model proved to be of good quality **[Cancet et al., 2010]** and could consequently be used to correct the CryoSat data in this region.

The importance of local tide models was also highlighted by COASTALT, as discussed in Section 3.4, below.

3.2.4.2.4 Recommendations from the state of the art

Given the characteristics of the existing tide correction models, we recommend using the most recent global models in the CryoSat products. In the North-East Atlantic ocean, we recommend to use the COMAPI regional model as is has been specifically tuned for this region and has the adequate resolution to provide accurate ocean tide corrections for the altimetry sea surface heights in shelf seas.

3.2.4.3   Ionosphere correction review

The ionosphere impacts the propagation of electromagnetic waves. In the frame of radar altimeter on board satellites, one of the main issues is the propagation delay that can induce errors ranging from a few millimetres to two tens of centimetres for the estimation of the sea level. Therefore the correction of the ionospheric delay is one of the numerous challenges that satellite altimetry has to solve. The ionosphere dynamics is insensitive to the ground surface (open oceans, coast lines, ice sheet, etc.) but is particularly dependent to the sunlight, the solar activity and the geomagnetic field. The consequence is that the ionosphere climatology is related to the local time and the latitude. However, sudden events of extreme variability can affect the ionosphere, in particular during geomagnetic storms induced by solar eruptions. Such events generate preferentially strong and complex dynamics at high latitudes. In the polar regions, the aurora borealis and australis are consequences of these events.

3.2.4.3.1 Ionospheric corrections available in the CryoSat products

The CryoSat products Handbook gives the description of the ionospheric corrections provided within the CryoSat products. As CryoSat radar altimeter is a single frequency one, the system cannot assess the ionospheric correction by itself. Indeed, this special feature is limited to dual frequency radars like POSEIDON-2 for example.

The ionospheric correction available in the CryoSat products relies on the ionosphere model BENT and the Global Ionosphere Maps (GIM) produced by the JPL. For the Level 1b products, both corrections are available. For the Level2 products, only one ionospheric correction is provided: the Bent correction for near-real-time and fast delivery mode products, the GIM correction for the delayed-time processing.

The **ionosphere model Bent [Bent, 1972]** is an empirical model tuned by using thousands of observations profiles recorded between 1962 and 1969. Bent is function of the latitude, the longitude, the time, the season, and the solar radio flux. This model was created in 1972.

The **JPL Global Ionosphere Maps** are generated from data recorded by the worldwide network of GPS receivers **[Mannucci et al., 1999]**. The method

consists in combining the phase and code measurement of several dual-frequency GPS receivers and in using the inverse problem theory to estimate total electron content (TEC) maps and instrumental biases. The resolution of the maps is 5° in longitude, 2.5° in latitude and 2 hours in time. They cover the longitudes from -180°E to 180°E and the latitudes from -87.5°N to 87.5°N.

3.2.4.3.2 Other current and upcoming suitable ionosphere corrections

3.2.4.3.2.1 Ionosphere models

The ionosphere models provide a first possibility to estimate the ionospheric correction for satellite altimeters. These models are generally empirical or semi-empirical and have been developed by using ionospheric observations profiles from topside sounders (satellites) and bottom-side sounders (ionosondes). The oldest models still in use are the Bent model (previously described) and the Klobuchar model **[Klobuchar, 1987]**. The latter is used to compute the ionosphere correction broadcasted through GPS navigation message. However several other models have been developed and are still improved like the International Reference Ionosphere model (IRI) **[Bilitza et al., 1993]** and the NeQuick model **[Radicella, 2009]**. These models provide ionospheric profiles as function of latitude, longitude, time and solar activity. They are global models but their latitude extent is limited to ±80°N. The NeQuick model has been selected to provide the ionospheric correction broadcasted by the GALILEO navigation message.

These models propose a detailed modelling of the profiles of several ionospheric elements while the ionospheric correction for altimetry requires only the TEC under the satellite altimeters. On this basis, the NIC09 model **[Scharroo and Smith, 2010]** has been developed by using TEC maps.

3.2.4.3.2.2 Dual frequency altimeters

The ionosphere is plasma in a weakly magnetized environment. An electromagnetic wave that propagates in such plasma is delayed depending on the TEC along the propagation path and the frequency of the emitted wave. Therefore the combination of signals emitted by a dual-frequency system gives the possibility to compute the TEC. Altimeter radars on board satellites such as TOPEX, Envisat, Jason-1 and Jason-2 have exploited this feature.

However, dual-frequency systems have to deal with instrumental biases and/or high noise level. In the case of satellite altimetry the inherent noise level necessitates the application of an along-track smoothing filter to the TEC estimation. The filter size is consistent over the different missions. In the case of Jason-2 it is recommended to use a 150-200km filter for local time between 06h and 24h and a 100-150km filter between 00h and 06h. The use of different

filtering windows points out the need to set a trade-off between the lowering of the noise level and the smoothing of the ionospheric dynamics.

3.2.4.3.2.3   TEC maps

The development of the GPS system after the 1980's and the advent of the GPS dual-frequency receivers' networks opened the way to new technics for ionosphere monitoring. In this frame, several institutes developed methods to compute TEC maps from the GPS network. The extent of the GPS network to a worldwide size and the creation of the International GNSS Service (IGS) contributed to the development of Global Ionosphere Maps (GIM).

The GIM maps are still daily produced by JPL, CODE **[Schaer, 1999]** and UPC **[Hernandez-Pajares et al., 1999]**. They are provided by the IGS (http://igscb.jpl.nasa.gov/) and they respect the IONEX file format **[Schaer et al., 1998]** and resolutions (see description of JPL-GIM above). However, the methods of TEC estimation are slightly different for each institute and so are the results. The JPL-GIM maps have demonstrated the best efficiency for the ionospheric correction of altimeters **[Scharroo, 2002]**.

Very dense GPS receivers' networks exist at national scale. The three denser networks are the Japanese, the European and the American networks. Several institutes propose TEC maps above the corresponding areas. Let us call these maps Regional Ionosphere Maps (RIM). Several examples are the American RIM at NOAA (http://www.swpc.noaa.gov/ustec/index.html), the Japanese RIM at NICT (http://seg-web.nict.go.jp/GPS/GEONET/index_e.html), the South African RIM at HMO **[Opperman et al., 2007]**, and the European RIMs at DLR (http://swaciweb.dlr.de) and at NOVELTIS (http://www.noveltis.com/spectre/index.html).

We have to note that the accuracy of GIM maps depends on the geographic location. Indeed, the accuracy is better over and close to the dense GPS networks. The uncertainty (RMS) can reach more than 7 TEC units (uTEC) above the open ocean while the RMS is usually below 1 uTEC over America, Europe and Japan, for example. Therefore, in the frame of satellite altimetry, the ionospheric correction accuracy is better at coastal areas for the reported countries than in the open ocean. Moreover, the dense GPS networks that are used to produce RIMs allow getting the same number (hundreds) of GPS receivers over a limited area as the total number of GPS receivers used for GIMs. Consequently, the space resolution is generally improved for RIMs products to 2.5° x 2.5° and even 1° x 1° for denser networks (Japan).

3.2.4.3.2.4   Scaling factor for GPS-derived TEC maps

The use of GPS-derived TEC estimation to compute the ionospheric correction for satellite altimeters presents a major issue: the GPS satellites orbit at an altitude of

20,200 km while the altimeter satellites orbit between altitudes of 800 km and 1,400 km. The consequence is that the TEC computed from GPS data overestimates the TEC below the altimeter satellites. A formula (here for Envisat at 800km) was suggested to scale down the GPS-derived TEC at a given time and place **[Iijima et al., 1999]**:

$$TEC_{<800km} = TEC_{GIM} \times \frac{TEC_{IRI95<800km}}{TEC_{IRI95<1400km}}$$

This formula necessitates an ionosphere model (here IRI95) to compute the scaling factor. However, we note that the scaling factor takes into account an ionospheric profile limited to 1,400 km of altitude while GPS satellites fly at 20,200 km. This choice was made because IRI95 overestimate the ionosphere upper part. Subsequently, the modeling of the topside ionosphere has been investigated in models like IRI2007 using the NeQuick topside electron model **[Coïsson et al., 2006]**, and Standard Ionosphere-Plasmasphere Model (SPIM) using the Russian Standard Model of the Ionosphere to model the plasmaspheric contribution **[Gulyaeva et al., 2002]**.

3.2.4.3.2.5   Discussion on the ionosphere corrections accuracy

The different ionospheric corrections for altimetry were compared to the smoothed dual-frequency correction. The errors were respectively 35% for IRI2007, 18% for NIC09 model and 14% for JPL-GIM products **[Andersen and Scharroo, 2011]**. These results suggest that the ionospheric correction derived from JPL-GIM products is the best for single frequency altimeters.

Recently, it has been suggested that a constant scaling factor depending on the satellite mission can be used without a significant decrease of the accuracy **[Scharroo and Smith, 2010]**. However the distribution of the electron density along altitude and its variability with location, local time and solar activity prove the necessity to accurately model the scaling factor **[Webb and Essex, 1999] and [Webb and Essex, 2001]**.

In conclusion, it is difficult to justify the absolute necessity of a modeled scaling factor without demonstrating the reliability of the recent models of the ionosphere topside and plasmasphere electron profiles or without demonstrating a better accuracy of the ionospheric correction derived from a modeled scaling factor. However, it seems reasonable to expect an improvement of the ionospheric correction at regional level by using RIM products instead of GIM.

3.2.4.3.3 SPECTRE TEC maps

In the frame of this project we propose to use RIM produced by NOVELTIS. The SPECTRE service is an operational service providing TEC maps over Europe from GPS network with an accuracy of 2-3 uTEC. This accuracy estimate is not

the RMS estimated conjointly with the TEC maps by inverse theory (which is significantly lower) but the errors assessed by multiple comparisons with GIMs (JPL, CODE, UPC), altimeter satellites (TOPEX, Jason-1, Envisat) and ionosondes **[Crespon et al., 2007]**.
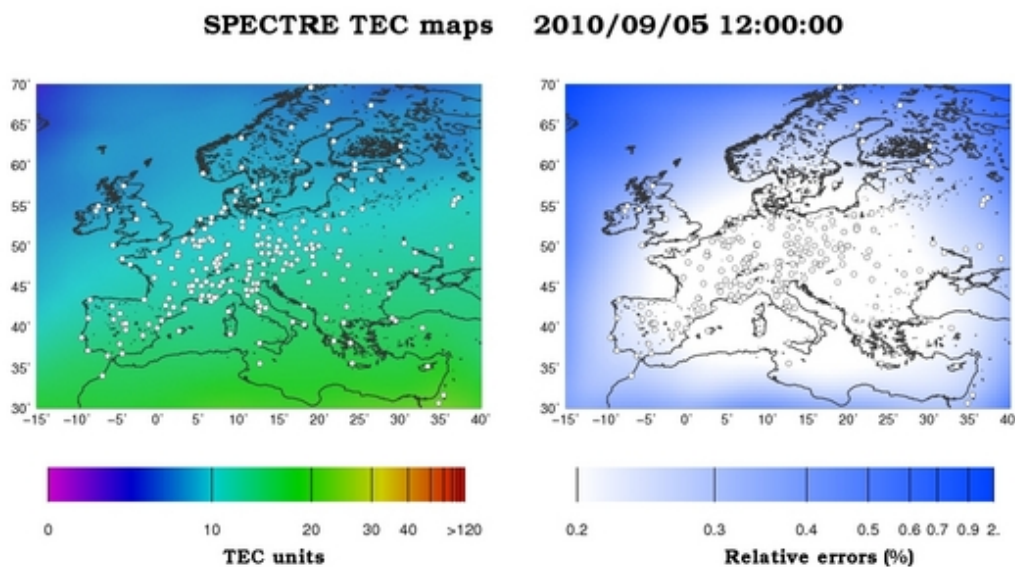
Figure 3.37 TEC and RMS (in percent) maps estimated by the SPECTRE service from the GPS receivers (white dots) of the European network.

The TEC maps (see Figure 3.37) extent from -15°E to 40°E and from 30°N to 70°N. The space resolution of the SPECTRE-TEC maps is 2.5° x 2.5° which provides a longitudinal resolution twice better than the GIM products. However the best improvement concerns the time resolution, which is 30 seconds for SPECTRE products while it is 2 hours for GIM products. Increase of space and time resolutions allows estimating the ionospheric perturbations at smaller space and time scales. The European map product covers the Mediterranean Sea and the North-East Atlantic area for the entire period from April 2004 to present.

SPECTRE algorithms have been adapted to produce TEC maps over different regions like Japan and the North Pole, but only a few days have been processed. High latitude mapping of the TEC is of particular interest for the CryoSat mission. Indeed, the ionosphere is affected by sudden and extreme increase of the TEC is this region due to the occurrence of geomagnetic storms (see Figure 3.38). Moreover, the space and time scales of ionization patterns during storms are smaller than the ionosphere dynamics patterns at mid and low latitudes. Therefore, RIM products with increased resolutions may significantly improve the accuracy of the ionospheric correction for satellite altimeters.
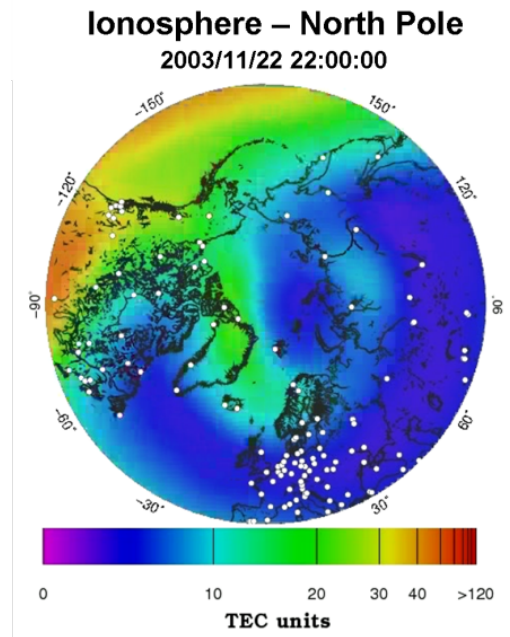
Figure 3.38 : SPECTRE-TEC map for the North Pole during 2003 Halloween geomagnetic storm.

3.3   WP2300 – Survey of Auxiliary Data

3.3.1   Satellite Altimeter data over the Oceans (through RADS)

Section 3.4.1 provides more information on the RADS initiative, which concerns one of the most used and consistent archives of satellite altimeter data to date. Having all historical and operational data in one data base also with the most up-to-date corrections, models and auxiliary data makes RADS very suited as a source of auxiliary data; *e.g.* the operational Jason-1 and Jason-2 data concurrent with CryoSat-2 data in a number of flavours, being ESA original, ESA improved and the re-tracked RADS product. Clearly in the validation of the LRM and pseudo-LRM CP4O products these data will be used and inter-compared, as well as the involved models and corrections, and including the comparison between RADS products and CPP products, and that all on a global scale. RADS also includes alternative variables, partly from models, partly from other data sources that allow the user to assess the possible influence of model errors on sea level, and to correlate it with wind speed, wave height, and sea surface temperature.

3.3.2   Gravity data for Polar regions

Figure 3.39 shows the recent result from the Lomroc 2009-2010 airborne surveys North of Greenland, which will be used for the sea floor/gravity validation.
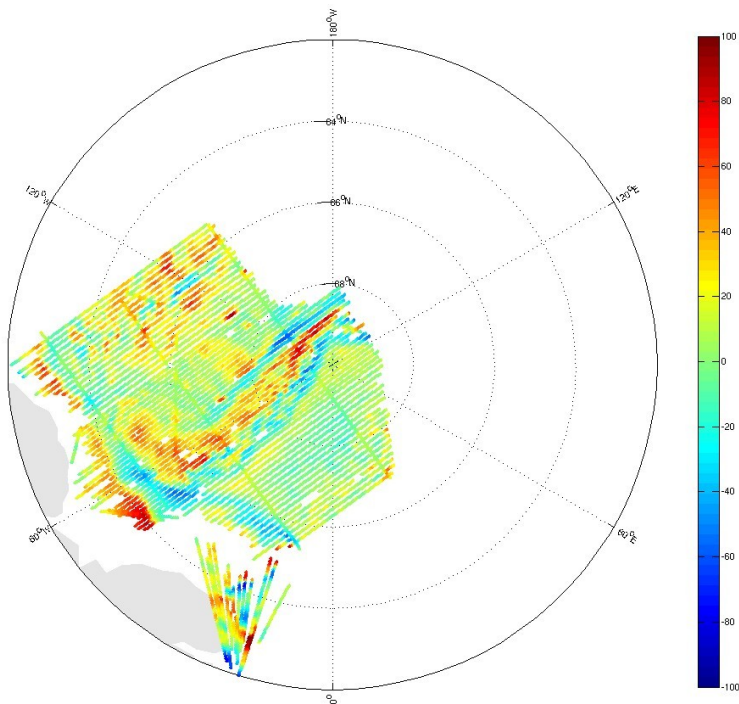
Figure 3.39 Gravity results from recent airborne surveys (Lomroc 2009-2010).

Table 3-13 CryoVEx/Icebridge 2011 and 2012 data overview.

Location	Airborne activity	CryoSat Orbit #	CryoSat passage time	CryoSat Mode	CryoVEx ASIRAS	CryoVEx ALS	IceBridge ATM	IceBridge DMS
Beaufort, Chukchi	15/3-2012	10262 10263	15/3-2012 16:50 UTC 15/3-2012 18:23 UTC	SAR			X	X
Alaska	17/3-2012	10291 10292	17/3-2012 16:47 UTC 17/3-2012 18:20 UTC	SAR			X	X
North Pole Transect	21/3-2012	10346	21/3-2012 11:40 UTC	SAR			X	X
Wingham Box	26/3-2012	10421	26/3-2012 15:45 UTC	SARin			X	X

Lincoln Sea	28/3-2012	10450	28/3-2012 15:37 UTC	SAR			X	X
Alert	29/3-2012	10462	29/3-2012 11:34 UTC	SAR	X	X	X	X
Nares Strait	30/3-2012	10491	31/3-2012 11:33 UTC	SAR	X	X		
Lincoln Sea	2/4-2012	10520	2/4-2012 11:29 UTC	SAR	X	X	X	X
Lincoln Sea	2/4-2012	10524	2/4-2012 18:03 UTC	SAR				
Lincoln sea	3/4-2012	10540	3/4-2012 20:30 UTC	SAR	X	X		
Lincoln sea	4/4-2012	10555	4/4-2012 21:19 UTC	SAR	X	X		
Wigham Box	5/4-2012	10565	5/4-2012 13:54 UTC	SarIN	X	X		
Svalbard	27/4-2012	10885	27/4-2012 15:03 UTC	SAR	X	X		
Station Nord	29/4-2012	10915	29/4-2012 16:40 UTC	SAR	X	X		

3.3.3 Review in situ and Globwave data

This section reviews sources of independent data that could be used for the validation of CryoSat-2 SAR data over the ocean and the coastal zone. Both data that are relevant to the validation of CryoSat-2 SAR sea surface height and significant wave height are considered, from both satellite and in situ sources.

3.3.3.1 Sea surface height

Satellites

CryoSat-2 SAR data are available for scientific analyses and exploitation dates from July 2010 onwards. CryoSat-2 SAR SSH can be compared and validated against SSH from other contemporaneous altimeters, subject to appropriate space/time colocation. Satellite altimeter SSH measurements are available from:

- Jason-2 (current)
- Jason-1 (current)
- ERS-2 (up to 4 July 2011 but only within range of ground stations)
- Envisat (up to 8 April 2012)

In situ: tide gauges and bottom pressure recorders

There is a large global network of tide gauges and other instruments that provide in situ information about sea level.

The Global Sea Level Observing System (GLOSS) is an international programme that aims at the establishment of high quality global and regional sea level networks for application to climate, oceanographic and coastal sea level research. The main component of GLOSS is the 'Global Core Network' (GCN) of over 290 sea level stations around the world for long-term climate change and oceanographic sea level monitoring (see Figure 3.40).
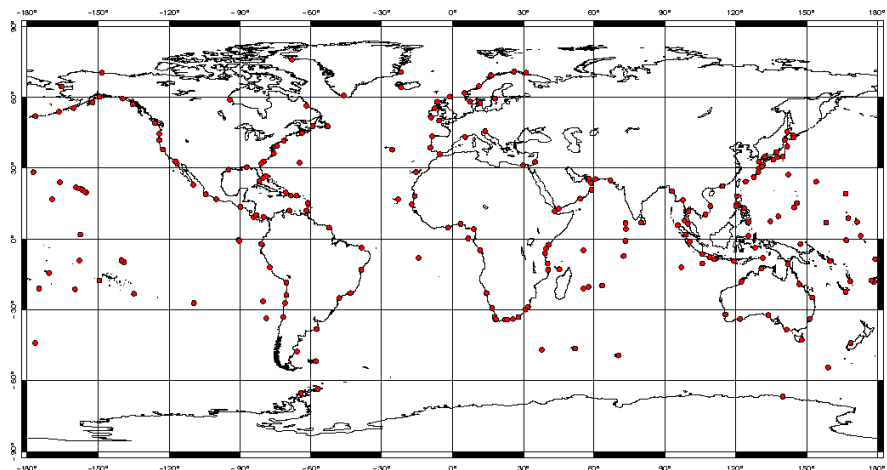
Figure 3.40 GLOSS network of tide gauges

Several services provide access to the data from the GLOSS and other tide gauge networks. Data are typically provided as relative level measurements with respect to a local datum, and are available as hourly, daily, monthly and annual averages. For some stations, data is available as 10 minutes averages.

The quality of tide gauge data is very variable, however, so it is important to consider what data quality control and vertical referencing is available for each station.

The Permanent Service for Mean Sea Level (PSMSL; http://www.psmsl.org) was established in 1933 and has been responsible for the collection, publication, analysis and interpretation of sea level data from the global network of tide gauges. It is based in Liverpool at the National Oceanography Centre (NOC), which is a component of the UK Natural Environment Research Council (NERC).

PSMSL features various data visualization tools (e.g. via Google Earth), online data catalogue viewers (see Figure 3.41) as well as information about quality control.
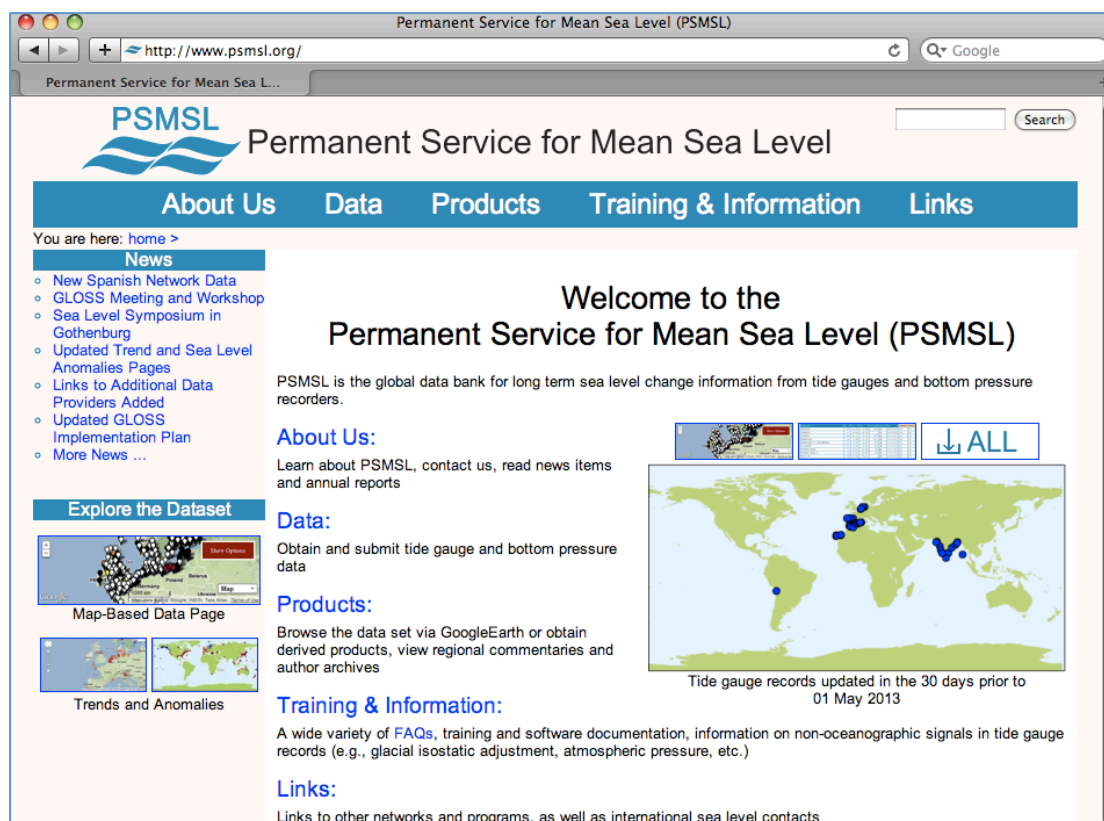
Figure 3.41: Web page of the Permanent Service for Mean Sea Level (PSMSL) providing access to global in situ sea level networks, data visualization and data access tools.

Similarly, the Systeme d'Observation du Niveau des Eaux Littorales (SONEL; http://www.sonel.org) aims to provide high-quality continuous measurements of sea- and land levels at the coast from tide gauges (relative sea levels) and from modern geodetic techniques (vertical land motion and absolute sea levels) for studies on long-term sea level trends, but also the calibration of satellite altimeters. SONEL serves as the GNSS data assembly centre for GLOSS and works closely with the PSMSL by developing an integrated global observing system, which is linking both the tide gauge and the GNSS databases for a comprehensive service to the scientific community (see Figure 3.42)
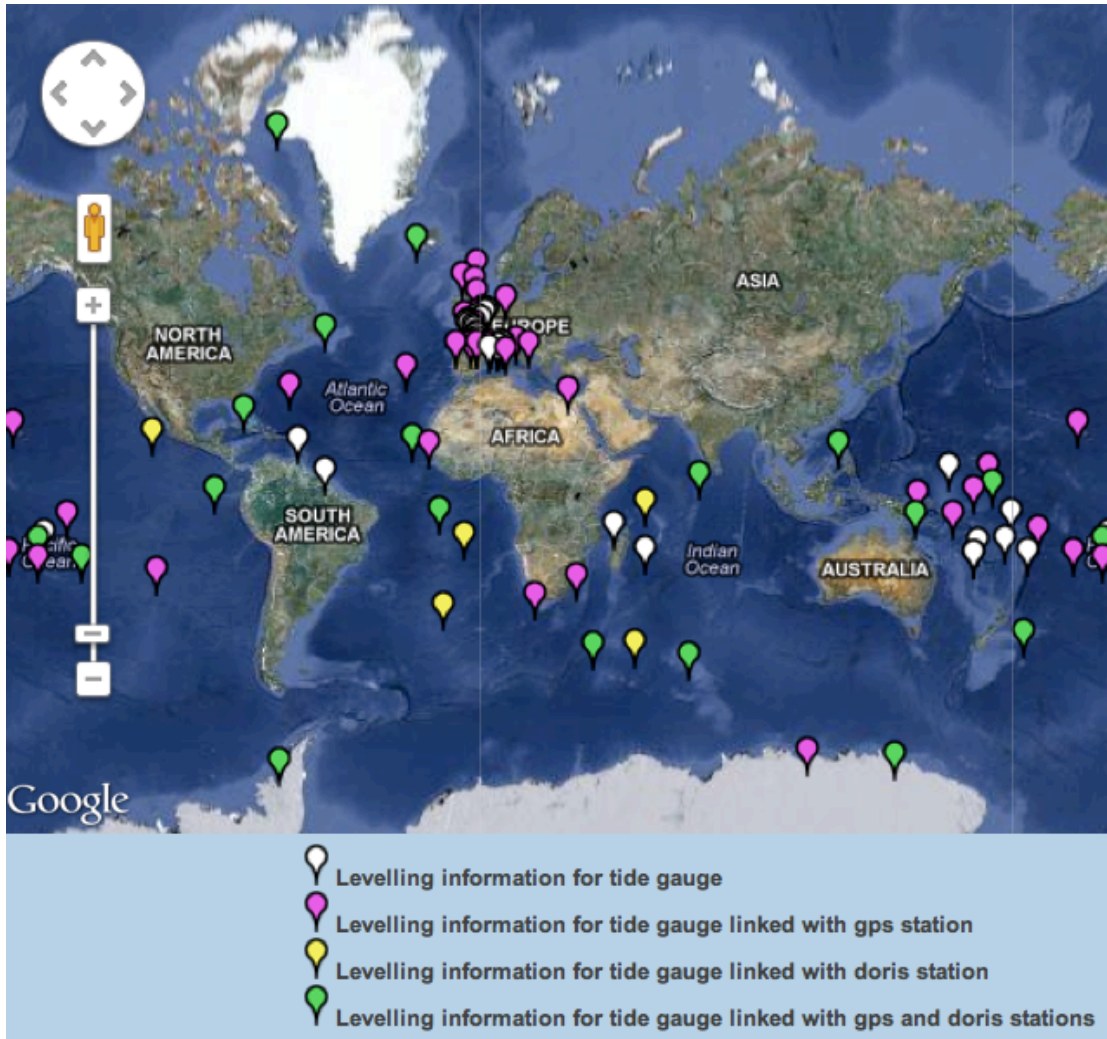
Figure 3.42 Origin of tide gauges geodetic leveling information (from http://www.sonel.org/-Stability-of-the-datums-.html)

Sea level data are available also from Bottom Pressure Recorders (BPR) such as those used in tsunami warning systems of the Deep-ocean Assessment and Reporting of Tsunamis (DART) network operated by the US National Data Buoy Center (NDBC). The DART system consists of a seafloor BPR capable of detecting tsunamis as small as 1 centimetre, and a moored surface buoy for real-time communications. There are some 39 US owned stations, mainly in the Pacific and the Atlantic, for which data is available in NRT every 15 minutes (see Figure 3.43).
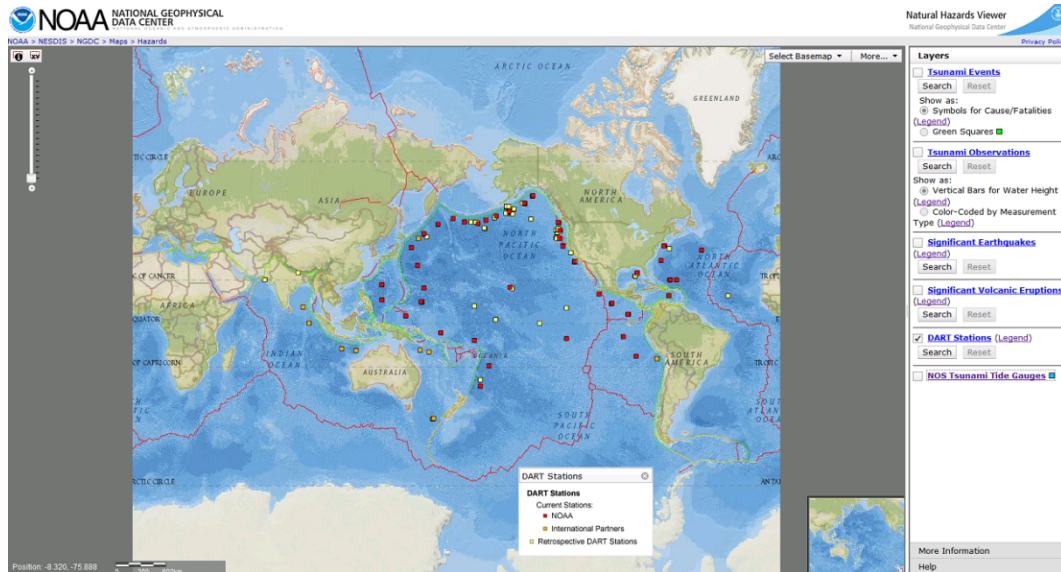
Figure 3.43 The DART network of Bottom Pressure Recorders providing sea level information every 15 minutes via NDBC (from http://maps.ngdc.noaa.gov/viewers/hazards/)

3.3.3.2 Ocean surface wave measurements

Satellite wave data: Globwave

GlobWave is an initiative funded by ESA (and subsidised by CNES) through the Data User Element (DUE) of Earth Observation Envelope Programme 3 (EOEP-3). The project aims to improve the uptake of satellite-derived wind-wave and swell data by the scientific, operational and commercial user community. It allows easy access to a harmonised set of satellite altimeter and SAR wave products provided in NetCDF format. Match-up databases of satellite wave data collocated with buoys were also developed within GlobWave, for both altimeters and SAR.

While the GlobWave project came recently to a close (April 2013), the GlobWave data products and portal is expected to continue to be maintained by Ifremer for the foreseeable future. Access to data is by ftp hosted by Ifremer after registration via mailto:fpaf@ifremer.fr.

In situ wave measurements

Wave buoy data are available from the National Oceanographic Data Centre (NODC; http://www.nodc.noaa.gov), the National Data Buoy Centre (NDBC; http://www.ndbc.noaa.gov), and the Coastal Data Information Program (CDIP; http://cdip.ucsd.edu). The online NOAA Marine Environmental Buoy Database contains wave height, wave period and wave spectra data, with an increasing

number of buoys reporting also directional wave spectra. Buoy measurements are provided usually hourly, sometimes every 30 minutes. These buoys are located primarily around the coast of the US (Figure 3.45).
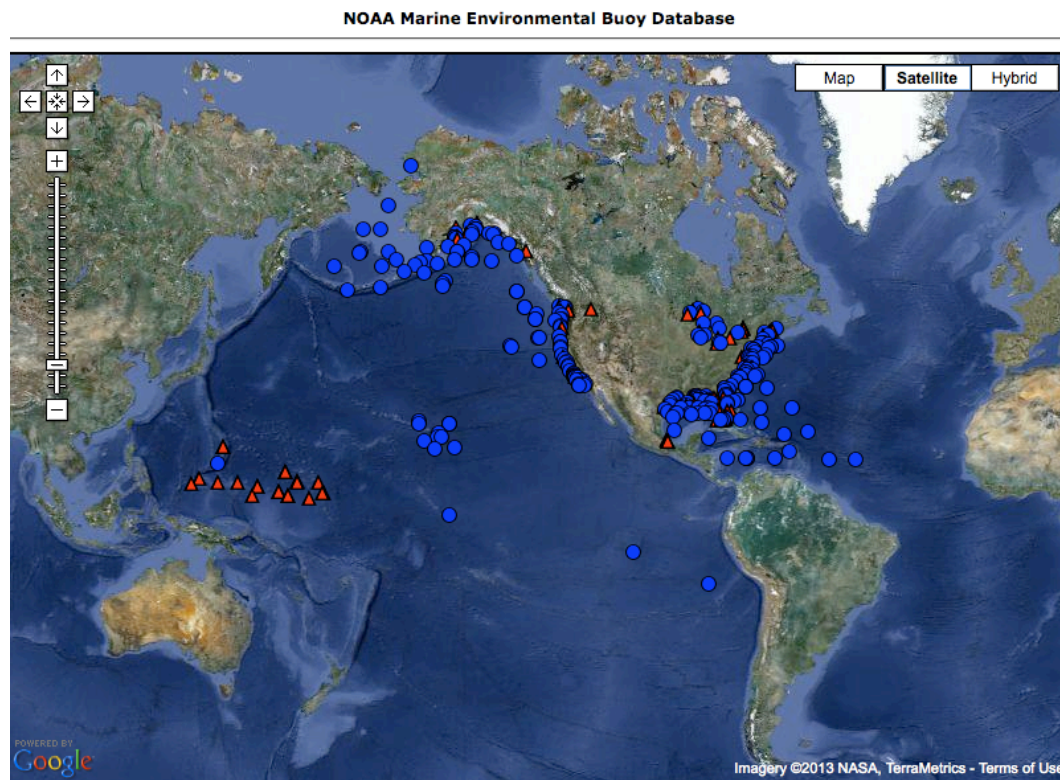
Figure 3.44 Data finder interface of the NOAA Marine Environmental Buoy Database (from http://www.nodc.noaa.gov/BUOY/)

The National Data Buoy Centre also provides access to some wave buoys not operated by NDBC in other regions of the World. Over the European continental shelf, this provides access to recent data from buoys operated by the UK Met Office and MeteoFrance (Figure 3.45).
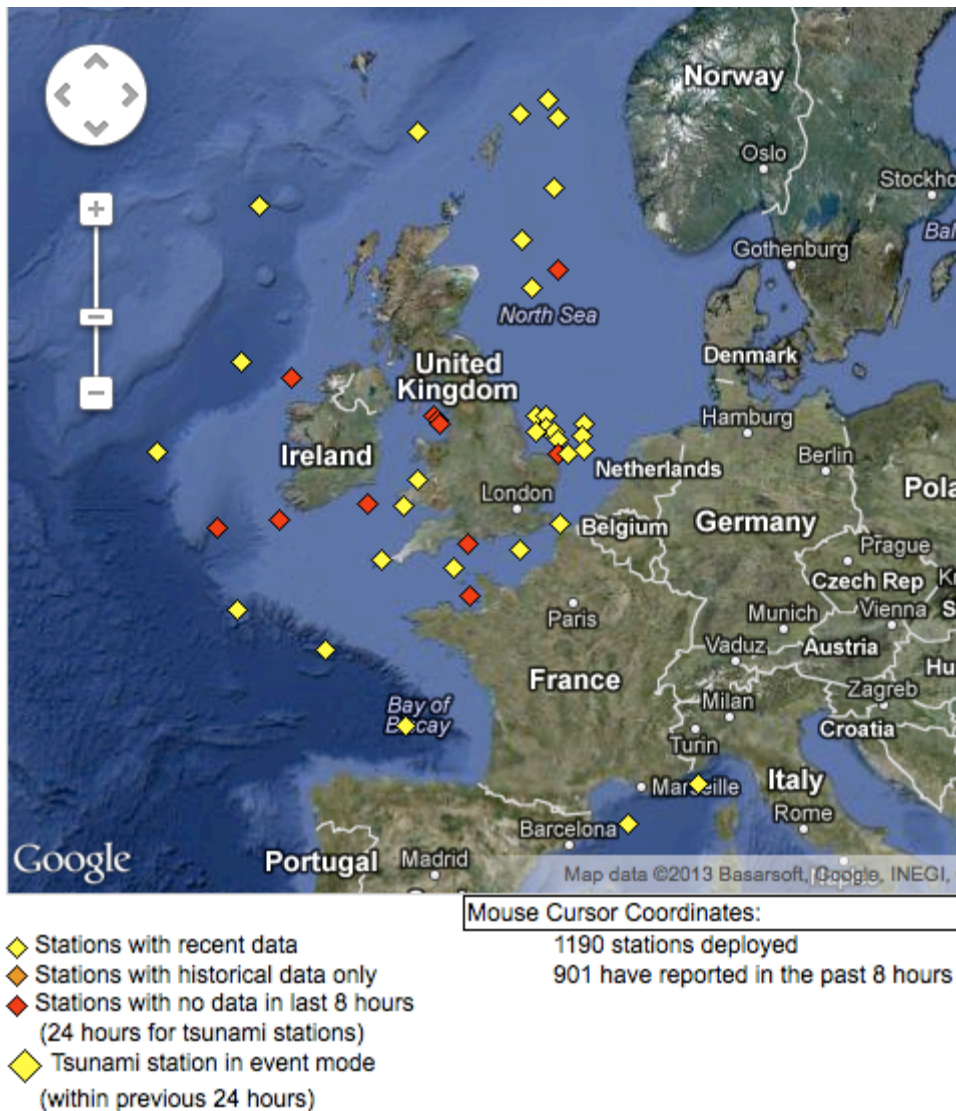
Figure 3.45 Moored stations reporting wind speed and direction, wave height and wave period in near real time via the US National Data Buoy Centre (from http://www.ndbc.noaa.gov/)

Other national services that provide access to buoy data around Europe include:

- Real-time data from the MeteoFrance automatic fixed stations (http://www.meteo.shom.fr/real-time/)
- The Centre d'Archivage National de Donnees de Houle In Situ (http://candhis.cetmef.developpement-durable.gouv.fr/carte/)
- Access to the latest marine observations from the UK Met Office (http://www.metoffice.gov.uk/weather/marine/observations/map.html)

CP4O	Preliminary Analysis Report	D2.1	

- Data search and access service of the UK Coastal Channel Observatory (http://www.channelcoast.org; see Figure 3.46)
- The UK WaveNet strategic wave-monitoring network for England and Wales (http://www.cefas.defra.gov.uk/our-science/observing-and-modelling/monitoring-programmes/wavenet.aspx), which provides a single source of real-time wave data from a network of wave buoys located in areas at risk from flooding.
- Access to real time and historical wave data through the Puertos del Estado website (http://www.puertos.es/oceanografia_y_meteorologia/redes_de_medida/index.html)
- Access to real time and historical wave data of the Italian wave buoy network (15 buoys) (http://www.telemisura.it)

Figure 3.46 Map viewer and data search interface of the UK Coastal Channel Observatory showing the location of directional wave buoys and tide gauges (http://www.channelcoast.org)

CP4O	Preliminary Analysis Report	D2.1	

3.4 WP2400 – Relevant Past and Current Initiatives

This section reviews a number of past and current projects that have had or have an impact on the development and applications of SAR altimetry, especially in the coastal zone where this technique is most promising. This impact can be indirect, as in the case of the COASTALT project which was not specifically dealing with SAR altimetry but nevertheless achieved a number of relevant results in terms of corrections and product specifications, or direct such as for the eSurge and LOTUS projects in which SAR altimetry data are processed and used.

3.4.1 RADS (TU Delft)

The Radar Altimeter Database System (RADS) has grown to become a mature altimeter database that focuses on consistent multi-mission products. Over the last 15 years it is continuously being developed, first at TUDelft, now at the NOAA and Altimetrics. It serves as a prototype for a fundamental Climate Data Record for sea level. Because of the multiple users involved in scrutinizing the data and the regular updates to the database, RADS is one of the most accurate and complete data bases of satellite altimeter data around. Data from nine altimeter missions are presently available in RADS, forming the basis for a prototype Level 2 sea level CDR. The 20 years of "reference missions" (TOPEX/Poseidon, Jason-1, and Jason-2) are complemented by "mesoscale missions" (Geosat, GFO, ERS-1, ERS-2, and Envisat) and the "polar mission" CryoSat-2. The latter two groups increase the spatial coverage of sea level change and start yielding stability comparable to the reference missions through some recent developments in corrections, like orbits and ionospheric corrections. A lot of effort went into the establishment of a homogenous dataset. Although the principle of satellite radar altimetry is fairly simple, properly accounting for all the geophysical corrections makes it rather complex. Also putting all the different missions and mission phases in a consistent reference is not an easy job. Nowadays, RADS provides a multitude of additional variables needed to convert the original satellite range measurement into a climate-quality sea level record, and RADS includes alternative variables to allow the user to assess the possible influence of model errors on sea level, and to correlate its variations with those in wind speed, wave height, and sea surface temperature. All measurements have been supplied with most up-to-date corrections and models: e.g. FES2004, GOT4.7 and GOT4.9 ocean tide models, consistent pole and solid Earth tides, EGM2008 geoid, EGM2008, CLS11, and DTU10 mean sea surfaces, DTU10 bathymetry, wind/waves from WaveWatch3 model, high resolution MOG2D dynamic atmosphere correction, NCEP/ECMWF full resolution atmospheric path delays, and smoothed dual-frequency and JPL GIM and NIC09 ionosphere corrections.

CP4O	Preliminary Analysis Report	D2.1	

RADS takes care of both delayed precision products, near real-time (NRT) and interim products, so that you always will find the best data available for your purpose at the time you access the servers. The machine at Altimetrics (Cornish) function as development machine, whereas the NOAA server serves as the operational server targeted to NRT uses in the US, and the Delft server serves as data server for the rest of the world. Meanwhile as all users are mirroring the database RADS has many copies all over the world. Figure 1 shows the locations of the current users of the RADS system.
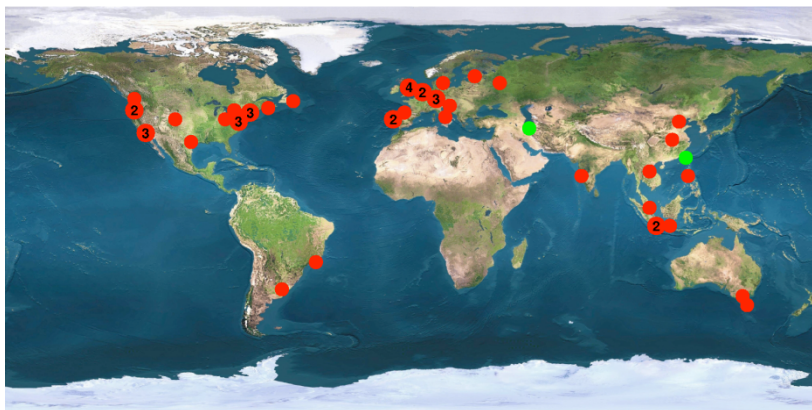
Figure 3.47 50 institutes in 24 countries mirror the RADS database

Besides the data content of RADS, the system also holds a number of tools that facilitate easy access to the data, cross-calibration of data and other data analyses like time tag biases and drifts through crossover difference minimization. With this RADS serves as the perfect platform to perform the CryoSat-2 data analyses involved in the CP4O project. ESA's product is readily available and can be intercompared with improved products like RADS' own Level1b re-tracked product and the products that will be developed in CP4O frame. Also individual corrections and models can be intercompared.

3.4.2   REAPER (CLS, isardSAT, Altimetrics)

REAPER is an ESA-funded project to reprocess the ERS-1 and ERS-2 altimeter data using a single set of algorithms to produce a consistent high quality data set that is as similar as possible in character and format to Envisat RA2 data. This required

- the compilation of the best available algorithms, correction models and auxiliary data
- the regeneration of precise orbits across the 12 year period of ERS-1 and ERS-2
- the sourcing and assembly of as complete a set of Level 0 data as possible.

CP4O	Preliminary Analysis Report	D2.1	

The source data and auxiliary data have now been assembled and the processing chain implemented and tested, and production of the final REAPER products is expected to start in the summer 2013.

3.4.3 SAMOSA

3.4.3.1 Overview

SAMOSA was an ESA-funded project to study ocean and inland water applications of Synthetic Aperture Radar (SAR) mode (or Delay Doppler mode) altimetry. The original Project was extended to support technical implementation of the improved theoretical echo models

The SAMOSA project was initiated in 2007 to investigate the improvements that SAR mode altimetry can offer in measurements over ocean, coastal and inland water surfaces, developing practical implementation of new theoretical models for the SAR echo waveform as part of this process.

The SAMOSA project team was led by Satellite Oceanographic Consultants (SatOC,UK) and included: The Danish University of Technology (DTU, Denmark), De Montfort University (DMU,UK), the National Oceanography Centre (NOC, UK) and Starlab Barcelona S.L (STARLAB, Spain). This consortium also benefitted significantly from the external participation of Dr. R.K. Raney (Applied Physics Laboratory at the Johns Hopkins University, USA).

The project team succeeded in defining novel retracking techniques for SAR Mode (SARM) altimeter echoes over water surfaces and in evaluating the performance of SARM altimetry compared to conventional pulse-limited altimetry. The performance of SARM in terms of range retrieval accuracy was analysed by retracking simulated CryoSat data, airborne data and CryoSat-2 data, and with estimates of achievable precision of SARM through the Cramér-Rao Lower Bound (CRLB) method. In addition, the "Berry Expert System" (BEST) was applied to simulated data over complex inland water scenarios to assess SARM performance over lakes, estuarine and wetlands.

3.4.3.2 SAMOSA1 and SAMOSA2 Models and Implementation

The SAMOSA project led to the definition of two new theoretical models for SAR waveforms over water. The first model ("SAMOSA1") assumes Gaussian ocean wave statistics and a circular antenna pattern, and includes the effect of Earth curvature and antenna mispointing in the along track direction only. An enhancement of the SAMOSA1 formulation ("SAMOSA1_Enhanced") addresses numerical singularities in the trailing edge of the SAMOSA1 SAR waveforms in low sea state conditions. The SAMOSA1 Enhancement allows waveform fitting to use data over the full gate range and produces an almost ten-fold reduction in computation time. The SAMOSA2 SAR model is a more complex formulation that includes non-Gaussian ocean wave statistics, Earth curvature and a better representation of mispointing effects both along- and across-track. The

SAMOSA2 model also comprises radial velocity effects and an elliptical antenna pattern. All SAMOSA theoretical models were implemented as SAR ocean retrackers and applied successfully to simulated and CryoSat-2 SAR waveforms.

Waveform retracking applied to simulated CryoSat data over ocean surfaces allowed for quantitative comparison of "Low Rate Mode" (LRM - conventional altimeter approach) and "SAR mode" (SARM) over identical sea state conditions. The SAMOSA1 SAR ocean retracker was applied to simulated SARM data to estimate the retrieval accuracy for range and significant wave height (SWH) in SAR mode, while LRM waveforms for the same ocean surfaces were retracked using a Brown-type ocean retracker. A technique was developed for the reduction of SARM data to emulate LRM and implemented in the "RDSAR" software. Retracking the "pseudo-LRM" RDSAR waveforms with a Brown-type ocean retracker showed that the RDSAR data offer the same retrieval accuracy than LRM. This work also showed an almost two-fold improvement in range retrieval with SARM compared to LRM and RDSAR, thus confirming earlier results from **[Raney, 1998]**. However, results with simulated data were not fully conclusive as no improvement was found in the retrieval of SWH from SARM data compared to conventional altimetry.

The SAMOSA1 ocean retracker performance was evaluated against airborne SAR altimeter data acquired with ASIRAS during the Cryovex'2006 campaign. Over 96% of the waveforms were successfully fitted by the SAMOSA1 model when the ASIRAS data was processed to have 64 pulses per burst and a maximum look angle of 1.4 degrees.

The SAMOSA1 Enhanced model was used to successfully retrack real CryoSat-2 SAR waveform data from different oceanic regions. The retrieval accuracy of SAR and LRM in different sea states was estimated for range and significant wave height using CryoSat-2 SAR and Jason-2 LRM data from a small region of the Norwegian Sea between July 2010 and March 2011. Results confirmed a marked, almost two-fold, improvement in range retrieval accuracy with CryoSat-2 SAR compared to Jason-2 LRM. Results also indicated that retrieval of significant wave height is at least as good for SARM as for LRM, although SARM overestimated SWH slightly compared to LRM, particularly in low sea states.

The SAMOSA2 waveform model was also implemented as a SAR ocean retracker and applied to simulated data and a small number of CryoSat-2 L1B SAR waveforms. The SAMOSA2 waveform model being more complex, it required longer computation time than SAMOSA1. Consequently, there was insufficient time within the project schedule to fully evaluate the performance of the SAMOSA2 retracker against CryoSat-2 data. Results with SAMOSA2 applied to simulated SAR data confirmed the findings with SAMOSA1 of an approximately two-fold improvement in range retrieval accuracy with SAR compared to LRM. Analytical solutions were identified to speed-up the computation of SAMOSA2 and were subsequently incorporated in later work.

CP4O	Preliminary Analysis Report	D2.1	

The performance of both SAMOSA1 and SAMOSA2 models were evaluated numerically in terms of precision with Cramér-Rao Lower Bound techniques. The SAMOSA2 model was found to be more robust than SAMOSA1. The impact of the various model improvements was investigated and quantified separately in terms of their effect on the precision of range retrieval. The modification of the model to include non-Gaussian ocean statistics had the greatest effect on precision. However, the change in precision resulting from these improvements was found to be small in terms of the overall precision error budget.

Simulated LRM and SARM data were obtained also for scenarios representing inland waters, including a lake scenario, an estuarine scenario and a wetland scenario. These were processed with BEST and successful retracking of the SAR waveforms (more than 62% for the wetland, and up to 85% for the lake scenario) and recovery of small-scale topographic features was demonstrated, although the waveforms did not conform to the expected shapes (specifically in the case of sigma0 response) in the case of the wetland simulations. Real CryoSat-2 data over the Mekong Delta region were recovered and processed, and the waveform shapes for these data were found to conform to expectation. Over 58% of the waveforms could be re-tracked without averaging though significant mirroring was found in the waveforms, which impacted the re-tracking

3.4.3.3   SAMOSA3 Model and Implementation

Under a further contract, the SAMOSA3 model was developed, which applied geophysical and mathematical approximations to the mathematically complex, and computationally expensive SAMOSA2 model.

After the mathematical formulation was modified, and the effect of this modification on the numerical form was evaluated, an analytical implementation was achieved and evaluated in terms of accuracy of retrieval of sea surface height and significant wave height, in terms of sensitivity to key input variables including mispointing, and in terms of computational performance.

The final output was a Detailed Processing Model for Sentinel-3 SAR mode altimeter ocean retracker **[Gommenginger et al 2012]**

3.4.4   COASTALT

COASTALT, a study on the development of altimetry in the coastal zone for Envisat, started in 2008 and finished in 2012 (ESA/ESRIN Contract No. 21201/08/I-LG led by the National Oceanography Centre, Southampton (UK)). Despite being specifically targeted at conventional pulse-limited altimetry, this project achieved a number of results that affect the field of SAR altimetry. These achievements and their impact are discussed below.

3.4.4.1   Establishing the user requirements for coastal altimetry data

COASTALT carried out a joint survey with the PISTACH project, funded by CNES, to gather the user requirements for coastal altimetry products. The results

from a sample of 53 replies to the questionnaire, mostly from public research institutions, highlight the interest of a wide community in having reprocessed coastal altimetry with improved accuracy and precision for a number of different applications **[Dufau et al., 2011]**; **[COASTALT URR, 2008]**. For the research community the main focus is on the analysis of ocean processes, while the operational community tends to require altimeter data more for model validation or assimilation into models. Wind and wave parameters are also of great value for operational forecasting centres, and there is an interest also in Near Real Time products.

The results of the survey remain naturally valid also for SAR altimetry, even in consideration of the fact that in the coastal zone SAR altimetry is expected to perform at least as well as, if not better than conventional altimetry; indeed this could bring some users to propose even more stringent requirements for the SAR coastal altimetry data.

3.4.4.2 Drawing the product specifications for coastal altimetry

Building on the experience of existing altimetric archives like RADS, and following the recommendations by the user community, COASTALT set the specifications for the reprocessed coastal altimetry products (CGDRs – Coastal Geophysical Data Records) in NetCDF format, and provided complete documentation for the product **[COASTALT2 PSD, 2011]** as well as a comprehensive user handbook **[COASTALT2 APH, 2011]**. This documentation gives a complete introduction to the field of coastal altimetry, which is crucial, both to ensure exploitation of the current products and as a starting point for the development of similar coastal altimetry products (CGDRs) for SAR altimetry.

3.4.4.3 A framework for coastal altimetry processing

COASTALT has implemented a software processor that ingests Envisat Sensor Geophysical Data Record (SGDR) data (and is fully compatible with the recently reprocessed V2.1 SGDR) and produces the reprocessed coastal altimetry data – i.e. the CGDRs – by retracking and updating some of the corrections. Sample CGDRs in COASTALT were produced over a number of pilot areas in European Seas and are available via http://www.coastalt.eu/. The COASTALT Processor is not an operational processor, but has always been intended as a research and development tool, that as well as providing the standard products (i.e. the L2 products propagated from the SGDR) outputs the L2 results from a custom suite of retrackers. The features included in the latest version of the processor are detailed in **[COASTALT2 ProcI, 2011]**.

Some of the modules of the COASTALT processor (for instance input-output) have been taken as starting point for the implementation of the eSurge multi-mission processor, presented in the next section. A key recommendation of COASTALT that extends to the development of SAR altimetry processors is that, in order to facilitate the work of developers, testers, and the uptake of the data by

'expert users', processors must be open, flexible, expandable, easily upgradable and fully documented.

3.4.4.4   Investigation of bright targets in the coastal zone

COASTALT and its related project PISTACH have highlighted the need for a significant improvement of retracking techniques in the coastal zone **[Gommenginger et al., 2011b]**. A lot of effort has been put into looking at new retracking techniques. One of the foci for innovative retracking research in COASTALT has been on the analysis of the returns due to bright targets near the coast, when the waveform is affected by proximity of land or other target peculiarities **[Gómez-Enri et al., 2010]**; **[Scozzari et al., 2012]**. This research led to the design and implementation of a hyperbolic pre-tracker specifically for the Envisat RA-2 altimeter **[COASTALT2 HypPrt, 2011]**. This technique is much better at coping with multiple discrete targets than an approach that treats each waveform in isolation thus neglecting the contextual information from neighbouring waveforms. The sequential retracking of waveforms with Bayes Linear techniques has also been investigated, but encountered numerical difficulties in its implementation that led to unsatisfactory results from this particular retracker.

While the effect of bright targets in SAR altimetry is different from conventional altimetry (in particular, due to multi-looking there is no 'migration' of bright features in a hyperbolic fashion as seen for Envisat), the idea that adjacent along-track resolution cells in SAR altimetry could be retracked in a batch, accounting for the contextual information in neighbouring resolution cells, warrants further investigation.

3.4.4.5   The GPD wet tropospheric correction

As amply discussed in Section 3.2 above, crucial issue for coastal altimetry is the correction of the path delay due to water vapour ('Wet Tropospheric' correction) [10]. The design, development and assessment of a new correction of this kind, the GNSS-Derived Path Delay (GPD) correction has been one of the most successful aspects of COASTALT. In particular this has achieved:

- Full design and implementation of the GPD technique as described in **[Fernandes et al., 2010]**.
- A global assessment of the correction, which showed in particular that the ECMWF-derived Zenith Hydrostatic (i.e. 'dry') Delay (ZHD), is the most suitable dataset to separate the GNSS-derived Zenith Total Delay (ZTD), at global scale, into the dry and wet components **[COASTALT2 tropcor, 2010]**.
- The GPD wet tropospheric correction has been successfully computed for the COASTALT CGDR 1Hz points and interpolated to 18Hz, alongside an interpolation flag and a formal error field **[COASTALT2 GPDout, 2011]**.
- A global implementation of the GPD algorithm was carried out at University of Porto enabling the computation of the wet tropospheric

correction, everywhere over ocean, including the coastal areas and the high latitude regions. Figure 3.48 shows an example of the global GPD correction for Envisat cycle 58. The correction is continuous with respect to the original MWR correction, replacing this one whenever a point is considered to have an invalid MWR value. There is a very good agreement between the Zenith Wet Delay (ZWD, i.e. the Wet tropospheric correction) derived from the GNSS path delays and the corresponding value determined from ECMWF. The mean difference has an absolute value less than 3 mm and the standard deviation is 13 mm **[COASTALT2 GPDimp, 2011]**.

- A study was then conducted on the variability of the spatial correlation of the ZWD field using global ECMWF grids, accompanied by a comparison of the GPD correction with other approaches (models, 'mixed-pixel' algorithm or MPA and 'land proportion' algorithm or LPA) – this is the only validation possible at the moment in the absence of a ground truth. One example of this comparison is shown in Figure 3.49. It showed the GPD estimates to produce more reliable corrections than the other two algorithms, which can show some noisy behaviour. However one of the COASTALT recommendations is that a mixed approach, for example, a mixed MPA and GPD approach, could improve the Path Delay retrieval in some of the most problematic configurations and therefore should be explored further **[COASTALT2 GPDval, 2011]**.
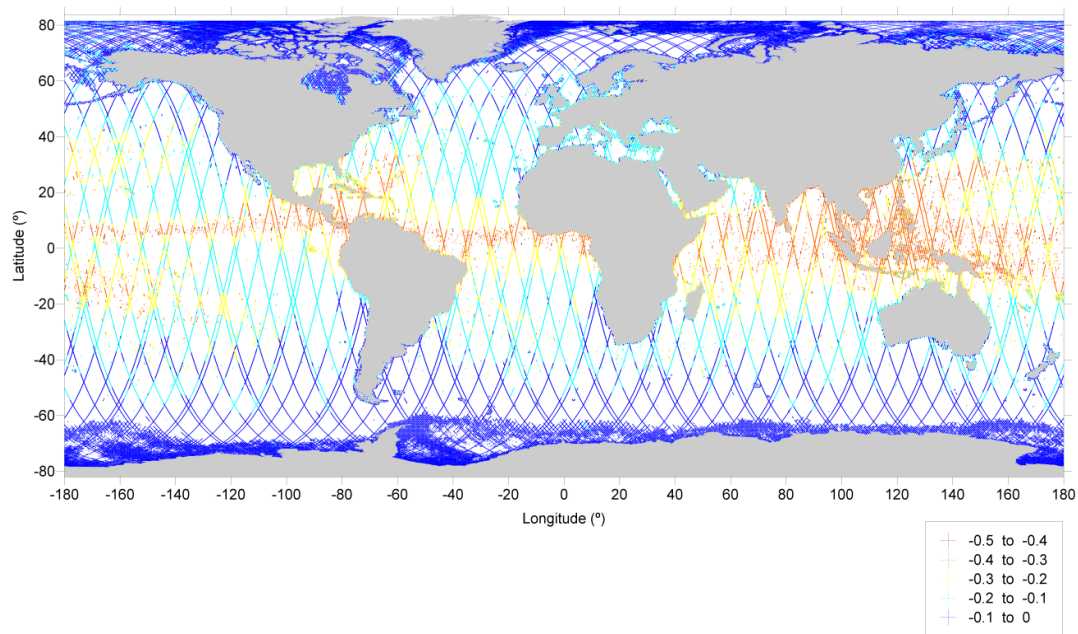
Figure 3.48 Estimated GPD wet tropospheric correction (in m) for Envisat cycle 58, plotted only in those locations where the original MWR-derived correction is not valid.

The conclusions of the research on the GPD naturally extends to SAR altimetry: the GPD, or a 'mixed' correction as explained above, should be the correction of choice for SAR altimetry and can significantly contribute to the precision and accuracy of SAR-derived sea surface height in the coastal zone. Further studies are encouraged on developing a mixed approach that explore the effectiveness of combining different wet tropospheric techniques by mean of Objective Analysis.
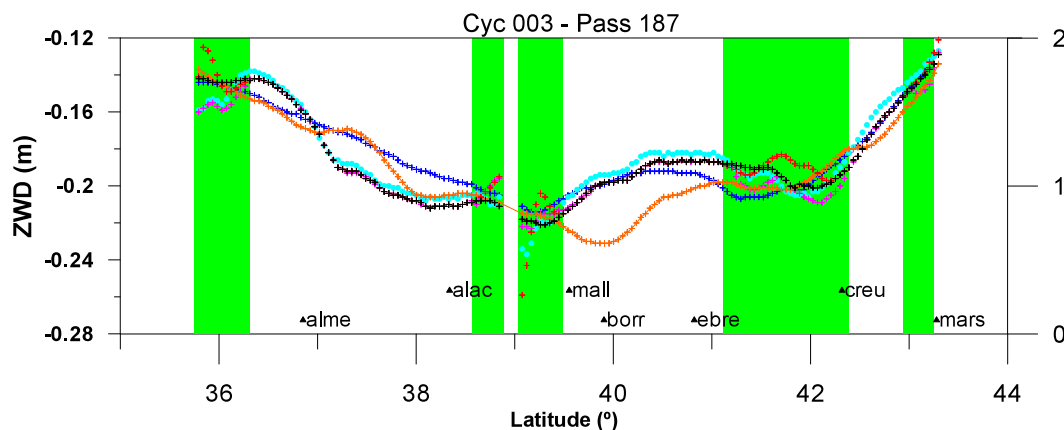
Figure 3.49 Wet tropospheric correction (ZWD) for Jason 2 pass 187, cycle 3: ECMWF (blue), ALADIN (orange), GPD (black), MPA (cyan), LPA (pink) and original MWR correction (red).

3.4.4.6   The importance of local tide models

Another issue that heavily affects the retrieval of sea level and ocean dynamics in the coastal zone is the availability of good regional tidal models. In COASTALT this was investigated on the West Iberian coast with the development of a regional model **[COASTALT2 LTM, 2010]**. The recommendation, which is valid for SAR altimetry too, is that further case studies based on local accurate tidal models should be demonstrated.

3.4.4.7   Further recommendations from COASTALT

Further recommendations from COASTALT that apply to SAR altimetry in the coastal zone are:

- The importance of outreach: we need more investments in outreach and capacity building, including careful selection for user-friendly example material aimed at non-experts;
- The whole issue of filtering for the various corrections in the coastal zone needs to be revisited, with correlation scales clearly identified and data screening and filtering schemes clearly recommended (these may depend on the application to some extent);

- The sea state bias correction needs a reassessment in the coastal zone, with the investigation of specific models – this is even more urgent for SAR altimetry;
- Validation of coastal altimetry data is crucial and should be supported further, and applications should be supported and encouraged, with easy data access;
- The techniques developed in COASTALT and similar projects (such as PISTACH), and the relevant processors should be extended to ensure multi-mission capability, also to enable comparison between the different missions.

3.4.4.8   COASTALT and the coastal altimetry community

One of the main achievements of COASTALT is its crucial contribution to the formation and growth of a lively community of international scientists working on coastal altimetry. The successful *Coastal Altimetry* workshop series has been firmly established with a strong influence by the COASTALT project, and remains the main focus for the international coastal altimetry community, who is coordinated via the COASTALT site at http://www.coastalt.eu/community. Recent editions of the workshop (San Diego, 2011; Riva del Garda, 2012) have had dedicated sessions and many presentations and posters on SAR altimetry and CryoSat-2. The COASTALT project coordinator moderates the COASTALT-SWT (Coastal Altimetry Science Working Team) mailing list, with more than 200 subscribers, and has led the Community White paper on "The role of Altimetry in Coastal Observing System" written for the OceanObs'09 Conference in Venice **[Cipollini et al., 2010]**. COASTALT has strongly contributed to the *Coastal Altimetry* book by Springer **[Vignudelli et al., 2011]**, which in many respects is a reference also for the extension of SAR altimetry to the coastal zone.

The coastal altimetry community remains the forum of choice to bring forward the discussion on technical issues and applications of SAR altimetry in the coastal zone.

3.4.5   *eSurge*

Amongst the most promising applications of coastal altimetry there is the study of storm surges. The understanding and realistic modelling of surges supports both preparation and mitigation activities and should eventually bring enormous societal benefits, especially to some of the world's poorest countries (like Bangladesh). Earth Observation data have an important role to play in storm surge monitoring and forecasting, but the full uptake of these data by the users (such as environmental agencies and tidal prediction centres) must be first encouraged by showcasing their usefulness, and then supported by providing easy access.

Having recognized the above needs, ESA has launched for 2011-2014 a Data User Element (DUE) project called eSurge. The main purposes of eSurge are:

CP4O	Preliminary Analysis Report	D2.1	

1. To contribute through Earth Observation to an integrated approach to storm surge, wave, sea-level and flood forecasting as part of a wider optimal strategy for building an improved forecast and warning capability for coastal inundation;
2. To increase the use of the advanced capabilities of ESA and other satellite data for storm surge applications.

The project is led by Logica UK, with NOC (UK), DMI (Denmark), CMRC (Ireland) and KNMI (Netherlands) as scientific partners.

In practice eSurge aims at building an end-to-end system **[eSurge TS, 2012]** including a database of surge events with the associated Earth Observation and in situ data, and to demonstrate that by assimilating those data in the surge models the forecast improve. A very important component of eSurge is the development, validation and provision of dedicated multi-mission coastal altimetry products. Coastal altimetry has a prominent role to play as it measures directly the total water level envelope (TWLE), i.e. one of the key quantities required by storm surge applications and services. But it can also provide important information on the wave field in the coastal strip, which helps the development of more realistic wave models that in turn can be used to improve the forecast of wave setup and overtopping processes. A multi-mission coastal altimetry processor is being integrated in the eSurge system; the general architecture (visible in Figure 3.50) and some of the modules of this processor follow closely the COASTALT processor, and the products comply with the CGDR NetCDF product specifications defined in COASTALT **[COASTALT2 PSD, 2011]**. We note explicitly that this processor will work on CryoSat-2 SAR data, using the SAMOSA3 retracker, in addition to the conventional Envisat, Jason-1/2 and ERS-1/2 data. CryoSat-2 LRM data will also be processed, using the coastal retrackers developed for the other conventional pulse-limited missions.

The delayed-time reprocessed coastal altimetry data will be blended with tide gauge data to extract the main modes of variability in the coastal regions. Then data from the tide gauges can be used to estimate the water level in real time, based on the modes of variability found, as done in **[Madsen et al., 2007]**.

3.4.5.1   CryoSat-2 SAR processing in Near Real Time (eSurge Live)

In a later phase of the project called eSurge Live, starting in summer 2013, the eSurge coastal altimetry processor will be extended to be able to ingest NRT raw SAR altimeter waveforms and generate the relevant NRT products, a definite first for coastal altimetry. The pilot region for this application will be the North Indian Ocean. On request from the eSurge project, ESA have updated the CryoSat-2 acquisition mask in October 2012 adding a SAR mode polygon around the coasts of the Indian subcontinent and the Bay of Bengal (see Figure 3.51).
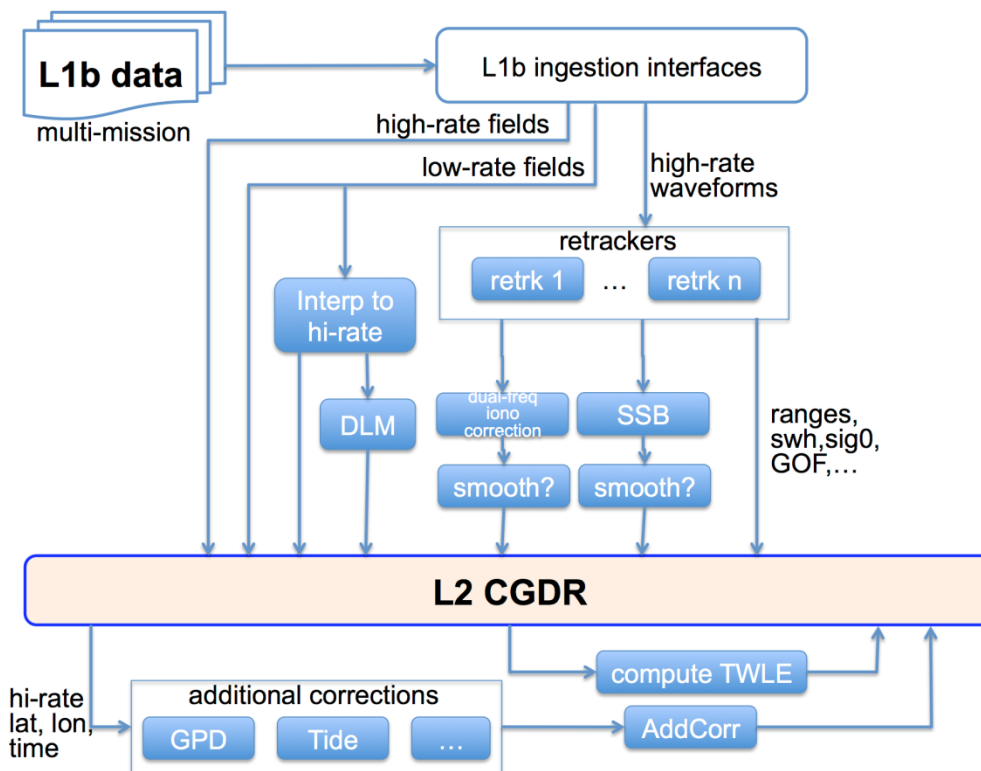
Figure 3.50 Schematic of the coastal altimetry processor for the ESA eSurge Project.
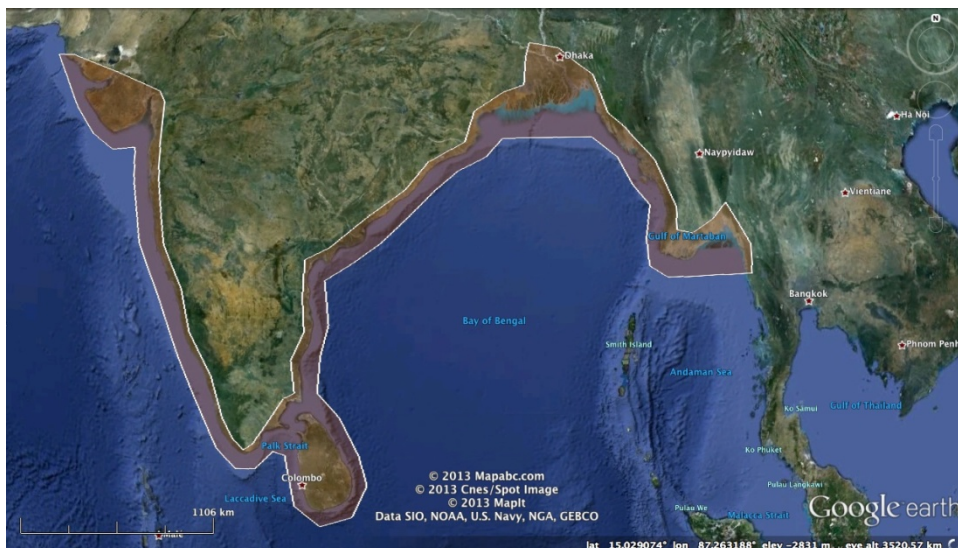
Figure 3.51 CryoSat-2 SAR mode acquisition polygon around the Indian Ocean coast, in effect from 1st October 2012 (Acquisition mask v. 3.4).

In summary, we expect eSurge to be one of the first pre-operational applications of coastal altimetry and a proof of the benefits to society that can be brought by this relatively new branch of marine remote sensing. SAR altimetry and CryoSat-2 will play a substantial part in all this, in particular with the Near Real Time demonstration phase (eSurge Live).

3.4.6 LOTUS

The new EU FP7 LOTUS (preparing Land and Ocean Take Up from Sentinel-3) project, led by DTU Space and starting in 2013, aims at supporting the development of Copernicus (the former GMES) by developing applications of Sentinel-3 to complete the space observation infrastructure designed for land and ocean monitoring for Copernicus.

In more detail, LOTUS deals with the methodologies and data processing that need to be developed to prepare the take-up of the Sentinel-3 data by the users. The LOTUS project will develop new algorithms, data processing chains, and applications of the Sentinel-3 data for the high resolution sea surface heights, wave heights and wind speeds in the open oceans, coastal seas as well as in sea ice covered regions for operational marine services.

LOTUS is necessarily relying on CryoSat-2 SAR data for preparation of test datasets over ocean, inland waters and land that can be used in place of Sentinel-3 data prior to launch. These will be used to develop and test new value-added applications for the Copernicus ocean and land services.

3.4.7 CNES SAR Studies

The CNES team has developed SAR retracking over ocean and the demonstration has been done for CryoSat-2 at Venice OSTST **[Boy et al., 2012]**. In order to validate the results obtained with the SAR processing, an LRM-like processing (RDSAR retracking) has been developed to allow close comparisons since the 20 Hz data have the same date and location.

It was shown by **[Boy et al., 2012]** that the SAR provides a very nice SLA spectrum that allows retrieving spatial scales down to 30 to 50 km in the along track direction, thanks to the true 300 m resolution offered by the SAR technique.

The comparison with RDSAR aims at checking the quality of the SAR processing at the centimetre level, especially that the SAR processing does not introduce any long wavelength errors. On the other hand, SAR processing should be more robust to backscattering events (sigma blooms) and thus provide higher quality data.

CNES is also performing several studies to develop suitable methods in Coastal areas and to review the stacking method currently based on Raney method.

CP4O	Preliminary Analysis Report	D2.1	

3.4.8 PISTACH Project

The CNES PISTACH project has carried out several studies to improve altimetry in the costal areas and inland waters. High-resolution Jason-2 products dedicated to coastal altimetry and hydrology are distributed since November 2008 in Near Real Time. The Level 2 products are provided at a sampling of 20 Hz over the whole globe while level 3 products (sampled at 5 Hz) are distributed over dedicated areas (currently: Agulhas Current, Mid Atlantic Bight, Oregon, Florida Keys).

In the coming months (2013-2014), CryoSat-2 and Jason-1 data (and tentatively SARAL) will be processed with the PISTACH algorithms. CryoSat-2 data will be processed with the CNES retracking algorithms both for LRM and SAR modes. The data will be distributed in IGDR mode and reprocessing of 2011 onward will be achieved. Therefore it will provide homogeneous high-resolution data sets for the three missions since 2011 and this will ease the comparison of different altimeter data sets (LRM and SAR) in coastal areas by scientific users.

3.4.9 CCI Project

The main objective of the sea level CCI project is to produce and validate a Sea Level Essential Climate Variable (ECV) product. It represents the first phase of the ESA Climate Change Initiative program that aims at setting up in a second phase an "operational processing capacity of Earth Observation data". The synergy of CP4O with the CCI project mainly relies in the comparison philosophy. The same approach has been used in the CP4O-WP5000 by developing metrics that will be applied to all the retracking algorithms provided by the WP4000. Indeed, the metrics have been revisited to be fully relevant for retracking assessment.

3.5   WP2500 - Selection of Test Areas for Validation Activities

3.5.1   Selection of open ocean LRM areas for global comparison with other altimeters

For the open ocean LRM product to be developed and validated we do not restrict ourselves to a particular region. The asset of RADS is that it has all the historic LRM altimetry up to current date and will serve as comparison platform. For the "open ocean" LRM we therefore take all possible CryoSat-2 measurement locations for when in LRM mode and when in SAR mode the locations of the reduced SAR data (referred to as pseudo-LRM). The only restriction will be the period over which the products will be developed which also restricts the active satellites being used in the comparison.

3.5.2   Selection of open and coastal ocean SAR areas: sites with in situ data, especially directional wave buoy data, if possible collocated with tide gauges (Starlab, NOC, CLS, SatOC)

The selection of test areas for the validation of CryoSat-2 SAR mode over the open and coastal ocean is determined by:

- the data need given the specific objectives of the validation (i.e. location, duration)
- the availability of CryoSat-2 data in the required mode for the required location and the required duration to make validation possible
- the availability of CryoSat-2 data processed with the appropriate processor baseline

The availability of CryoSat-2 data in different modes (LRM, SAR and SARIN) is determined by the data acquisition mode mask. Figure 3.52 shows some of the main versions of the mask, together with the approximate periods covered by each version of the mask in the right-hand column. As can be seen in Figure 3.52, the mask evolved significantly during the mission lifetime.

Note that the dates in Figure 3.52 are approximate (being derived from direct experience of using the data) as no official record about the periods of applicability of each version of the mask could be found.

In addition, over the period of the mission, data processing at the ESA Instrument Processing Facility (IPF) also evolved. While there were incremental changes affecting various products at various stages of the mission, one notable change to the processing that is particularly relevant for SAR mode over water surfaces was the transition from Baseline A to Baseline B IPF processor. The transition to Baseline B processing for the CryoSat-2 products available on the data

dissemination ftp server became effective for products from February 2012 onwards.

There are two main aspects of the Baseline B processing which are relevant to SAR mode over water surfaces (from the CryoSat Product Handbook), as already discussed above in Section 3.1:

a) Since 01 February 2012, raw complex SAR echoes are oversampled in the FBR to level-1b processor (baseline B products) in order to avoid aliasing over strongly specular targets (e.g. sea ice). Given that the number of samples per waveform remains unchanged (i.e. 128 samples), this results in the truncation of the trailing edge of the waveforms.

b) Baseline B processing is characterised by the application of a Hamming window in azimuth direction, to all samples of all echoes of every burst at the very beginning of the beam-forming step. The windowing process is performed with the following parameters from the processor configuration file:

   o Apply_Azimuth_Hamming: which defines whether or not to apply the window
   o Azimuth_Hamming_c1 and Azimuth_Hamming_c2: which are used to change the shape of the window, H(x) as:

$$H(x) = c_1 + c_2 \left(\cos((\pi x/N) - (\pi/2)) \right)^2$$

where N is the number of echoes in burst, always 64 in SAR mode.

In the latest IPF1 processor release (VK 1.0, February 2012), for both SAR and SIN specialized processors, these parameters are set to:

Apply_Azimuth_Hamming: on

Azimuth_Hamming_c1:   0.08

Azimuth_Hamming_c2:   0.92

The effect of the Hamming window is to increase (broaden) the along-track resolution of the SAR system by a factor of approximately 1.3. This effect, which helps to address aliasing issues over highly specular reflections over sea ice, is nevertheless detrimental to the exploitation of SAR data over water, where some of the benefits of SAR altimetry will be lost. Thus, for ocean applications, if IPF L1B products are to be used, it seems more appropriate to use data obtained with Baseline A.

To date, Baseline A processing applies to data from July 2010 to December 2011, while Baseline B processing applied to data from February 2012 to today (May

CP4O	Preliminary Analysis Report	D2.1	

2013 at time of writing). A further change of processing, to Baseline C, is scheduled for the end of 2013.

a) V3.0

1 July 2010
– 19 April
2011 ?

b) V3.2

20 April
2011?
– 30 April
2012
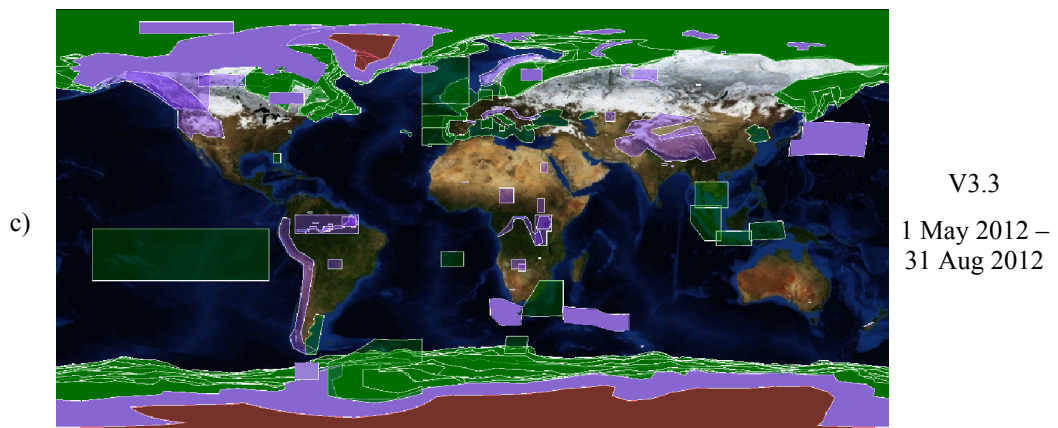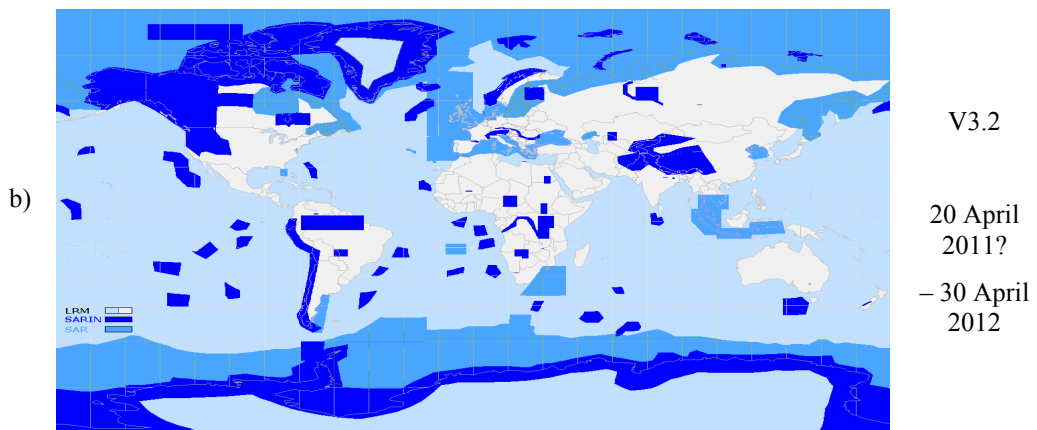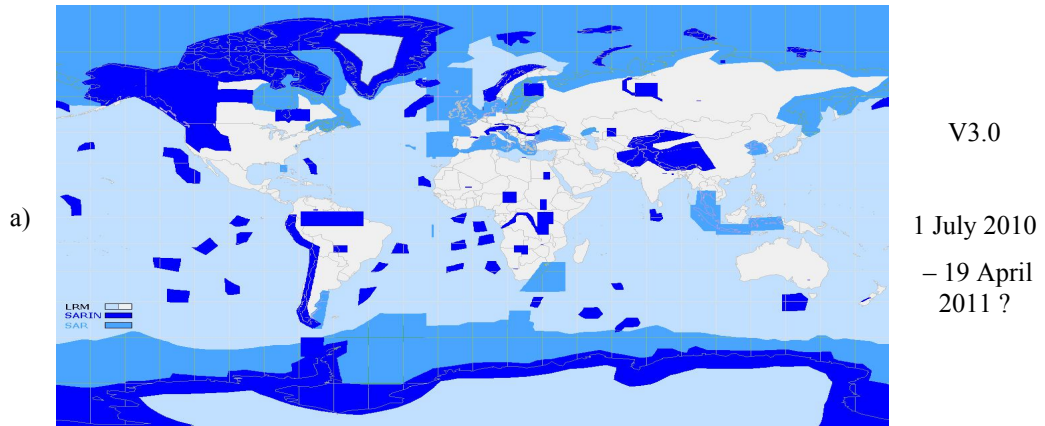
c) V3.3
1 May 2012 –
31 Aug 2012
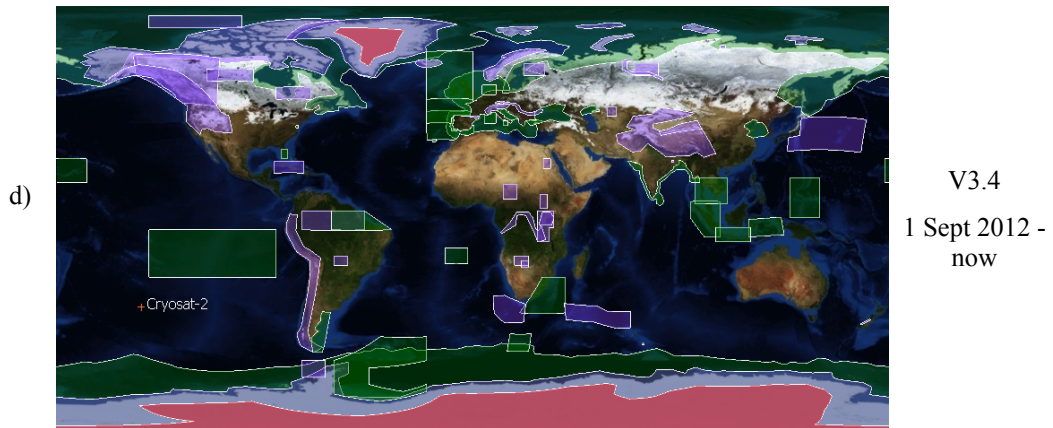
d) V3.4
1 Sept 2012 - now

Figure 3.52: Four main versions to date of the CryoSat-2 mode mask with approximate periods of applicability: a) v3.0; b) v3.2; c) v3.3; d) v3.4

3.5.2.1 Selection of open ocean SAR areas (Starlab, NOC)

The NOC contribution to the validation experiment of CryoSat-2 SAR mode over ocean has the following specific objectives:

- To define and validate the optimal SAR retracking methodology, considering different theoretical SAR waveform models and different L1B multi-looked waveform products and the effect of platform mispointing
- To compare the performance of CryoSat-2 SAR mode SSH and SWH against data from other satellites (e.g. Jason-2) and from in situ measurements (e.g. offshore wave buoys)

In view of the above, the NOC validation activities over ocean will focus over the North-West European shelf. This area has the advantage of having been observed in SAR mode over the whole duration of the mission, thus providing approximately equal amount of data in Baseline A (18 months) and Baseline B (16 months). In addition, the area also benefit from the availability of in situ measurements (UK Met Office and MeteoFrance buoys) as well as frequent satellite overpasses in the Northern part of the region, in view of the high latitude.

3.5.2.2 Selection of coastal ocean SAR areas (NOC, Noveltis)

In addition to the above, the NOC validation activities proposed with CryoSat-2 SAR mode over coastal regions include the following specific objectives:

- To ascertain the quality of C2 SAR mode waveforms within 10 kilometres of land compared to conventional pulse-limited altimeters
- To validate and optimise the SAR retracking methodology defined for open ocean conditions to the case of SAR waveforms in coastal regions.
- To assess the performance of CryoSat-2 SAR mode SSH and SWH against data from other satellites (e.g. Jason-2) and from in situ measurements (e.g. inshore wave buoys and land-based tide gauges).

The comparisons of the C2 SAR SSH with sea level measurements from tide gauges calls for suitable orbit and L2 geophysical corrections. In the coastal zone, this would require dedicated corrections for wet tropospheric delay, tides and (to lesser extent) ionospheric delay. Since no correction exists to date to correct for the effect of sea state on SAR mode SSH (so-called "SAR sea state bias"), some consideration will be given during the validation to the effect of sea state on retrieved SSH, in particular with regards to swell and swell direction.

In view of the above, the NOC validation activities over the coastal ocean will focus on the south coast of the UK, where in situ measurements of waves and sea level are available, as well as dedicated coastal corrections provided by our CP4O partners.

3.5.3 Selection of open ocean SAR areas for sea-floor mapping: sites with high-resolution marine gravity information (DTU)

Within the CryoSAT-2 mode mask version 3.4 a region was selected for the investigation of high resolution marine gravity information by DTU. The region was selected from the following criterias.

1) The depth should not in average be larger than 2000 meters
2) The region should contain significant gravity signal.
3) The ocean signal should be small to moderate.
4) The region should have a relative dense distribution of known sea mounts as this is the region where unknown sea mounts can potentially be found.
5) The region should have marine gravity and bathymetry for comparison.

For a retrieval of short wavelength signal we need data from at least 1 complete repeat cycle of the CryoSat-2 orbit, which is 369 days (a little over 1 year). Furthermore for the suitable region(s) and a suitable time period the best SAR products (from the open, coastal and polar ocean altimetry themes) should be processed by the CP4O consortia in order to be used to chart the marine gravity and the sea floor. The Cryosat-2 SAR Mask was installed prior to October 2012, and covers the region between 15N and 30N and 175E to 195E, so for part of the region data from more than one year will be studied after the completion of one year of observations to evaluate the high resolution gravity field for sea floor mapping.

3.5.4 Selection of coastal ocean SARIn areas (isardSAT)

The isardSAT investigation using SARin data needed from the beginning of the CP4O project a new geographical SARin mask to cover the two nominal scenarios of coastal lines with respect to the satellite track in non-ice coastal ocean zones: perpendicular and parallel. This need has been satisfied with the CryoSat mode mask version 3.4, with a SARin mode mask zone covering the entire Cuban archipelago.

This new SARin mask zone is the main geographical coastal area used for the SARin particular investigation. In this area one can easily find perpendicular tracks with respect to the coastline, and a large range of geographical features. Moreover, the coast of Chile will cover the parallel tracks cases.

In addition, isardSAT will search all around the globe any other interesting zone based not only in the geometry of the track with respect to the coast line, but also taking into account the coastal land topography. SARin mode masks coastal zones over Norway, Canada and Finland have been also detected and are sensible to be used in summer periods to ensure the non-ice sea conditions.

3.5.5 Selection of polar ocean SAR areas: SSH validation data in the Arctic region, tide gauges and mean sea surfaces

The region initially selected for the Polar Ocean validation experiment is Baffin Bay, in the Davis Strait, west of Greenland, where CryoSat-2 already operates in SAR mode and where independent data are available for validation.

This region has been chosen for another important reason: the region is sea-ice covered for only part of the year, and this makes it possible to obtain SAR estimates of SSH over water (with the SAMOSA SAR retrackers) in summer and over ice (with the polar retrackers) in winter. Assuming the seasonally varying CryoSat-2 SAR mask allows, this offers the unique possibility of comparing the SSH for the same region in winter conditions (with extensive sea ice coverage) and in summer conditions, when high precision SSH can be retrieved using the SAMOSA retracker.

The region is defined as follows: Latitude [64° – 74°N], Longitude [70°W-55°W]. We will retrack the CryoSat-2 SAR L1B products for this region using the SAMOSA retracker for the summer months of 2011 for this region, and using the polar retrackers for winter months. We foresee working on a small demonstrator region due to the huge amount of data to be processed. However, early work revealed that the study should be carried out over a larger area of the Arctic so that the effect of mode switching between LRM and SAR could be fully investigated.

4 WP 2000 themes

In Chapter 3 all results have been discussed as they have been compiled per (sub) work package within WP2000. Essentially that chapter provides the complete overview of the state of the art for CryoSat over the oceans, including identified risks of availability of data, auxiliary data and test areas. In this chapter we take another cut through these results and issues by summarising them in relation to the different CP4O themes: "open ocean altimetry", "coastal ocean altimetry", "polar ocean altimetry", and "altimetry for sea floor mapping". Integrated in all these themes is the choice of the best and most up-to-date geophysical corrections like ionosphere delay, wet troposphere delay, and tide models. As coastal altimetry and polar altimetry require higher resolution solutions for these corrections regional and local improvements have been sought in models fed with local/regional in situ data.

4.1 Open Ocean Altimetry

The open ocean theme of CP4O concerns data from the Low Rate Mode (LRM) and SAR modes of the CryoSat-2 SIRAL altimeter instrument over the open ocean. Due to the nature of the sampling characteristics of Cryosat (both orbit driven and instrument driven) and the improved performance offered at small scales, the focus for open-ocean is on the exploration of meso-scale and sub-mesoscale ocean processes. Existing data products are investigated together with possibilities for developing and validating improved products produced by members of the project team, hence the name "CryoSat +". Accuracy and continuity with respect to previous and concurrent missions are also assessed. New products are foreseen for the LRM product, an LRM-like product from the SAR mode, also referred to as RDSAR processing and we propose and investigate new SAR re-tracking schemes. All of these developments are aimed to improve the ability to accurately map fine scale features in the ocean surface.

4.1.1 Existing products and availability

For open ocean applications the ESA SAR, LRM and FDM L1B and L2, CPP LRM, RDSAR, and SAR, and RADS LRM and RDSAR products were assessed. Analyses carried out by the project team partners identified problems with SSB (sigma$_0$), ionosphere and timing bias. These findings, when considered alongside the open issues identified on ESA CryoSat Product Status Page https://earth.esa.int/web/guest/missions/cryosat/product-status (also see Table 3-2) which also impacted on performance over the oceans led to the conclusion that the currently available ESA "operational" products had too many problems for direct

application in this project dedicated to ocean applications. The next version of the processor (Baseline C) should address many of these problems, but data from this processor will not be available until 2014[1].

Because of time constraints on the CP40 project it was not practical to wait for the product update planned by ESA (baseline C, available early 2014), so it was instead decided to use RADS LRM and RDSAR, and CPP LRM, RDSAR and SAR, which are based on either L1b or L1a (FBR) data. Re-tracked FDM L1b appears very well suited for NRT altimetry.

Global corrections on ESA product need to be revised to adhere to the latest correction/model developments; *e.g.* GOT4.9 ocean tide model, DTU10 or CLS11 mean sea surfaces, high resolution MOG2D dynamic atmosphere correction, NCEP/ECMWF full resolution atmospheric path delays, and proper JPL GIM implementation for the ionosphere correction. Also a need remains for an updated SSB both for LRM and for SAR.

RADS products are available through the RADS distribution channels and CPP products will be made available to the project by CNES.

4.1.2   Techniques, models, and data integration

The best way to reduce the RMS of CryoSat-2 LRM crossovers (either from own single crossovers or dual-crossovers with Jason-1 or -2), is to re-track the L1b product and then recalculate significant wave height, backscatter, and range (sea height), and adjusted (best matching) SSB. This is done in both RADS and CPP, whose products will be inter-compared and compared with other altimeters to identify the key differences.

The approach chosen for SAR processing was to work from the Level 1a (or FBR) product, and apply the SAR techniques/models developed and available in the CP4O consortium, that is, numerical, semi-analytical and fully analytical re-tracking. For most of these analyses, CPP level1B will be used as the starting product in order to have the same "baseline" for the retracking comparison.

From our "state-of-the-art" analysis we also conclude that special attention has to be paid to tailor-made hybrid SSB models, and it is also clear that the SSB for LRM cannot be used for the SAR, which needs a different approach. Other issues to be studied thoroughly are the sensitivity of the retracking with respect to the off-nadir angle of the platform (mispointing), for this an accurate platform orientation (attitude) information is required. A possible sensitivity to long waves in the sea surface will also be investigated, for which wavelength and wave direction information in certain study areas will be needed.

---

[1] Most of the key necessary changes have been incorporated in the FDM (Fast Delivery Marine) processor, and new data from this processor have been available since February 2013. However, reprocessing of data prior to that date will not take place until 2014.

CP4O	Preliminary Analysis Report	D2.1	

The testing of new retrackers will also address the problem of getting accurate sigma0 values, and by that accurate wind and SSB, for both LRM and SAR. For SSB a hybrid (non-parametric) approach is described and recommended.

For the open ocean a requirement was to provide continuity across the SAR portions of the ocean with an LRM-like product by reducing the SAR information. This process is known as RDSAR and produces pseudo-LRM or PLRM. An important issue here is the smooth transition from the LRM data product to the PLRM product and back. Other issues concern the noise in the PLRM. Three different approaches will be considered: SAMOSA, CPP (CNES) and RADS (NOAA). All these methods process FBR (level 1a) data into LRM waveform data and applying retracking dealing with the differences in PRF for LRM and SAR. The SAMOSA approach processes subsets of waveforms; remaining issues concern the optimization of the subset and dealing with the time tag bias. For the first time it will be applied to actual data from CryoSat. The CPP approach is different because it is based on averaging all pulses from 4 SAR bursts (256 FBR echoes). The CPP product is already tested and validated for CryoSat and the CPP RDSAR data are routinely ingested in the CNES/SALP product. NOAA's approach is similar to the CPP approach taking all SAR echoes in the calculation but there are differences in the way the echoes are stacked and averaged. In the CP4O project the three techniques will be applied and validated.

Presently used corrections and models on ESA product should be replaced by state-of-the art: e.g. for the wet troposphere no on-board MWR is available. The solution currently applied to Cryosat data uses ECMWF and NCEP analysed meteo fields (for dry and wet troposphere) and seems sufficiently accurate for open ocean data where variability is low. CP4O is working on improving this correction by developing an optimal data combination technique (objective analysis) in which the ERA model, MWR from altimeter and non-altimeter missions and GNSS solutions are combined. The latter data source in particular will contribute to improvements near coasts and islands, and so benefit coastal applications. Because CryoSat's SIRAL instrument is a single-frequency altimeter we cannot make use of the dual-frequency first order ionosphere correction estimate, so we revert to TEC models and external sources like GNSS. The option applied to the ESA products (the BENT ionosphere) is only available for latitudes to 82°. The proposal is to replace it by the JPL GIM product which is provided to 87.5° However discrepancies have been detected between the ESA implementation and the RADS implementation. This could be due to what TEC fields are used (operational vs. final) and/or altitude cut-off and should be further investigated. Regionally, the ionosphere correction can be improved by a regional ionosphere TEC, *e.g.* from the Spectre project. This would help both coastal and polar altimetry. On the subject of ocean tides; globally it is advised to use high-resolution empirical or hydro-dynamical models like DTU10, EOT10a, TPXO7.2, GOT4.8, or FES2012. Current RADS default is GOT4.8, but this is not well suited for shallow waters in the coastal regions. Thus for coastal areas the

recommendation is to use regionally tuned higher resolution models like the COMAPI model for the NE Atlantic.

4.1.3 Auxiliary data, test areas, and supporting initiatives

Independent sources of data and appropriate methodologies are needed to validate and verify the open ocean products: LRM, SAR and RDSAR. Sources will include data from concurrent altimeter satellites (Jason-1, -2, Envisat and hopefully Saral (Altika altimeter)). Both CNES/CLS (SSALTO/DUACS) and NOAA/TUDelft (RADS) have altimeter data base systems that carry all the altimeter data to date with up-to-date corrections, models and references, and these will be used in the global open ocean validation of the new CP4O products. In situ data sources will also be used. These will include tide gauge data (PSMSL), (directional) wave buoy data (NDBC), and wave height and period data from moored stations. Although these sources are predominantly located in the coastal ocean, some open-ocean sources are available in the form of offshore wave buoys, a number of tide gauges on isolated islands, and a selection of bottom pressure recorders (DART system). Another interesting initiative which will be used is GLOBWAVE (ESA/CNES). Though this project officially has ended relevant auxiliary information on global wave height and wave direction is still maintained and distributed by Ifremer, and will be valuable to the CP4O project.

LRM data will be produced and validated on a global basis (where there is LRM and PLRM, according to the CryoSat mode mask). True global comparisons will be possible against other satellite data, whereas the in situ validation will take place over the locations of the in situ data.

The availability of the SAR data is more localized (where there is SAR according to the mode mask), so validation opportunities will depend on the collocation of SAR data availability and on the availability of in situ validation data. Also the required processing effort is higher for SAR data. For these reasons a more restricted area, the NE Atlantic, was chosen for the development, validation and intercomparison of SAR data products. The same considerations apply to RDSAR; so this work will focus on the same area, the NE Atlantic.

Interesting initiatives that have been identified that will benefit CP4O are RADS, REAPER, SAMOSA, LOTUS, CPP (CNES SAR studies), and CCI.

4.2 Coastal Ocean Altimetry

The coastal ocean theme within CP4O concerns the data from the SAR and SARIN (SAR Interferometric) modes of the CryoSat-2 SIRAL altimeter instrument over the coastal zones. The SAR mode offers increased spatial

sampling characteristic with respect to conventional (LRM) altimetry, and so potentially enables the detection of short spatial scale ocean features, which dominate the dynamics in the coastal zone. The SAR mode also allows retrieval of data closer to the coast and so will support development of new approaches to minimise the effect of land contamination in the SAR altimeter footprint. SARIn data will also be used to analyse the potential to discriminate and mitigate contamination from off-nadir land targets.

4.2.1 Existing products and availability

SAR and SARin data will be used. The issues with the existing (open ocean) products have already been extensively discussed in Section 4.1.

4.2.2 Techniques, models, and data integration

The same SAR-retracking issues apply as for the open ocean, so we refer again to Section 4.1. An important additional point of concern is the requirement to get as close as possible to the coast and to analyse methods to minimise footprint land contamination effects. To gain in both temporal and spatial resolution in the coastal zones we also investigate data integration methods to combine different altimeter sources.

For the state-of-the-art altimeter corrections Section 4.1 already provides the overview for open ocean altimetry. Problems with regard to the corrections available on the ESA products have been identified in the previous sections for which both global and regional/local replacements are proposed. The latter provide usually higher spatial and temporal resolution much needed in the coastal zones where the wet troposphere correction is highly variable. For instance, it is possible to improve on the current correction provided by the ECMWF meteo data by optimally combining the ECMWF re-analysis interim model (ERA) with a number of sources of wet path delay data like MWR on-board other satellites and from GNSS stations. Basically this gives a global update that can be used for open ocean, coastal zones and polar regions, though the application in coastal zones creates some particular problems; the location of coastal inland GNSS stations and land contamination in MWR products. Dedicated techniques to efficiently detect contamination problems will be investigated.

A number of new global models for ocean tides are available, including DTU10, EOT10a, TPXO7.2, GOT4.8, and FES2012. The RADS default choice is GOT4.8, but of course being a global model this is not tailor-made for the shallow waters of coastal regions. As mentioned before the advice for the coastal region is to use regionally tuned higher resolution models. For CP4O the COMAPI model for the NE Atlantic will be adopted. For the ionosphere correction a number of global solutions are available, (e.g JPL GIM and NIC09) together with improved regional solutions. Again the coastal zone altimetry will benefit from the use of high-resolution regional total electron content (TEC) maps. CP4O will use and investigate the maps from the SPECTRE initiative (Noveltis). SPECTRE is a

distribution service providing detailed 2D maps of TEC over Europe, including the continental shelf areas.

4.2.3 *Auxiliary data, test areas, and supporting initiatives*

The same basic auxiliary data sources as mentioned in Section 4.1 for the open ocean are also applicable for validating coastal products. Of particular relevance for the coastal areas are in situ measurements of sea level from tide gauges (GLOSS, PSMSL, and SONEL) and bottom pressure recorders (DART), and of waves from wave buoys and moored stations (NODC, NDBC, CDIP). Another important source on wave height and wave direction is GLOBWAVE (Ifremer).

The selection of test areas for coastal products is determined by the availability of the SAR/SARIN data (according to the CryoSat mode map), by the location of in situ measurements sites and on the availability of dedicated coastal altimeter corrections provided by the CP4O partners. Initial development and validation will focus on the south coast of the UK where in situ measurements of waves and sea level are readily available. The large-scale assessment later in the project will consider regional areas like the Gulf of Cadiz, NW Mediterranean, and the German Bight where partners have access to in situ data. The investigations using the SARIN product will take place over Cuba and coastal Chile, where tracks perpendicular to and parallel to the coastline are available.

The most important initiatives on coastal altimetry, from which CP4O benefits, are COASTALT and PISTACH. COASTALT is an ESA study on the development of altimetry in the coastal zone (2008-2012) led by NOC (UK). Though being targeted at conventional pulse-limited (LRM) altimetry (mainly Envisat), this project achieved a number of results that apply to SAR altimetry. A coastal processor has been built that carries a number of improvements in retracking, especially dealing with waveforms affected by the proximity of land. Lessons learned in this project will play a major role in the development of CP4O coastal CryoSat SAR products. While the effect of bright targets in SAR altimetry is different from conventional altimetry (in particular, due to multi-looking there is no 'migration' of bright features in a hyperbolic fashion as seen for Envisat), adjacent along-track resolution cells in SAR altimetry could be retracked in a batch, accounting for the contextual information in neighbouring resolution cells, and will be investigated further. As mentioned above, an important issue in coastal altimetry is the provision of regional and high-resolution corrections. IN addition the SSB needs special attention in coastal waters. As most CP4O partners are directly involved in the large COASTALT community it is clear that each project can benefit form the other. PISTACH is also a project to improve altimetry in the coastal areas and inland waters. It is led by CNES and until recently dealt mainly with NRT Jason-2 products. It is foreseen that in 2013-2014 CryoSat-2 data will be processed with the PISTACH (CNES) retracking algorithms both for the LRM and SAR mode, and that these data can be used by CP4O for comparison studies.

Other interesting initiatives include eSurge and the CPP CNES SAR studies in coastal areas. eSurge is an integrated approach to a storm surge, wave, sea level and flood forecasting system, led by Logica UK with NOC (UK) and KNMI (NL), among others, as scientific partners. It builds on the ideas and results from COASTALT. In the NRT demonstration phase, which soon will go live in the 2nd half of 2013, eSurge will be one of the first operational systems for coastal altimetry applications, and CryoSat-2 and SAR altimetry will play a large role. CP40 will closely follow the developments in eSurge.

4.3   Polar Ocean Altimetry

The polar ocean theme within CP4O will consider LRM, SAR and RDSAR products over the polar oceans. The ultimate aim is to improve representation of the large scale, mesoscale and sub-mesoscale ocean features characteristic for the polar region. The high inclination of the CryoSat-2 orbit enables research at latitudes never visited before by other altimeter satellites: one of the important assets of the CryoSat mission. A drawback of these specific high latitude areas is the presence of sea ice. Therefore CP4O activities concentrate on the development and evaluation of tailored processing schemes that can be applied to sea-ice affected areas. Because no other altimeters have flown here, special interest goes to improvements in mean sea surface, mean dynamic topography, and polar ocean circulation. At the same time, if the record is long enough, improvements in polar ocean tide models can also be expected.

4.3.1   Existing products and availability

Unsurprisingly, for polar ocean altimetry the same problems are encountered as for open ocean altimetry (Section 4.1) and coastal altimetry (Section 4.2). In addition there are a larger number of regions in different modes (LRM, SAR, SARIN) so beside the standing issues to do with each of these modes, incidental issues arise to ensure continuity across the transitions (jumps in sea height in the ESA products). A further issue is that the re-tracker applied in the ESA product has known shortcomings in providing accurate sea height readings in oceans with sea ice. These are the typical things that need investigation and for which alternative methods have to be sought.

In principal the correction issues are the same as for open-ocean and coastal ocean, and so the need to investigate alternatives for wet troposphere, ionosphere and tides also applies in polar regions. The Bent model included in the product only extends to 80° latitude, the JPL GIM is available up to 87.5° North and South, whereas the SPECTRE maps do not go beyond 70° North. For the wet troposphere the methods proposed and investigated by UPorto are recommended: though the wet troposphere is less variable in the polar regions the available MWR data are also more sparse. In addition a tailored polar ocean tide model is

needed, as is an update of mean sea surface model (as sea level anomaly reference) because the older models (as on the standard product) are erroneous in the high latitudes and lack the short-wavelength features.

4.3.2 Techniques, models, and data integration

Based on the fact that no specific sea ice retracker is applied in the ESA data, DTU investigated and proposed new retrackers targeted to areas with sea ice. The best results (out of a selection of 7 different retrackers) were obtained with the leading edge threshold retracker and the DTU prototype threshold retracker. The CryoSat-2 Level 1B data processed with these two improved waveform retrackers clearly show better statistics (in terms of standard deviation) in both sea surface height and marine gravity, revealing that they perform better than the traditional retrackers (especially the one used on the ESA product) that work on the complete waveform. This proves the assumption that applying retracking just on the leading edge of the power waveform results in improved sea surface height determination in areas with sea ice. For open water in the polar regions where there is no ice or little ice one can suffice with any of the new SAR retrackers proposed by CP4O for open ocean altimetry (*e.g.*, the SAMOSA retracker). DTU will continue improving their prototype threshold retracker, which seems most promising for CP4O.

4.3.3 Auxiliary data, test areas, and supporting initiatives

Available auxiliary data for validation include altimeter data from Envisat (and earlier missions), and laser altimetry from ICESAT augmented with data from specific field experiments. Especially interesting in this respect is the use of CRYOVEX-IceBridge data from the 2011/2012 campaigns that have become available. Operation Icebridge closes the gap between the ICESAT laser mission that ended in 2010 and its successor that will not fly before 2016. This is realised by airborne campaigns using a number of different radar instruments. Meanwhile CRYOVEX provides the airborne validation data by flying simultaneously along certain CryoSat tracks. The CRYOVEX/IceBridge campaigns combine these flights.

The region selected for the Polar Ocean validation experiment is Baffin Bay, in the Davis Strait, west of Greenland, where CryoSat-2 already operates in SAR mode and where independent data are available for validation. This region is also chosen because it is ice-covered for only part of the year and by that we can compare winter and summer conditions, though both need a tailored retracking methods (SAMOSA in Summer, and polar/sea-ice retracker in Winter). An investigation of the effect of mode switching between LRM and SAR would require a study over a larger Arctic area. It is also dependent on available tide gauge data and a detailed mean sea surface model.

CP4O	Preliminary Analysis Report	D2.1	

4.4   Altimetry for sea floor mapping

The sea floor mapping theme within CP4O especially focuses on data from the SAR mode of the CryoSat-2 SIRAL altimeter instrument over regions that have a high chance of presence of uncharted seamounts and or trenches, in other words exploiting the SAR finer along-track spatial resolution. The ultimate aim is to assess the ability to resolve the short-wavelength sea surface signals caused by sea-floor topography and marine gravity. For a complete view on these short-wavelength signals, besides the full spatial resolution of the SAR, data from at least 1 complete repeat cycle of the CryoSat-2 orbit (369 days) are needed. For (a) suitable region(s) and a suitable time period the best SAR products (from the open, coastal and polar ocean altimetry themes) will be used to chart the marine gravity and the sea floor.

4.4.1   Existing products and availability

This activity will require the application of SAR altimetry to make use of the along-track spatial sampling which will enable the capture of small-scale features. To maximise also the cross-track sampling at least 1 repeat cycle of 369 days worth of SAR data over a suitable area, is needed. This means that the CryoSat mode mask should be kept fixed for at least a year, or at least should be fixed for a year for the chosen area. Issues concerning existing (SAR) products, their availability and their problems (including corrections) are covered in the earlier sections on open ocean altimetry (4.1), coastal ocean altimetry (4.2) and polar ocean altimetry (4.3).

4.4.2   Techniques, models, and data integration

In work presented in this document assessing the potential application of CryoSat data to sea floor mapping, three months (September to November 2010) of SAR L1b, LRM L1b and LRM L2 data over the Baffin Bay were analysed (**[Stenseng and Andersen, 2012]**). The L1b data were retracked with three different retrackers and compared with an independent marine gravity dataset. This first investigation found very promising results in the comparison with the mean sea surface for both LRM and SAR data. The comparison with the marine gravity field was also promising and preliminary tuning of the processing indicates that significant improvements can be achieved. The inclusion of three months of CryoSat-2 data also improved the local gravity field compared with the ERS-1 derived benchmark gravity field.

Furthermore sea-ice and sea-ice debris were found to be present in the November SAR data and this increases the error on the residual geoid used for the gravity field calculation. A future editing scheme will therefore be required to reject sea-ice contaminated data using SSMIS or equivalent data to avoid degradation of the derived sea surface and thereby the derived gravity field. This will be investigated further in the course of the CP4O project.

4.4.3   Auxiliary data, test areas, and supporting initiatives

The full-scale ocean floor altimetry work will be carried out on one complete (369 day) cycle of SAR mode data, in the region of the North Pacific first implemented in Mask 3-4 on 1st October 2012. Thus it will not be possible to complete this activity until the entire cycle of data is available and has been processed, which is expected late 2013. Availability of in situ validation data for this region will be investigated.

Meanwhile, for sea floor and marine gravity validation purposes we will also work on polar regions and for that exploit the gravity data from the Lomroc 2009-2010 airborne surveys North of Greenland.
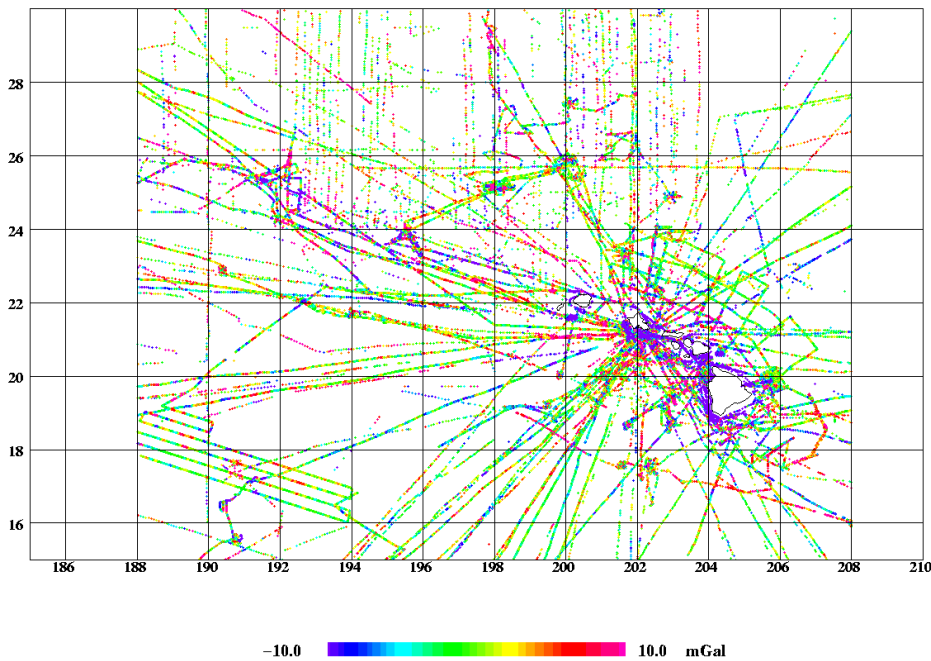
Figure 4.1 Location of marine gravity and presumably marine geophysical parameters like bathymetry for the evaluation of marine gravity and bathmetry prediction using SAR altimetry.

A study into the auxillary data available for the control of the predited gravity field in the Pacific region was initially conducted with the assistance of the National geospatial-intelligences un-classified marine gravity field data base and we found more than adequate data for the comparison with marine gravity.

In this context we assume that most of the tracks shown in Figure XX.1 will also have associated geophysical information recorded like bathymetry. However no detailed survey into this has yet been conducted.

5 Conclusions and recommendations

5.1 Conclusions

ESA's CryoSat-2 mission is the first one carrying a radar altimeter that can operate in SAR mode. Although the primary aim is land and marine ice monitoring, this SAR mode capability offers potential benefits for ocean applications. The project "CryoSat Plus for Oceans" (CP4O) exploits CryoSat-2 data over the ocean. CP4O aims at building a sound scientific basis for new applications of CryoSat-2 data over the open ocean, polar ocean, coastal seas and for sea-floor mapping. In addition new methods and products are proposed, investigated and evaluated that should enable the full exploitation of the capabilities of the CryoSat-2 SIRAL altimeter. The ultimate goal is to maximise the scientific return of the CryoSat-2 mission and be prepared for the full exploitation of the upcoming SAR enabled altimeter missions Sentinel-3 and Jason-CS.

In this report a preliminary analysis of the state-of-the-art of CryoSat-2 products has been carried out. This comprised a comprehensive review of the state-of-the-art, relevant current initiatives, algorithms, models and Earth-observation based products and datasets that are relevant in the context of innovative ocean applications for CryoSat-2 data. In this review we have focussed on low and high-resolution open ocean altimetry, high-resolution polar ocean and coastal zone altimetry and high-resolution sea-floor altimetry. It included:

- A detailed review, assessment and cross-comparison of existing products, datasets, methods, models and algorithms, as well as related range of validity limitations, drawbacks and challenges;
- A detailed analysis of the suitable models and data integration approaches as well as their related limitations, drawbacks and challenges;
- A survey of all accessible data sets associated (space, airborne and in situ) that could be of use in helping ESA to perform an adequate development and validation activity. Investigation of problems such as the lack of sufficient data and identification of practical solutions;
- A survey of current and upcoming initiatives and projects related to CryoSat-2 innovative ocean applications;
- An analysis and identification of the best candidate test areas to be used in the upcoming development and validation of products, including a complete analysis and description of the available data over those test areas.

Considering our analyses and the known problems in the CryoSat-2 data products published by ESA we have come to the conclusion that currently, for oceanographic applications, LRM L2 and SAR L2 are not useful and that SAR

L1b is sub-optimal. At the same time the CP4O team recognizes the exceptional performance of the SIRAL altimeter on CryoSat-2, and is confident that in due course the high-quality state-of-the-art products possible will be available from the ESA processing chain and CP4O hopes to contribute to this adequately. Meanwhile alternative data sets come from CNES CPP and RADS.

For a complete summary per CP4O theme we refer the reader to Chapter 4. For the open ocean the general aim is to contribute to mesoscale and sub-mesoscale oceanography, and the ability to map fine scale features. We used both LRM and SAR mode data, assessed accuracy and sought continuity with respect to previous and concurrent missions. We also have investigated LRM-like products from SAR mode (RDSAR) to ensure continuity from coastal zone to open ocean, and continuity from LRM to SAR mode. New SAR retracking schemes have been proposed, developed and investigated with a focus on mapping fine scale features in the sea surface height. In the coastal zone even finer scales are wanted; for this we explored dedicated SAR retracking with the purpose of minimizing the effect of land contamination in the radar echo, and investigated SARIN mode data also with a focus on mitigating contamination from off-nadir land targets. The polar ocean is not much different from the open ocean, although challenges arise in the form of sea ice and the fact that no altimeter satellite has gone beyond 81.5° latitude. So here we also looked at (to be improved) LRM, SAR and RDSAR products, and developed and evaluate processing schemes applicable to sea-ice affected regions, and targeted to improving mean sea surface models, mean dynamic topography models, polar ocean circulation, and polar ocean tide models.

In the sea-floor mapping theme we investigated the ability to resolve short-wavelength sea surface signals caused by marine gravity and sea-floor topography and the ability to map uncharted seamounts and trenches. For this we exploit the CryoSat-2 SAR mode data to enable the highest along-track sampling resolution. To achieve highest cross-track sampling resolution we need to wait for at least 1 year of continuous data over a suitable region, for which we chose the SAR area (according to the latest mode mask) in the North Pacific.

A lot of effort also went into the assessment of the necessary geophysical corrections, and updates are proposed for the ionosphere, wet troposphere, and ocean tide corrections.

The clear advantages of the CryoSat-2 SAR data over the conventional LRM data is that more independent looks (multi-look) leads to improved retrieval precision, thought the theoretical factor 2 is not yet practically achieved. In terms of height precision this is closer to a factor 1.5 improvement. SAR has finer spatial resolution along-track (about 300 metres), reaches a higher SNR (about 10 dB more), also provides a better performance close to land, especially tracks that incident land at about 90° (perpendicular to coastline), and is also less sensitive to sea state. In the near future we will have the Sentinel-3 surface topography mission that will provide LRM over the open ocean and SAR globally over all coastal areas and over sea ice. We are convinced that our efforts in the CP4O

project not only benefit the exploitation of CryoSat-2 data but also pave the way for proper exploitation of SAR data from Sentinel-3 (1st of 2 to be launched in 2014) and later from Jason-CS (to be launched in 2017).

5.2   Outlook

The heart of CP4O is the development and validation of algorithms and processing schemes for new CryoSat-2 ocean products. From our state-of-the-art analysis we conclude that this should involve the creation of 7 new experimental altimeter data sets, and 4 data sets with new geophysical corrections, of which Table 5-1 gives an overview. The Development and Validation Plan (the other deliverable of the WP2000 work package) provides the details on the definition of these data sets and the plans for development and validation.

Table 5-1 CP4O product development overview

		Initial Development and Validation	Large scale assessment
1	**LRM** for **Open Ocean**	Global (RADS & CLS)	
2	**RDSAR** for **Open Ocean**	NE Atlantic / Pacific	Global
3	**SAR** for **Open Ocean**	NE Atlantic / Pacific	Global
4	**SAR** for **Coastal Ocean**	South Coast UK	Global / regional Gulf of Cadiz, North-West Mediterranean & German Bight
5	**SARIn** for **Coastal Ocean**	Cuba, Chilean Coast	N/A
6	**SAR** for **Polar Ocean**	Arctic (initially Baffin Bay)	
7	**SAR** for **Sea Floor** Mapping	Pacific / North Pacific	
8	Improved **wet trop correction**	Global, full C2 mission	

9	Improved **iono correction**	Mediterranean Sea, European continental shelf
10	Improved **regional tides**	North East Atlantic (coastal)
11	**Other** improved **corrections**	Global (RADS)

 The next steps in CP4O concern impact assessment by applying a "round robin" methodology to all data sets and future exploitation by drawing a scientific road map that should ensure the fullest possible exploitation of CryoSat-2 data over the oceans, and transfer of the results into scientific and operational activities. We plan to organize open workshops to present latest findings and invite others working in this field to present their work. We also want to establish an external expert group to provide independent evaluation of our work. Figure 5.1 provides an overview of the next steps (work packages) in the CP4O project.

SAR mode altimetry offers an exciting opportunity to oceanographers. Aim is to maximise the exploitation of CryoSat-2 data in oceanography, and to build a scientific base for future SAR-enabled satellite missions, starting with Sentinel-3.

| CP4O	Preliminary Analysis Report	D2.1	
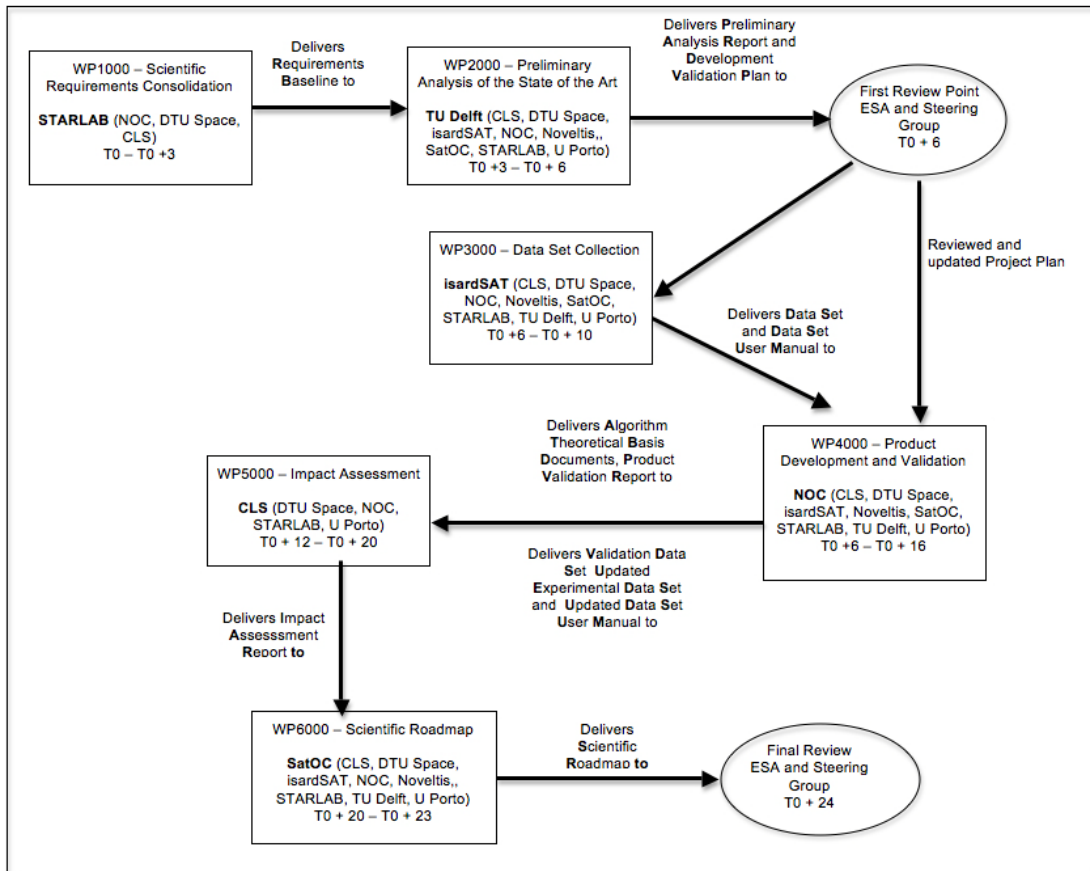
Figure 5.1 Links and flows between the CP4O tasks.

6 References

[Abdalla, 2007]: S. Abdalla, S., "*Ku-band radar altimeter surface wind speed algorithm*", in Proc. of the 2007 Envisat Symposium, Montreux, Switzerland, 23-27 April 2007, ESA SP-636, European Space Agency, The Netherlands.

[Amarouche et al., 2004]: L. Amarouche, P. Thibaut, O.-Z. Zanifé, J.-P. Dumont, P. Vincent, and N. Steunou, "*Improving the Jason-1 ground retracking to better account for attitude effects*", Mar. Geod., 27, 171–197, doi: 10.1080/01490410490465210.

 [Andersen et al., 2005]: O.B. Andersen, P. Knudsen and R. Trimmer, "*Improved High Resolution Altimetric Gravity Field Mapping (KMS2002 Global Marine Gravity Field)*", in F. Sanso (Ed): A Window on the Future of Geodesy, IAG symposium, 128, 326-331, Springer Verlag, Heidelberg, Germany.

[Anderson and Scharroo, 2011]: O.B. Andersen, and R. Scharroo, "*Range and Geophysical Corrections in Coastal Regions And Implications for Mean Sea Surface Determination*", S. Vignudelli et al. (eds.), Coastal Altimetry, doi:10.1007/978-3-642-12796-0_5, Springer-Verlag Berlin Heidelberg.

[Bao et al., 2009]: L. Bao, Y. Lu, Y. Wang, "*Improved retracking algorithm for oceanic altimeter waveforms*", Prog Nat Sci.

[Bent et al., 1972]: R.B. Bent, S.K. Llewellyn, and P.E. Schmid, "*A Highly Successful Empirical Model for the Worldwide Ionospheric Electron Density Profile*", DBA Systems, Melbourne, Florida, 1972.

[Bevis et al., 1994]: M. Bevis, S. Businger, S. Chiswell, T.A. Herring, R.A. Anthes, C. Rocken, and R.H. Ware, "*GPS Meteorology - Mapping Zenith Wet Delays Onto Precipitable Water*", J. Appl. Meteorol, 33 (3):379-386. doi:10.1175/1520-0450.

[Bilitza et al., 1993]: D. Bilitza, K. Rawer, L. Bossy, and T. Gulyaeva, "*International Reference Ionosphere - Past, Present, Future: I. Electron Density*", Adv. Space Res. 13, #3, 3-13, 1993.

[Boy et al., 2011]: F. Boy et al., "*CryoSat Processing Prototype, LRM and SAR processing on CNES side*", oral presentation given at OSTST'2011.

[Boy et al., 2012]: F. Boy, J.-D. Desjonqueres, N. Picot, T. Moreau, S. Labroue, J.-C. Poisson, and P. Thibaut, "*CryoSat Processing Prototype: LRM and SAR processing on CNES side*", OST Science Team meeting, Venice, 27-28 Sept 2012, Available from: http://www.aviso.oceanobs.com/en/courses/sci-teams/ostst-2012.html

[Brown, 2010]: S. Brown, "*A novel near-land radiometer wet path-delay retrieval algorithm: Application to the Jason-2/OSTM advanced microwave radiometer*", IEEE Transactions on Geoscience and Remote Sensing, Vol.48, no.4, 1986-1992.

[Cancet et al., 2010]: M. Cancet, M. Lux, C. Pénard, et al., "*COMAPI: New regional tide atlases and high frequency dynamical atmospheric correction*", presented at the Ocean Surface Topography Science Team meeting, Lisbon, Portugal.

[Cancet et al., 2012]: M. Cancet, F. Lyard, F. Birol, L. Roblou, J. Lamouroux, M. Lux, E. Jeansou, D. Boulze, E. Bronner, "*Latest improvements in tidal modeling: a regional approach*", Proceeding of the 20 Years of Progress in Radar Altimetry Symposium, Venice, Italy.

[Carrère et al., 2012]: L. Carrère, F. Lyard, M. Cancet, A. Guillot, and L. Roblou, "*FES2012: A new global tidal model taking advantage of nearly twenty years of altimetry*", Proceeding of the 20 Years of Progress in Radar Altimetry Symposium, Venice, Italy.

[Cipollini et al., 2010]: P. Cipollini, J. Benveniste, J. Bouffard, W. Emery, C. Gommenginger, D. Griffin, J. Høyer, K. Madsen, F. Mercier, L. Miller, A. Pascual, M. Ravichandran, F. Shillington, H. Snaith, T. Strub, D. Vandemark, S. Vignudelli, J. Wilkin, P. Woodworth, and J. Zavala-Garay, "*The Role of Altimetry in Coastal Observing Systems*", in Proceedings of OceanObs'09: Sustained Ocean Observations and Information for Society (Vol. 2), Venice, Italy, 21-25 September 2009, Hall, J., Harrison, D.E. & Stammer, D., Eds., ESA Publication WPP-306, 2010.

[COASTALT URR, 2008]: "*Report on User Requirements for Coastal Altimetry Products*", COASTALT Deliverables 1.1/1.2, v 1.1, 13 Oct 2008.

[COASTALT2 APH, 2011]: "*Envisat Coastal Altimetry Product Handbook*", COASTALT2 Deliverable 4.1b, COASTALT2-D41b-201, (ESA ref: ENVI-DTEX-EOPS-TN-09-0006), v2.0.1, 16/09/2011.

[COASTALT2 GPDimp, 2011]: "*GPD global implementation*", COASTALT2 Deliverable 2.1c, COASTALT2-D21c-11, v 1.1, 05/08/2011.

[COASTALT2 GPDout, 2011]: "*GPD output for CGDR for European coasts*", COASTALT2 Deliverable 2.1b, COASTALT2-D21b-11, v 1.1, 08/02/2011.

[COASTALT2 GPDval, 2011]: "*Data combination and GPD validation*", COASTALT2 Deliverable 2.1d, COASTALT2-D21d-11, v 1.1, 29/09/2011.

[COASTALT2 HypPrt, 2011]: "*Development and Implementation of the Hyperbolic Pretracker*", COASTALT2 Deliverable 3.3, COASTALT2-D33-20, v2.0, 21/12/2011.

[COASTALT2 LTM, 2010]: "*Local Tide Model for the West Iberian Region*", COASTALT2 Deliverable 2.2, COASTALT2-D22-11, v 1.1, 10/10/2010.

CP4O	Preliminary Analysis Report	D2.1	

[COASTALT2 ProcI, 2011]: "*COASTALT Processor v.2. Processor improvements: technical note*", COASTALT2 Deliverable 1.2a, COASTALT2-D12a-10, v 1.0, 25 July 2011.

[COASTALT2 PSD, 2011]: "*Product Specification Document*", COASTALT2 Deliverable 4.1a, COASTALT2-D41a-203 v 2.0rev3, 20/06/2011.

[COASTALT2 tropcor, 2010]: "*Global assessment of GNSS-derived tropospheric corrections*", COASTALT2 Deliverable 2.1a, COASTALT2-D21a-11, v 1.1, 26/07/2010.

[Coïsson et al., 2006]: P. Coïsson, S.M. Radicella, R. Leitinger, and B. Nava, "*Topside electron density in IRI and NeQuick: features and limitations*", Adv. Space Res., 37(5), 937-942, doi:10.1016/j.asr.2005.09.015.

[Cotton, 2010]: D. Cotton, "*SAR Altimetry MOde Studies and Applications*", (SAMOSA) project web page (including links to project presentations and reports).

[Crespon et al., 2007]: F. Crespon, E. Jeansou, J. Helbert, G. Moreaux, P. Lognonné, P.E. Godet, R. Garcia, "*SPECTRE (http://www.noveltis.fr/spectre): a web Service for Ionospheric Products*", in Proceedings of 1st Colloquium Scientific and Fundamental Aspects of the Galileo Programme, Toulouse, France, October, 2007.

[CryoSat DQS, 2013]: "*CryoSat Data Quality Status Summary*", ESA report ESRIN-EOP-GQ, CS-TN-ESA-GS-808 Version 5, 08 March 2013, 23 pp. Available from ESA website: https://earth.esa.int/web/guest/missions/cryosat/product-status

[CryoSat MDD, 2007]: "*CryoSat Mission and Data Description*", Document no. CS-RP-ESA-SY-0059, Jan. 2007. http://esamultimedia.esa.int/docs/CryoSat/Mission_and_Data_Descrip.pdf

[Davis et al., 1985]: J.L. Davis, T.A. Herring, I.I. Shapiro, A.E.E. Rogers, and G. Elgered, "*Geodesy by radio interferometry: effects of atmospheric modelling errors on estimates of baseline length*", Radio Science 20(6):1593-1607.

[Davis, 1995]: C.H. Davis, "*Growth of the Greenland ice sheet: a performance assessment of altimeter retracking algorithms*", IEEE Trans Geosci Remote Sens 33(5).

[**Davis, 1997]**: C.H. Davis, "*A robust threshold retracking algorithm for measuring ice-sheet surface elevation change from satellite radar altimeter*", IEEE Trans Geosci Remote Sensing 35(4).

[Desportes et al., 2007]: C. Desportes, E. Obligis, and L. Eymard, "*On the wet tropospheric correction for altimetry in coastal regions*", IEEE Transactions on Geoscience and Remote Sensing, Vol.45, no.7.

[Dinardo, 2008]: S. Dinardo, "*Technical Note: Methodology For SAR To LRM Reduction*", ESA EOP-SER, July 2008.

[Ducet et al., 2000]: N. Ducet, P.-Y. Le Traon, and G. Reverdin, "*Global high resolution mapping of ocean circulation from Topex/Poseidon and ERS-1 and -2*", J. Geophys. Res., 105 (C8), 19477-19498.

[Dufau et al., 2011]: C. Dufau, C. Martin-Puig, and L. Moreno, "*User requirements in the coastal ocean for satellite altimetry*", in Coastal Altimetry, Eds S. Vignudelli, A. Kostianoy. P. Cipollini, J. Benveniste, Springer, 2011.

[eSurge TS, 2012]: "*eSurge Technical Specification*", Deliverable D.110, v 3.1, 24/07/2012, 80 pp., available http://www.storm-surge.info/sites/storm-surge.info/files/eSurge_D110_TS_v3.1.pdf

[Fernandes et al., 2010]: M.J. Fernandes, C. Lázaro, A.L. Nunes, N. Pires, L. Bastos, and V.B. Mendes, "*GNSS-derived Path Delay: an approach to compute the wet tropospheric correction for coastal altimetry*", IEEE Geosci. Rem. Sens Lett., vol. 7, NO. 3, pp. 596−600.

[Fernandes et al., 2012]: M.J. Fernandes, N. Pires, C. Lázaro, and A.L. Nunes, "*Tropospheric Delays from GNSS for Application in Coastal Altimetry*", Advances in Space Research, Vol. 51(8). doi:10.1016/j.asr.2012.04.025.

[Gaspar et al., 1994]: P. Gaspar, F. Ogor, P.-Y. Le Traon, O.-Z. Zanife, "*Estimating the sea state bias of the TOPEX and POSEIDON altimeters from crossover differences*", J.Geophys. Res., 99(C12), 24,981-24,994, 1994.

[Giles et al., 2012]: K. Giles, D. J. Wingham, N. Galin, R. Cullen, and W. Smith, "*Precise estimates of ocean surface parameters from CryoSat*", OST Science Team meeting, Venice, 27 - 28 Sept 2012, Available from: http://www.aviso.oceanobs.com/en/courses/sci-teams/ostst-2012.html

[Gómez-Enri et al., 2010]: J. Gómez-Enri, S. Vignudelli, G.D. Quartly, C.P. Gommenginger, P. Cipollini, P.G. Challenor and J. Benveniste, "*Modeling Envisat RA-2 waveforms in the coastal zone: Case-study of calm water contamination*", IEEE Geosci. Rem. Sensing Lett., vol. 7, no. 3, pp 474−478, July 2010.

[Gommenginger et al., 2011a]: C. Gommenginger, C. Martin-Puig , S. Dinardo, D. Cotton, M. Srokosz, and J. Benveniste, "*Improved altimetric accuracy of SAR altimeters over ocean: Observational evidence from CryoSat-2 SAR and Jason-2*", OST Science Team meeting, San Diego, 19 - 21 Oct 2011, Available from: http://www.aviso.oceanobs.com/en/courses/sci-teams/ostst-2011.html.

[Gommenginger et al., 2011b]: C. Gommenginger, P. Thibaut, L. Fenoglio-Marc, G. Quartly, X. Deng, J. Gómez-Enri, P. Challenor, and Y. Gao, "*Retracking altimeter waveforms near the coasts - A review of retracking methods and some applications to coastal waveforms*", in Coastal Altimetry, Eds S. Vignudelli, A. Kostianoy. P. Cipollini, J. Benveniste, Springer, 2011.

[Gommenginger et al., 2012]: C. Gommenginger, C. Martin-Puig , M. Srokosz, M. Caparrini, S. Dinardo, and B. Lucas, "*Detailed Processing Model of the*

Sentinel-3 SRAL SAR altimeter ocean waveform retracker", SAMOSA3 WP2300 technical Note, ESRIN Contract No. 20698/07/I-LG "Development of SAR Altimetry Mode Studies and Applications over Ocean, Coastal Zones and Inland Water", Version 2.1.0, 16 March 2012, 75 pages.

[Gulyaeva et al., 2002]: T.L. Gulyaeva, X. Huang, and B.W. Reinisch, "*Ionosphere-plasmasphere model software for ISO*", Acta Geodaetica et Geophysica Hungarica, 39/3,.143-152.

[Hernandez-Pajares et al., 1999]: M. Hernandez-Pajares, J.M. Juan, and J. Sanz, "*New approach in global ionopsheric determination using ground GPS data*", Journal of Atmospheric and Solar-Terrestrial Physics, 61, p. 1237-1247.

[Ignatov and Laszlo, 2004]: A. Ignatov A., and I. Laszlo, "*Equator crossing times for NOAA, ERS and EOS sun-synchronous Satellites*", Int. J. Remote Sensing, VOL. 25, NO. 23, 5255–5266.

[Iijima et al., 1999]: B.A. Iijima, I.L. Harris, C.M. Ho, U.J. Lindqwister, A.J. Mannucci, X. pi, M.J. Reyes, L.C. Sparks, and B.D. Wilson, "*Automated daily process for global ionospheric total electron content maps and satellite ocean altimeter ionospheric calibration based on Global Positioning System data*", Journal of Atmospheric and Solar Terrestrial Physics, 61, 1205-1218.

[Jensen, 1999]: J.R. Jensen, "*Radar altimeter gate tracking: Theory and extension*", IEEE Trans. Geosci. Rem. Sens., 37 (2), 651–658.

[Keihm et al., 1995]: S.J. Keihm, M.A. Janssen, and C.S. Ruf, "*TOPEX/Poseidon microwave radiometer (TMR): III. Wet troposphere range correction algorithm and pre-launch error budget*", IEEE Trans. Geosci. Remote Sens., vol. 33, no. 1, pp. 147–161.

[Keihm et al., 2000]: S.J. Keihm, V. Zlotnicki, and C.S. Ruf, "*TOPEX microwave radiometer performance evaluation, 1992–1998*", IEEE Trans. Geosci. Remote Sens., vol. 38, no. 3, pp. 1379–1386.

[Klobuchar, 1987]: J. Klobuchar, "*Ionospheric Time-Delay Algorithms for Single-Frequency GPS Users*", IEEE Transactions on Aerospace and Electronic Systems (3), pp. 325-331.

[Kouba, 2008]: J. Kouba, "*Implementation and testing of the gridded Vienna Mapping Function 1 (VMF1)*", Journal of Geodesy 82:193-205 doi:10.1007/s00190-007-0170-0.

[Lee et al., 2008]: H. Lee, C.K. Shum, A. Braun, C.Y. Kuo, "*Laurentia crustal motion observed using Topex/Poseidon radar altimetry over land*", J. Geodyn. 46.

[LeTraon et al., 1998]: P.-Y. Le Traon, F. Nadal, and N. Ducet, "*An Improved Mapping Method of Multisatellite Altimeter Data*", J. Atmospheric Oceanic Technol., 15, 522-534.

[Lyard et al., 2006]: F. Lyard, F. Lefevre, T. Letellier, et al., "*Modelling the global ocean tides: modern insights from FES2004*", Ocean Dyn., 56, 394-415.

[Madsen et al., 2007]: K.S. Madsen, J.L. Høyer, and C.C. Tscherning, "*Near-coastal satellite altimetry: Sea surface height variability in the North Sea–Baltic Sea area*", Geophys. Res. Lett., 34, L14601, doi:10.1029/ 2007GL029965.

[Mannucci et al., 1999]: A.J. Mannucci, B. Iijima, L. Sparks, X. Pi, B. Wilson, and U. Lindqwister, "*Assessment of global TEC mapping using a three-dimensional electron density model*", Journal of Atmospheric and Terrestrial Physics, vol. 61, p. 1227-1236.

[Marquez et al., 2010]: J. Marquez et al., "*RDSAR Software Documentation*", ESA Contract Report D4 for SAMOSA CCN, contract no. 20698/07/I-LG, Oct. 2010.

[Mendes et al., 2000]: V.B. Mendes, G. Prates, L. Santos, and R.B. Langley, "*An evaluation of the accuracy of models of the determination of the weighted mean temperature of the atmosphere*", In: Proceedings of "ION 2000 National Technical Meeting", Anaheim, CA.

[Obliges et al., 2010]: E. Obligis, A. Rahmani, L. Eymard, S. Labroue, and E. Bronner, "*An Improved Retrieval Algorithm for Water Vapor Retrieval: Application to the Envisat Microwave Radiometer*", IEEE Transactions on Geoscience and Remote Sensing, V. 47, no. 9, pp. 3057−3064.

[Obliges et al., 2011]: E. Obligis, C. Desportes, L. Eymard, J. Fernandes, C. Lázaro, and A. Nunes, "*Tropospheric corrections for coastal altimetry*", In: Vignudelli S, Kostianoy A, Cipollini P, Benveniste J (eds) Coastal Altimetry. Springer, Heidelberg, 560 pp. doi:10.1007/978-3-642-12796-0_6.

[Opperman et al., 2007]: B.D.L. Opperman, P.J. Cilliers, L-A. McKinnell, and R. Haggard, "*Development of a regional GPS-based ionospheric TEC model for South Africa*", Advances in Space Research, Volume 39, Issue 5, 2007, Pages 808–815, http://dx.doi.org/10.1016/j.asr.2007.02.026.

[Phalippou and Demeestere, 2011]: L. Phalippou and F. Demeestere, "Optimal retracking of SAR altimeter echoes over open ocean: Theory versus results from SIRAL2 data", OST Science Team meeting, San Diego, 19 - 21 Oct 2011, Available from: http://www.aviso.oceanobs.com/en/courses/sci-teams/ostst-2011.html

[Phalippoua and Enjolras, 2007]: L. Phalippou and V. Enjolras, "*Re-tracking of SAR altimeter ocean power-waveforms and related accuracies of the retrieved sea surface height, significant wave height and wind speed*", IGARSS: 2007 IEEE International Geoscience and Remote Sensing Symposium, Vols 1-12, 3533-3536.

[Quartly and Srokosz, 2003]: G.D. Quartly, and M.A. Srokosz, "*Rain-flagging of the Envisat altimeter*", in Proc. International Geoscience and Remote Sensing Symposium (IGARSS) 2003, vol. 5, 2984–2986.

[Radicella, 2009]: S.M. Radicella, "*The NeQuick model genesis, uses and evolution*", An. Geophys., vol. 52, N. 3/4, June/August 2009.

[Raney, 1998] Raney, R. K., *The Delay/Doppler Radar Altimeter,* IEEE Trans. Geosci. Remote Sensing, vol. 36, pp. 1578-1588, Sept.1998.

[Ray et al., 2013]: C. Ray, C. Martin-Puig, M.-P. Clarizia, G. Ruffini, S. Dinardo, C. Gommenginger, and J. Benveniste, "*SAR Altimeter Backscattered Waveform Model*", IEEE Transactions on Geoscience and Remote Sensing (under review).

[Ray, 1999]: R.D. Ray, "*A global ocean tide model from TOPEX/POSEIDON altimetry: GOT99.2*", NASA Tech. Memorandum 1999-209478, Goddard Space Flight Center, Greenbelt, MD.

[RDSAR SD, 2012]: Starlab's SAMOSA Team, "*RDSAR Software Description*", Deliverable D4 of the ESA Contract 20698/07/I-LG, Oct 2012.

[Rodriguez, 1988]: E. Rodriguez, "*Altimetry for Non-Gaussian Oceans: Height Biases and Estimation of Parameters*", Journal of Geophysical Research, 93, 14107-14120.

[Sandwell et al., 2011]: D.T. Sandwell, E. Garcia, and W.H.F. Smith, "*Improved Marine Gravity from CryoSat and Jason-1*", OST Science Team meeting, San Diego, 19 - 21 Oct 2011: http://www.aviso.oceanobs.com/en/courses/sci-teams/ostst-2011.html

[Schaer et al., 1998]: S. Schaer, W. Gurtner, and J. Felstens, "*IONEX: The Ionosphere Map Exchange Format Version 1, February 25, 1998*", in Proceedings of the 1998 IGS Analysis Centers Workshop, ESOC, Darmstadt, Germany, February 9-11, p. 233-247.

[Schaer, 1999]: S. Schaer, "*Mapping and Predicting the Earth's Ionosphere Using Global Positioning System*", PhD., Astronomical Institute, University of Berne, Berne, Switzerland.

[Scharroo, 2002]: R. Scharroo, "*A Decade of ERS Satellite Orbits and Altimetry*", PhD thesis, Delft Univ. Press, Delft, Netherlands.

[Scharroo and Lillibridge, 2004]: R. Scharroo and J. Lillibridge, "*Non-parametric sea-state bias models and their relevance to sea level change studies*", In: Lacoste H, Ouwehand L (eds) Proceedings of the 2004 Envisat & ERS Symposium, ESA SP-572.

[Scharroo and Smith, 2010]: R. Scharroo, and H.F. Smith, "*A global positioning system-based climatology for the total electron content in the ionosphere*", J. Geophys. Res., 115 A10318, doi:10.1029/2009JA014719.

[Scharroo et al., 2013]: R. Scharroo, W.H.F. Smith, E.W. Leuliette, and J.L. Lillibridge, "*The performance of CryoSat-2 as an ocean altimeter*", in Proc. CryoSat-2 Third User Workshop, Dresden, 12-14 March 2013, Eur. Space Agency Spec. Publ., ESA SP-717, 5 pp.

[Scozzari et al., 2012]: A. Scozzari, J. Gómez-Enri, S. Vignudelli, and F. Soldovieri, "*Understanding target-like signals in coastal altimetry:*

experimentation of a tomographic imaging technique", Geophys. Res. Lett., 39, L02602, doi:10.1029/2011GL050237, 2012.

[Smith and Scharroo, 2011]: W.H.F. Smith, and R. Scharroo, "*Retracking range, SWH, sigma-naught, and attitude in CryoSat conventional ocean data*", OST Science Team meeting, San Diego, 19 - 21 Oct 2011: http://www.aviso.oceanobs.com/fileadmin/documents/OSTST/2011/oral/01_Wednesday/Splinter%201%20IP/03%20Smith_WHFSmith_IP_CS2_2.pdf

[Stenseng and Andersen, 2012]: L. Stenseng, and O.B. Andersen, "*Preliminary gravity recovery from CryoSat-2 data in the Baffin Bay*", Adv. Space Res., 50, 1158-1163, doi:10.1016/j.asr.2012.02.029.

[Stum et al., 2011]: J. Stum, P. Sicard, L. Carrère, and J. Lambin, "*Using Objective Analysis of Scanning Radiometer Measurements*", 3222 IEEE Transactions on Geoscience and Remote Sensing, VOL. 49, NO. 9.

[Vignudelli et al., 2011]: S. Vignudelli, A.G. Kostianoy, P. Cipollini, J. Benveniste (Editors), "*Coastal Altimetry*", Springer-Verlag Berlin Heidelberg, doi:10.1007/978-3-642-12796-0, 578 pp.

[Webb and Essex, 1999]: P.A.Webb, E.A. Essex, "*Modelling the Plasmasphere*", online: http://www.ips.gov.au/IPSHosted/STSP/meetings/aip/phil/phil.htm

[Webb and Essex, 2001]: P.A. Webb, and E.A. Essex, "*A dynamic diffusive equilibrium model of the ion densities along plasmaspheric magnetic flux tubes*", J. Atmos. Solar-Terr. Phys. 63, 1249-1260.

[Wingham et al., 1986]: D.J. Wingham, C.G. Rapley, and H. Griffiths, "*New techniques in satellite tracking system*", Proceedings of IGARSS 86 symposium, Zurich.

[Wingham et al., 2004]: D.J. Wingham, L. Phalippou, C. Mavrocordatos, and D. Wallis, "*The Mean Echo and Echo Cross Product From a Beamforming Interferometric Altimeter and Their Application to Elevation Measurement*", IEEE Transactions on Geoscience and Remote Sensing, 42**,** 2305-2323.

Other consulted material

CryoSat products handbook:

https://earth.esa.int/c/document_library/get_file?folderId=125272&name=DLFE-3605.pdf

Envisat products handbook:

CP4O	Preliminary Analysis Report	D2.1	

https://earth.esa.int/pub/ESA_DOC/ENVISAT/RA2-MWR/PH_light_1rev4_ESA.pdf

Jason-1 GDR products handbook:

http://www.aviso.oceanobs.com/fileadmin/documents/data/tools/hdbk_j1_gdr.pdf

Jason-2 GDR products handbook:

http://www.aviso.oceanobs.com/fileadmin/documents/data/tools/hdbk_j2.pdf